BED PACKING MODELS: INFLUENCE ON BED GEOMETRY AND HYDRODYNAMICS

A Dissertation

by

VENKAT KRISHNA SRIKANTH PANYARAM

Submitted to the Office of Graduate and Professional Studies of
Texas A&M University
in partial fulfillment of the requirements for the degree of

DOCTOR OF PHILOSOPHY

Chair of Committee,	Benjamin Wilhite
Committee Members,	Mark Holtzapple
	Victor Ugaz
	Simon North
Head of Department,	M. Nazmul Karim

May 2019

Major Subject: Chemical Engineering

ABSTRACT

Fixed Bed Reactors are multi-phase reactors where flow of gas, liquid or both phase reactants occurs over a packed bed of solid catalyst. These systems are common in industry as they are easy to construct, operate and maintain. They provide significant contacting of phases with low pressure drop and exhibit relatively low catalyst attrition rates. The complex flow patterns often lead to flow mal-distribution and liquid channeling which in turn leads to non uniform catalytic activity. A manifestation of such consequences is hot spot formation and catalyst and product degradation, which are key concerns with these reactors. This behavior is primarily dictated by the bed structure which influences the flow distribution and catalytic activity. Bed packing configurations produce contacting surfaces for the fluid phases and also aid in catalytic reactions. The configurations developed while packing the beds play an important role in the operation of reactor as they effect the hydrodynamics of the operation by altering the fluid flow behavior. Also, extremely dense beds are known to produce high pressure drops because of the highly tortuous paths. This leads to under utilization of catalyst beds, mal-distribution issues and eventually compromises the safety and product quality.

In this study, the bed characteristics of two highly relevant catalyst shapes, spheres and cylinders, are studied. Spherical particle structures comprised of mono-disperse and poly-disperse particle samples and cylinder particle structures comprised of mono-disperse particle samples with two different aspect ratios are generated using the Discrete Element Method (DEM). The beds are prepared using three different loading strategies: *Uniform, Sock* and *Wall*, wherein the radial entry position of the particles is varied. Geometric properties of these beds were studied and their potential influence on the flow phenomena is evaluated. Lastly, the spherical particle structures were analyzed using Computational Fluid Dynamics to study the interstitial flow behavior among the spherical particle beds.

DEDICATION

To my mother.

ACKNOWLEDGMENTS

Firstly, I would like to express my gratitude towards my adviser Dr. Benjamin Wilhite. Back in 2012, when I stepped into his office the dissertation idea was pitched to me in its nascent stage. In retrospection, the dissertation would not have been completed if not for his keen insights, constant support and motivation. He has always gone the extra mile to provide me the relevant resources to complete this work and has always been patient with me. Apart from our technical discussions, our journey to Longview site of Eastman created many memories which I will remember fondly.

I would like to thank my committee Prof. Holtzapple, Prof. North and Prof. Ugaz for providing their time to serve on my committee. Their key ideas during my prelim discussion have significantly benefited me and have improved my dissertation. I will fondly remember Prof. Holtzapple's anecdote of "Engineers have to always sell!" and Prof. North's visual demonstration of oscillating kinetics experiments. I would like to thank Prof. Arul Jayaraman who as graduate student adviser helped me with adviser selection and has been a fellow BITSIAN whom I could always look upto.

This project would not have seen the light of the day without the help of Eastman Chemical Company. In particular, Dr. Xianchun Wu, Dr. Ken Hampton and David Slivensky have provided strong technical feedback and ample opportunity to interact with Eastman Chemical Company and for hosting us on their plant site.

I am very grateful to Wilhite research group who were a constant source of support throughout my dissertation. Dr. Holly Butcher and Dr. Xiaohong Cui were always down for technical and personal discussions with whom I have spent some memorable times. I had a great time working with Puneet Kawatra and Rowan Appleman along with whom I could carry out experimental investigations for two phase flows which greatly enhanced my research work. Dr. Bhanu, Dr. Haomio, Dr. Elva and Dr. Daejin greatly helped me with professional discussions. The latest additions to the group Sunjeev and Naveen supported me during the last stage of my dissertation and I wish them good luck!

This work drew ideas from many interdisciplinary areas and executing them would not have been possible without the help of HPRC TAMU who were always helpful in providing me with suggestions and comments. Particularly, Amruth Kumar Juturu and Jian Tao provided key insights while developing numerical models and codes. Siva Praneeth provided key insights in developing CAD models and Tejasvi Khambampati, Manoj Myneni and Jay Pandian provided help with fluid dynamics analysis.

Towanna Arnold and Ashley Stokes have helped me with administrative work and ensured all documents were submitted in a timely manner. Jeff Polasek and Joel James have provided great support with computer infrastructure. Conversations with Doug White had provided me great information about lab practices and safety.

I like to thank my roommates Dr. Vamseedhar Reddy, Tejasvi Khamabampati for their company, Dr. Nirup and Dr. Susmita for their company during department lunch, Kashyap and Srinivas for their warm welcome in the initial days of graduate school. I am indebted to Dr. Akshay, Aditya, Dr. Shareq who provided support during tough times. This list is by no means a complete one and I heartfully thank everyone who has been a part of this journey.

Lastly, I cannot thank my family enough for their support and patience throughout this journey. They have shared my joy and troubles in equal parts and without them this work would not have been possible.

CONTRIBUTORS AND FUNDING SOURCES

Contributors

This work was supported by dissertation committee consisting of Dr. Benjamin Wilhite of the Department of Chemical Engineering.

All other work conducted for the dissertation was completed by the student independently.

Funding Sources

This work was sponsored by The Eastman Chemical Company, Longview, TX, USA through project number $C4690$. Additional financial support was provided by the Artie McFerrin Department of Chemical Engineering, Dwight Look College of Engineering.

Graduate study was supported by Graduate Teaching Fellowship from College of Engineering, Texas A&M University.

NOMENCLATURE

List of Symbols

B Bed property

CFD Computational Fluid Dynamics

D Diameter, m

DEM Discrete Element Method

E Young's Modulus, Pa

F Force, N

G Shear Modulus, Pa

H Enthalpy, J/kg

I Moment of Inertia, kg $\cdot$ m^2

K Stiffness coefficient, N/m

N Dampening coefficient, N·s/m

R Particle Radius, m

Re Reynolds Number

S Source term, J/m^3

T Temperature, K

e Coefficient of restitution

g Gravity, m/s^2

h Bed Height, m

m Particle mass, kg

p Pressure, Pa

$s(r)$ Arc length intersecting sphere, m

t Time, s

u Velocity, m/s

v Linear velocity, m/s

v' Fluctuating component, m/s

x Distance from wall to center of reactor, m

y Linear displacement, m

Greek Letters

α Coefficient of friction

χ Dimension

ϵ Voidage

$\epsilon(r, h)$ Axially averaged radial voidage

Γ Torque, N · m

κ Skewness

μ Dynamic viscosity, Pa·s

μ Mean

μ_t Turbulent Viscosity, Pa · s

ν Poisson's ratio, Pa

ω Angular velocity, rad/s

ρ Density, kg/m^3

σ Standard deviation

τ Stress tensor, Pa

θ Angular displacement, rad

$\vec{\omega}$ Angular velocity, rad/s

Subscripts

b Bulk, Body

eq Equivalent property of bodies

i Phase, Direction

n Normal direction

P Particle

r Radial

s Surface

$solid$ Solid property

t Tangential direction

TABLE OF CONTENTS

Page

LIST OF FIGURES

FIGURE Page

LIST OF TABLES

TABLE Page

1. INTRODUCTION

1.1 Multi-Phase Reactors

Multi-phase flows involving fluid-fluid and fluid-solid contact are commonly found in the chemical industry, facilitating many important chemical operations including absorption, adsorption distillation and catalytic reactions [1, 2, 3, 4]. The primary goal of devices in which these flows are housed is to enhance the contact area, resulting in increased mass and heat transport, and reaction rates [5, 6, 7]. Heterogeneous chemical reactions that rely on all the three mentioned phenomena are the workhorse of the chemical industry [8]. A wide range of gas-liquid-solid contactors have been devised with relative movement of phases to accomplish both heterogeneous and homogeneous reactions [9, 10]. The number of fluid phases, flow configurations and solid phase properties can be altered to meet desired needs. Figure 1.1 shows different multiphase reactor configurations where either the solid and/or fluid phase are in motion. In the Slurry reactor, the gas and liquid are fed into a slurry comprising of catalyst particles where the reaction occurs. In the Carberry reactor, the solid particles are fixed in a stationary basket around which continuous fluid flow occurs. In the case of Fluidized beds, the solid particles are suspended in a fluidized state by the fluid flowing within the interstitial volume. In the Moving Bed Reactor, the solid and the fluid phase undergo simultaneous motion with spent catalyst cycling through regenerator before re-entering the reactor, while the fluid phase is allowed to exit the reactor. Lastly, the Fixed Beds comprise of a stationary solid bed over which multiple fluid phases flow in either counter or co-current directions.

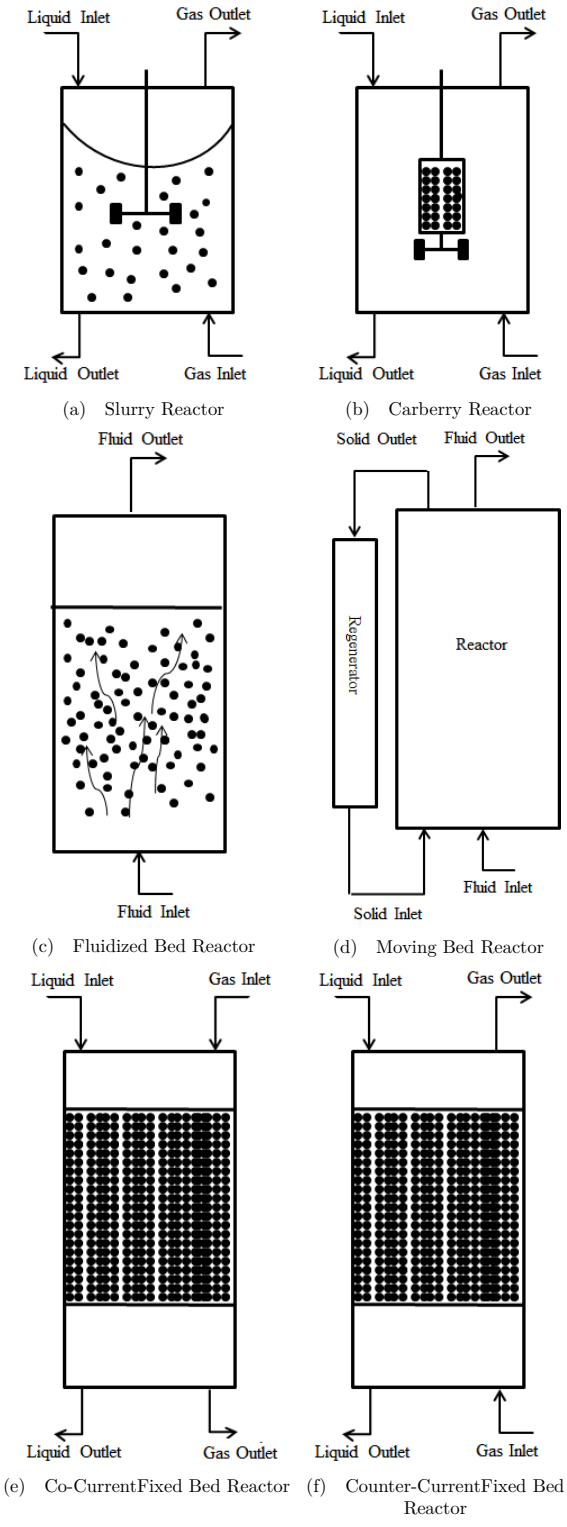

Figure 1.1: Multiphase reactors used in the chemical industry

Despite development of several techniques and devices for housing multiphase phenomena, fixed-beds have been the most commonly used in the industry. Fixed-Beds are usually preferred as they result in minimum damage to the solid entities, which often contain expensive catalysts and absorbents/adsorbents. The solid bed comprising of particles of various shapes (spheres, cylinders, trilobes etc) serves multiple purposes by providing contacting surfaces for different fluids and also housing catalyst particles that play a strong role in heterogeneous reactions [6, 11]. The stationary nature of the solid bed results in housing single or multiple fluid phases (trickle-bed reactors) [5] and different flow patterns (upflow,downflow etc) [4] as well. Fixed beds have also been used to house novel chemical processes like unmixed combustion [12], exo-endo coupling [13] and energy storage [14] and offer potential for process intensification. This flexibility in operation, ease of construction and absence of moving parts makes fixed beds a preferred choice for chemical processing.

Fixed beds have been of continuous interest to both academic and industrial researchers [15, 16, 17]. Studies have focused on packing, hydrodynamics and reaction studies associated with these fixed bed reactors. Initial studies focused on obtaining bulk parameters like overall voidage, pressure drop and liquid holdup [18, 19, 20]. These parameters coupled with relevant heuristic approaches dictated the guidelines for scale up and operations [10]. However, they do not provide insights into the local phenomena occurring inside the fixed-beds. With advancement in experimental visualization [21, 22] and modeling techniques [11, 23], better insights have been obtained into the working of fixed beds. Fixed Bed behavior is dictated by the solid particle activity, fluid flow distribution and the solid-fluid interactions. While the fluid phase serves the purpose of convective supply and removal of mass and heat, the solid particles house the expensive catalyst which results in the reactive conversion. Though in operation for more than half a century, the design and operational criteria for these fixed beds have been largely empirical. With increase in demand for more processed material, stringent energy and environmental constraints fixed beds are being re-investigated to enhance their performance. Although cheap and easily replaceable, optimizing fixed-bed performance can increase the efficiency of the process flow and aid in enhanced function-

ing of several other process units downstream of the fixed-bed. Importantly, malfunctioning fixed beds result in hot-spots, catalyst degradation, under-utilization of catalyst and excess energy usage leading to severe safety and economic consequences. In the current scenario, empiricism based approach for design of fixed-bed reactors has severe limitations and needs to be reconsidered. As a result, several researchers are employing advanced experimental and computational techniques to gain fundamental and mechanistic understanding of the fixed beds to develop better design, operational and control strategies. This requires development of mechanistic tools which can provide significant insights into operation and scale up of these units. To this end, important aspects of fixed bed operation are discussed below highlighting associated issues. Figure 1.2 provides a representation of the working of fixed beds, where the loading of particles dictates the solid phase structure. These solid phase structures impact the overall flow behavior, affecting the velocity and temperature fields. A summary of each component is provided in the following sections.

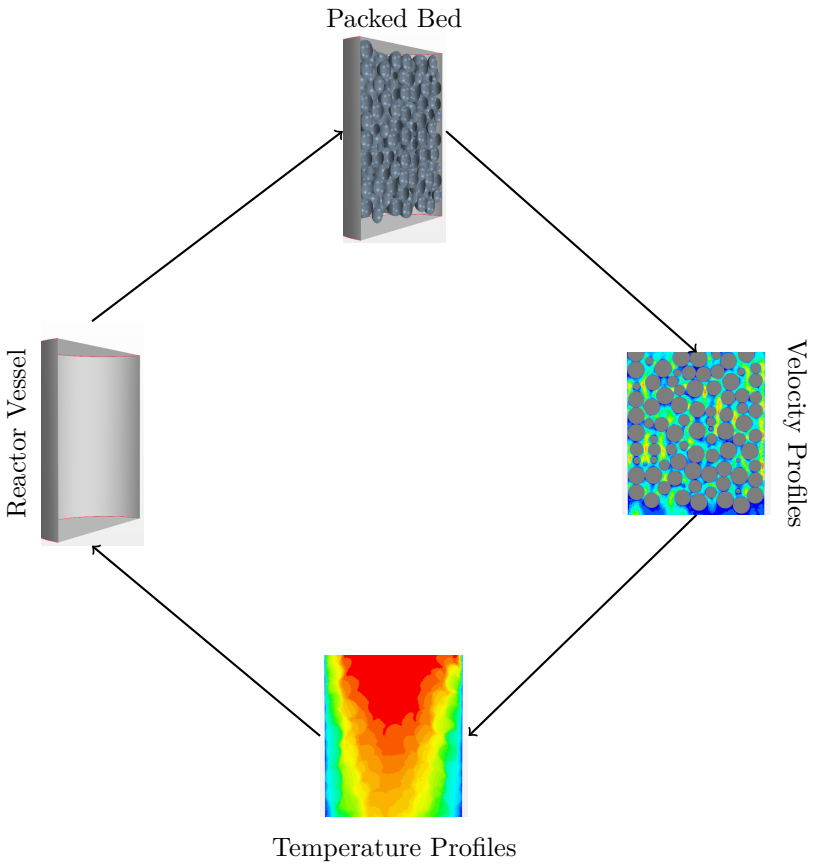

Figure 1.2: Schematic description of the work-flow

1.1.1 Solid Packing

The solid packing used in fixed beds significantly influences the mass transfer, fluid flow patterns and, in turn, the overall performance of fixed beds [24]. Different catalytic shapes as shown in Figure 1.3 have been used in fixed bed reactors. While the isotropic shape of spherical particles provides less resistance to the flow, the non-isotrpic shape of cylinder like particles provides more surface area for surface reactions. The choice of the catalyst shapes is dictated by factors including desired reaction rates, diffusion limitations and the overall pressure drop [25].

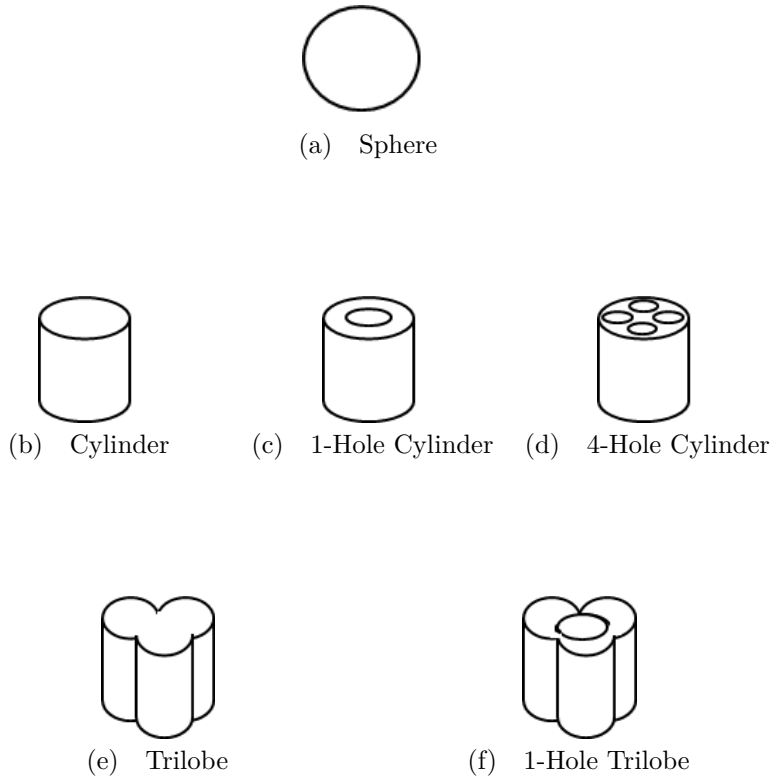

Figure 1.3: Catalyst shapes employed in the chemical industry

Initial studies accounted for the effect of solid packing through an averaged parameter bulk voidage ϵ_b, which represents the total empty space available for fluid flow [26, 27, 28]. This parameter provided an estimate of important properties like pressure drop and fluid hold-up through previously established empirical correlations [29, 30, 31]. With increase in bed diameter, continouos fluid flow and oscillations induced by vibration or tapping, bulk voidage is bound to reduce as a consequence of particle compaction [32]. However, the use of a global averaged parameter does not provide insights into the local heterogenities exhibited by the solid packing which affects the local transport and reaction rates [11, 22, 23, 33]. Solid structures comprised of spherical and non-spherical particles exhibit local variations in voidage. Figure 1.4 shows the radial variation in the voidage profiles along with the axial velocity fluctuations from the wall to the center of the bed as observed by Nguyen *et al.* [21] for the case of monodisperse sphere packed beds. The oscilla-

tions tend to create non-uniform velocity profiles. Variation of the voidage in both radial and axial direction has been of an important subject of study [34, 35, 36]. These variations arise from the local ordering of particles induced by wall [26] or any other perturbations induced during loading or bed operation [25]. These variations result in deviations from plug flow behavior within the fixed-bed. In case of cylindrical particles, orientational ordering of particles is also observed [37] and is known to create varied hydrodynamic [38, 39] and reaction behavior [40]. These effects need to be considered to gain a holistic understanding of fixed-bed operation.

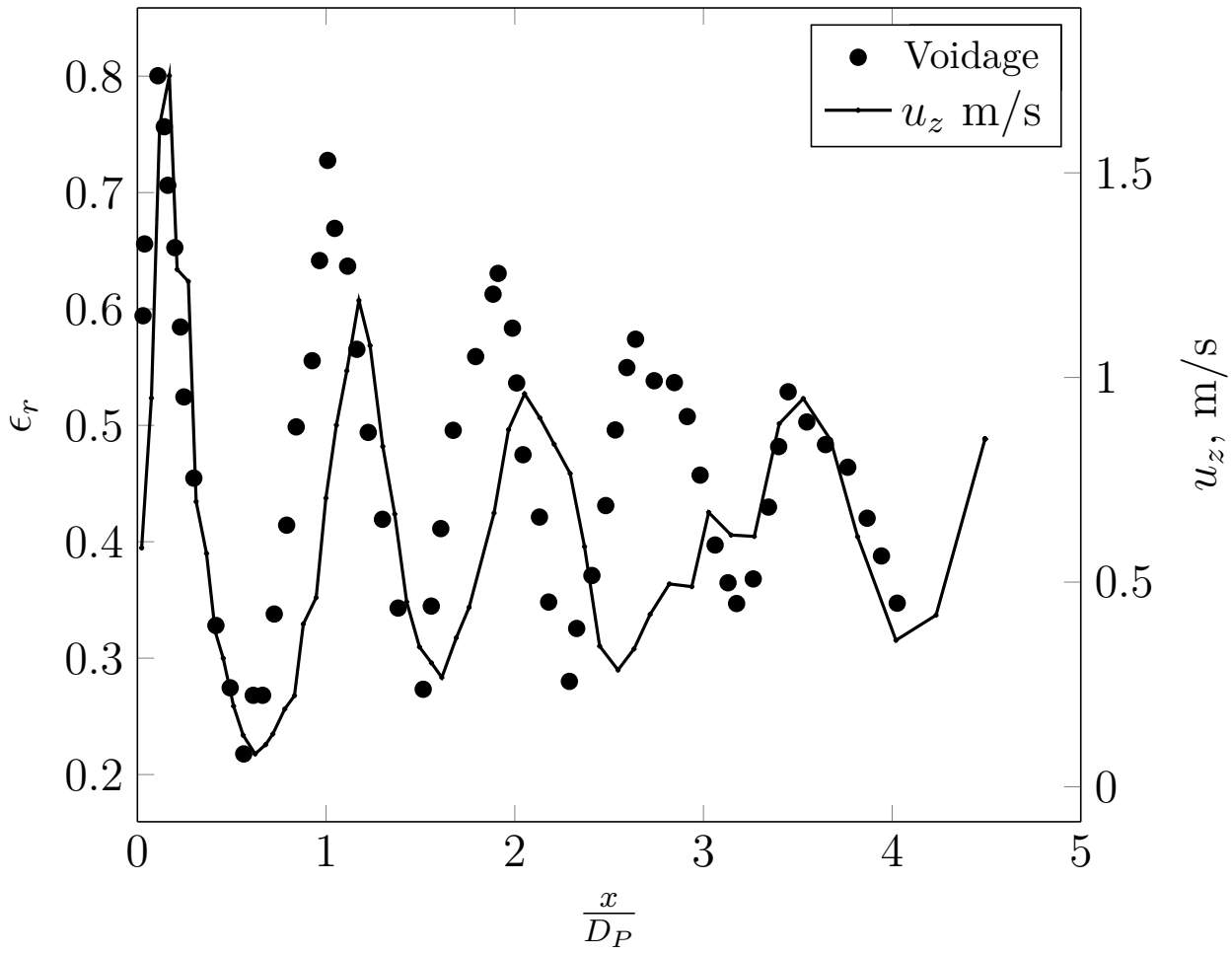

Figure 1.4: Radial Voidage profiles and corresponding axial velocity profiles [21]

With better computational and experimental techniques, significant insights into local structure of the bed packing have been gained [41, 42, 43, 44]. Spherical and non-spherical particle exhibit different characteristics in terms of bulk and local voidages, but more importantly the particle fluid interactions are different for each case. Recent advances in the experimental visualization techniques have provided insights into the local particle structure (position and orientation). Lately, loading/dumping methodologies used to load the solid particles into the bed have shown promising developments in terms of generating fixed beds with homogeneous voidages, less tortuous interstitial spaces and dense or loose packing of particles depending on the applications. Also, a wide range of operations like that of tapping and vibration are performed on the fixed bed to ensure any local instabilities are eliminated. This makes study of fixed bed structures with respect different particle shapes and different loading strategies pivotal to understanding and enhancing fixed bed behavior.

1.1.2 Fluid Flow

Fluid flow behavior is a key component of fixed-bed operation. A plethora of modeling and experimental studies exist which provide good understanding of the fixed-bed reactors [45,46,47]. Initial studies dealt with measuring global properties like overall pressure drop, fluid holdup and saturation which resulted in development of correlations widely used in scale up and operation of fixed beds [29, 48]. In case of two phase flows of gas-liquid, researchers have also identified different operation regimes based on measurements from the above mentioned parameters [49,50]. However, obtaining the flow and phase profiles from bed interior is still a limitation with very few studies able to address this issue [22,51,52,53]. Therefore the scale up and operation of these fixed beds is still largely driven by empirical correlations without accounting for the localised phenomena. Simultaneously, efforts have focused on developing both homogeneous and heterogeneous models for fluid flow prediction which are validated against the experimental studies [54, 55, 56]. The interstitial pores between the solid particles create tortuous flow paths for fluids and thereby result in complex flow patterns. In beds with tortuous flow paths high pressure drop, severe maldistribution and under utilization of catalyst bed is noticed with a decrease in reaction conversion.

In the case of gas-liquid flows, partial catalyst wetting is noticed which results in varying reaction rates across the bed structure. Lastly, with decreased fluid supply there is a reduction in effective mass and heat removal from the solid particles which results in hot spot formation which has severe safety and economic concerns. These observations imply that there are significant insights to be gained by studying the behavior of fluid flow among the solid packing.

1.2 Objectives

It is evident from the above discussion that overall operation of fixed beds is strongly dictated by the local packing structure and the ambient fluid and temperature fields. Current work aims at developing a work flow which can predict the behavior of a fixed bed reactor while accounting for the above aspects. The objectives of the current work are to study the impact of loading methods on the generation of packed bed structures comprised of both spherical and cylindrical particles. The generated fixed-bed structures are evaluated for the intrinsic properties like bulk voidage, radial voidage, orientation distribution and radial particle size distribution. The generated fixed bed structures of spherical particles are then used to study the flow behavior in a gas-solid downflow reactor and capture its impact on the hydrodynamics. The major tasks associated with the objectives are as follows:

- Develop a methodology to assemble a packing of spherical particles inclusive of the poldispersity of packing sample and loading methodology.
- Develop a methodology to assemble a packing of cylinders of different aspect ratios inclusive of loading methodology.
- Develop a computational fluid dynamics framework to study the impact of the particle scale geometry on the fluid flow behavior in a gas-solid downflow reactor.

1.3 Research Methodology

As a first step to achieve the objectives of the dissertation packing methodologies were developed. For this, two commonly used catalyst shapes have been selected: spheres and cylinders.

The packing structures were generated in cylindrical vessels using the Discrete Element Method (DEM). Three commonly used loading methodologies *Uniform, Sock and Wall* have been employed to load the solid particles. The generated output files comprised of the location and orientation of particles in the packed structure. This data was subjected to post-processing to obtain bed characteristics like bulk voidage, radial voidage and orientation details (in case of cylindrical particles). This study will quantify the effect of loading methods and particle poly-dispersity on the fixed-bed structure.

The solid geometry generated by above algorithms is used to obtain the volume domain through which the fluid flow occurs. This flow domain is suitable treated to obtain a mesh which is further used for finite volume analysis. The simulations are carried out using air as the fluid. Local velocity and pressure fields are obtained from these simulations. This study provides insights into the impact of loading methods and poly-dispersity on the fluid distribution in fixed beds. The Discrete Element Method and Computational Fluid Dynamics simulations were performed using the academic license of STAR-CCM+ 12.06.011 package [57].

1.4 Dissertation Outline

The above mentioned methodology is explained along with results in detail in the following chapters:**Chapter 2** provides a detailed literature review while explaining the novelty of current work taken up. **Chapter 3** provides description of the Discrete Element Methods and Computational Fluid Dynamics methods employed to study solid packing and fluid flow behavior. **Chapter 4** discusses the impact of different loading methods and polydispersity on the spherical packing structures. **Chapter 5** discusses the impact of loading methods on cylinder packed structures. **Chapter 6** provides a case study for the implementation of computational fluid dynamics to study flow fields in fixed beds of spherical particles. **Chapter 7** concludes the dissertation and provides recommendations for the future work.

2. LITERATURE REVIEW

2.1 Fixed Bed Reactors

Fixed-beds are characterized by fluid flow over stationary beds of solid particles retained by screens fixed at the bottom of the bed. Figure 2.1 represents a generic fixed-bed packed with mono-disperse spherical particles with downward interstitial fluid flow generated in STAR-CCM+ [57] (see chapter 3). The number of fluid phases, flow configurations and solid phase properties can be altered to meet desired needs.

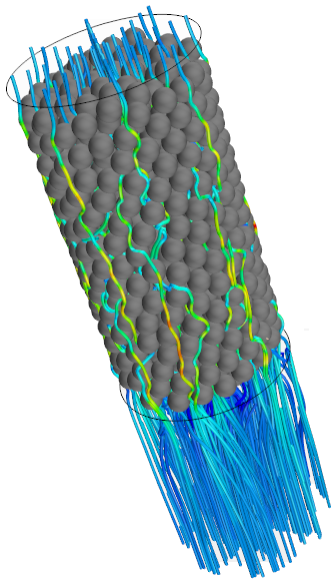

Figure 2.1: Schematic representation of a down flow fixed bed reactor

Initial studies on fixed-bed studies focused on quantifying the overall properties like pressure-drop [29, 30, 58], adiabatic temperature rise [59, 60], heat and mass transfer rates [61, 62], reaction rates [63, 64] and phase hold-up [15, 39, 50]. Studies have been performed to optimize the bed behavior by monitoring the above mentioned parameters as well [65, 66, 67]. Based on these observations, several mathematical models have been proposed to study the fixed-bed behavior.

Homogeneous and pseuod-homogeneous models treat the entire bed as as single interpentrable continua have been employed to model fixed beds [68, 69, 70]. Along with the classical reaction engineering models, these models have been effectively applied to predict reaction rates, adiabatic temperature rise and for multiplicity analysis in fixed-beds [71, 72, 73]. A common theme among the above models is the simplistic treatment of the fluid flow behavior and the fluid-solid interactions. A wide range of intrusive [42, 74, 75] and non-intrusive techniques [22, 33, 34, 44, 46] have been developed over the past few years which provide ample evidence regarding the heterogeneity in the local flow fields and the solid structure. Numerous non-intrusive techniqu1es have studied the variation of the local flow fields and showed that oscillatory velocity fields are related to the local voidage structure [21, 76]. These flow fields significantly impact the radial and axial thermal conductivity as evidenced by many researchers [67, 77]. These variations arise from the different flow, thermal and mass concentrations in the ambiance of the catalyst particle leading to varied reaction rates across the bed [78, 79, 80].

The classical homogeneous models do not account for the above mention variations and hence there is an increase in the number of studies dealing with heterogeneous models wherein individual phases are modeled inclusive of their heterogeneity. The fluid phase and solid phase are modeled separately and coupled through closure equations for heat and mass transfer. This heterogeneity impacts the overall bed behavior and has to be accounted in developing fixed bed models as depicted in Figure 2.2. The following sections explain relevant fluid and solid phase modeling studies performed to gain an understanding of fixed bed systems.

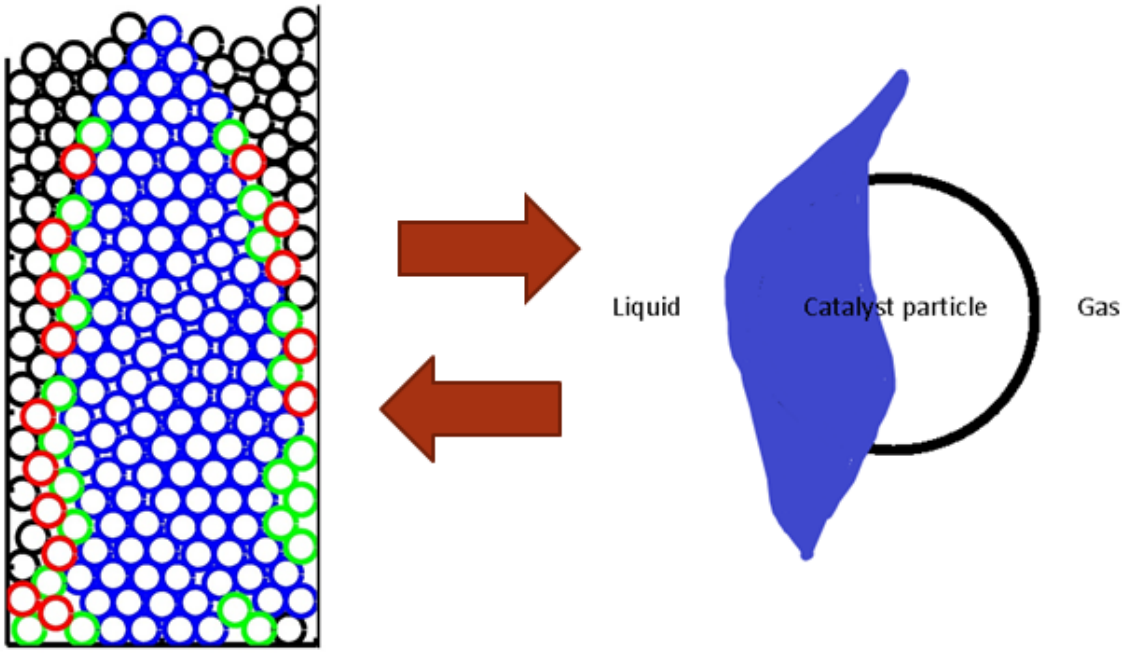

Figure 2.2: Schematic representing the interaction between fluid flow and solid catalyst

2.2 Fluid-Phase Modeling

Empirical models obtained from lab or pilot scale experiments served the community successfully regarding design and scale up of fixed beds. However, they suffer from universal agreement owing to their strong dependency on experimental conditions. Also, they provide rough estimate for averaged process parameters like pressure drop, fluid saturation and particle wetting but cannot predict the localized phenomenon occurring in the fixed beds. Hence, there is a strong drive in the research community to develop models with a mechanistic understanding of the flow physics. Several researchers have developed models for predictive analysis of fixed bed reactors involving single and multiple phases as described in Table 2.1.

Table 2.1: Mathematical models developed for analysis of fixed beds.

Models	Description	Application
Deans and Lapidus [68]	Discretized the bed into a two dimensional network of perfectly stirred tanks	Studied the radial mixing characteristics and extended the model to reactive systems
Ramachandran *et al.* [71]	Discretized the bed into a one dimensional network of connected perfectly stirred tanks	Applied the model to oxidation of formic acid and compared the results with a slurry and a trickle bed reactor
Holub *et al.* [48]	Developed a pore scale model by simplifying the pore scale voids as two parallel planes	Calculated two phase pressure drop and showed it to be a good match with experimental data
Attou *et al.* [81]	Developed a phenomenological model based from the principles of continuity and momentum balance	Predicted two phase pressure drop and compared with experimental correlations
Schnitzlein [82, 83]	Modeled fixed beds as an interconnected network of stirred tanks and plug flow reactors depending on the porous network of solid phase	Modeled single phase reactors to predict conversion and two phase reactors to predict liquid distribution
Funk *et al.* [84]	Generated a two dimensional random packing of fixed beds and employed a liquid distribution model to predict	Studied liquid distribution and reaction rates using multiple distribution schemes
Khadilkar *et al.* [85]	Developed a one dimensional unsteady state model comprising of particle scale and bed scale models	Studied the effect of periodic variation in fluid supply to reactor and found reactor enhancement with such modulations
Jiang *et al.* [86]	Developed a model combining the mixed cell approach and computational fluid dynamics	Compared the model predictions for local velocities and species conversion with experimental predictions
Dixon *et al.* [11]	Developed a full fledged 3D CFD models to study bed scale and particle behavior. Subsequently employed micro-kinetic models to predict reaction behavior inclusive of the random nature of bed packing.	Studied steam methane reforming and compared the local velocity, temperature and species concentrations with experimental predictions and found a good match.
Du Wei *et al.* [87]	Generated a network of uniformly spaced spherical a particles and employed CFD to study local liquid flow characteristics	Studied the impact of thermophysical properties on liquid distribution in 2 phase flows.

Solving the mechanistic models is computationally expensive and requires knowledge of particle scale geometry. Fortunately, better computational infrastructure have made mechanistic models a reliable approach for studying fluid flow in fixed beds. Computational fluid dynamics(CFD) has emerged as a reliable tool for analysis of fixed beds. With advancement in computational capacities it has become possible to resolve flow fields at low time and length scales [88]. The CFD models can be broadly classified into two sets: porous media (lumped or mixture models) approach [23, 89] or discrete phase approach [55, 90]. In lumped models the entire bed is assumed to behave like a homogeneous mixtures and flow fields are solved by using average bed properties. Momentum and heat balance equations are solved by using phase averaged thermo-physical properties. The solid phase effects are considered by using bulk and radial voidage profiles available in literature [91, 92]. Though these studies provide good insights into overall bed behavior and hydrodynamics, local interactions are not taken into consideration necessary to account for local particle effects.

In discrete models [93] each phase is treated like a separate entity along with accurate representation of the soli geometry and the phases are coupled through closure equations [48, 81]. Through representation of individual phases in lieu of averaged phase parameters, insights into local phase interactions can be obtained. Volume of fluid (VOF) approach has also been used to study two phase flows where the actual interface between the fluids can be reconstructed [42, 94]. Discrete models provide a reliable tool to study the effect of phase heterogeneity on the overall bed behavior. These models have the capability to account for the variations in the solid phase geometry to rigorously model the axial and radial variations in bed voidage along with the particle shape effect.

In this context, 3-D simulation of fixed bed reactors resolved at particle scale has emerged as a potential tool for fixed bed analysis [11, 95]. These models do not make any ideal assumptions of different phases involved and hence provide a rigorous analysis of fixed bed behavior. As the fundamental equations to be solved remain same compared to lumped models, a major challenge with discrete models is realization of actual geometry and overcoming meshing difficulties [95,96].

The Discrete models, commonly known as Particle-Resolved models are effectively applied for fixed-bed analysis. Dixon and Niejmeisland [93] provide an excellent review of the single phase flows in packed beds. Efforts have been focused on gaining understanding of localized flow phenomena and associated heat and mass transfer effects [42, 88]. With better computing power, along with hydrodynamics and energy distribution, chemical species balance through reactions also has been performed by researchers [97]. Recently, in order to be consistent with the length and time scales involved with CFD simulations, reduced micro-kinetic models have been included in the simulations [90,98,99]. However, efficient incorporation of these kinetic models is still a challenge for less complex CFD simulations and efforts are being directed to address this issue [100, 101]. Initially, researchers studied fluid flow among manually arranged set of small number of spheres to study momentum and heat transfer effects in fixed beds [93, 102]. Though not representative of the actual fixed bed scenarios, these studies are quite pivotal in validating the CFD simulations with experiments and developing meshing strategies. With access to rapid fixed-bed generation tools described in Section 2.3, researchers began to investigate 3D simulations of fixed beds with representative geometries. This has also allowed researchers to study other complex particle shapes used in industry [88,103,104]. It can be concluded that CFD provides a strong alternative for fixed bed analysis and heterogeneity introduced by solid phase can be accounted for through this method. In the following sections, solid phase heterogeneity and methods to model and capture them will be discussed in detail.

2.3 Solid-Phase Modeling

Solid phase morphology strongly impacts the flow phenomena and catalytic reaction occuring within the fixed-beds. Particle shape and size distribution have strong impact on the fluid behavior in terms of flow uniformity, pressure drop and thermal conductivity [105]. This impact also translates to the relevant transport phenomena at particle level affecting the mass and the thermal exchange between the fluid and solid phases [40, 106]. The loading practices employed to pack these fixed bed reactors has received significant attention and has been studied to increase catalyst loading density and minimize pressure drop [25, 107]. Though initial studies accounted for aver-

aged solid phase properties in terms of bulk and radial voidage, the spatial distribution of the solid phase is not taken into consideration. Particularly, the non-spherical particle studies have revealed interesting insights into the orientation distribution of the particles and their subsequent impact on the bed behavior [37]. This has motivated researchers to capture the local solid phase structure in fixed-beds [21, 33, 44]. However, this methodology relies on expensive measurement techniques and high resolution is required to capture the structure adequately. Alternatively, generation of synthetic beds using various mathematical models has been successfully employed. Particularly, the Discrete Element Method with classical Newtonian dynamics has demonstrated to be a potential tool for study of solid phase in fixed beds [90, 104]. The following sections describe experimental and modeling efforts to study spherical and cylinder packed structures and the impact of loading methods on packing structures

2.3.1 Sphere Packing

While a wide range of particle shapes have been employed for packing fixed-beds, spherical particles remain a preferred choice, owing to ease of manufacture, isotropic shape devoid of orientation effects [38] and availability of a wide range of impregnation techniques for patterning of catalyst [108].

The global and local properties of fixed-bed structures have been extensively investigated [26, 27, 28, 43, 44, 109, 110, 111, 112, 113] as summarized in Table 2.2. A wide range of structures exhibiting different global voidage are possible, depending on the packing method employed [114, 115]. Correlations have been developed by researchers to predict global voidage as a function of bed and particle properties [26, 27, 28, 116]. It has been consistently observed that bed voidage tends to an asymptotic value of 0.36-0.40 [26, 28] with an increase in bed diameter as any constraining effect of the bed wall diminishes. Both invasive and non-invasive techniques have provided significant insights into the local structure of particle packing, specifically the wall-induced oscillations in radial voidage profiles [109, 111]. Suzuki *et al.* [44] used X-ray micro-tomography on cylindrical beds packed with spherical particles to observe a damping oscillatory behavior in radial porosity consistent over a range of different particle and bed sizes. Based on

Table 2.2: Experimental studies on sphere packed structures

Author, Year	Experiment	Remarks
Roblee *et al.* [109]	Solidification of molten wax	Studied impact of wall on radial porosity
Benenati and Broslow [110]	Solidification using epoxy resin	Corroborated the work of Roblee,1958
Thadani and Peebles [111]	Radiography	Noticed the cyclic tendency in radial voidage
Dixon [26]	Weight measurement	Obtained correlations for overall voidage
Benyahia [27]	Image analysis	Studied radial voidage behavior for different catalyst shapes
Foumney and O'Neill [28]	Water displacement method	Improved overall voidage correlations by including shape factors
Ismail *et al.* [112]	Water displacement	Studied global bed properties of ternary mixtures
Ismail *et al.* [113]	Image analysis	Developed radial voidage correlations for ternary mixtures
deKlerk [43]	Weight measurement	Developed correlations for radial voidage in sphere packed beds to capture oscillations
Suzuki *et al.* [44]	X-Ray Radiography	Measured radial porosity and proposed a damped oscillation correlation.

these experimental observations, several correlations have been developed to predict these wall induced oscillations [43, 44], which tend to disrupt uniform fluid flow and impact the heat and mass transfer in the wall region [117] especially in the case of beds with $D_B/D_p < 20$ where D_B is the bed diameter and D_p is particle diameter.

Though experimental studies provide good insights into bed structure, replication of this data for further fluid flow analysis is a tedious task [118, 119]. As an alternative several modeling strategies with varying levels of complexities have emerged to provide insights into the complex fixed-bed structures. Geometrical modeling employs drop and roll calculations to add particles in a sequential fashion wherein each particle is placed in the most mechanically stable config-

uration [120, 121]. Nandakumar *et al.* [122] used an optimization algorithm to pack particles by placing them in the lowest stable position possible without any overlap between particles. Abreu *et al.* [123] used Monte-Carlo[MC] simulations to subject particles to a sequence of MC motions so that they ultimately converge to a final pseudo-thermodynamic equilibrium which is equivalent to a fixed-bed structure. These models are categorized as hard sphere models wherein particles cannot overlap. Salvat *et al.* [124] developed a soft sphere model which generated packed bed structures by minimizing the overlap between particles from an initially dense overlapping packing configuration. Though computationally easy to execute, these models are not dynamic in nature and do not consider the physical phenomena related to the packing process (eg. momentum transfer upon wall-particle and particle-particle collision). Likewise, they do not account for the filling method employed and often result in generating either overly loose or densely packed beds. In contrast, Caulkin *et al.* [125] developed a packing algorithm which relied on digitization of the vessel and packing particles such that each were represented by a collection of pixels/voxels. The movement of pixels was governed by principle that a pixel/voxel cannot be occupied by more than one particle and could be easily extended to particles with complex shapes. The model was later modified to include realistic forces associated with particle-particle collision during the bed loading [33]. Strategies implementing simplified mechanics, specifically soft-sphere approaches combined with a 'frozen-bed' assumption wherein each particle settles in the absence of friction and subsequently is frozen i.e. experiences infinite friction have proven to be effective in simulating non-spherical structures as well [126, 127]. However, these studies remain limited to mono-disperse particle samples with no variation in loading strategies employed for packing.

With the advent of high performance computing, Discrete Element Modeling [DEM] [128, 129, 130, 131] has become a preferred tool for generating packed bed structures. Similar to molecular modeling, interaction forces between particles are calculated by employing the principles of Newton's Laws and time integration. This process is repeated over several discrete time steps to capture the behavior of involved solid phases. This formulation provides the opportunity to study various interactions among the particles as well as surrounding fluid. Different time schemes have

been implemented for this integration and their pros and cons have been studied with respect to computational speed and stability of the solution [132, 133].

DEM methods have been employed to study the structure of fixed beds comprised of spherical and non-spherical particles. Theuerkauf *et al.* [134] have used this model to study voidage variation in low D_B/D_p beds. Ookawara [135] generated beds comprised of spherical particles for fluid flow analysis and commented on the impact of modifying friction parameter to generate realistic bed structures. Zobel *et al.* [117] studied the impact of wall structure on voidage distribution for monodisperse spheres using DEM methods. Schulze *et al.* [136] have used this methodology to pack $\sim 10^5$ particles to study the impact of polydispersity on porosity distribution in packed beds and subsequent flow behavior. DEM simulations provide accurate packing structures as they account for a wide range of forces acting among the particles and consider force and moment modeling.

2.3.2 Cylinder Packing

Cylindrical particles are of significant importance as they provide higher surface area compared to their spherical counterparts at the cost of increased pressure drop [25]. Also majority of industrial process employ cylindrical particles or suitable variants of them which makes study of these particles relevant [40]. In the current study, impact of cylindrical particles on fixed-bed structures is elucidated.

Significant amount of studies have focused on elucidating the properties of cylindrical particle structures as summarized in Table 2.3. Initial studies focused on obtaining the global and radial voidage of these structures. Roblee *et al.* [109] used wax impregnation techniques to obtain the radial voidage patterns in beds packed with equilateral cylinders. They observed dampened oscillatory patterns in the vicinity of the wall and an overall voidage of about 0.25. Stephenson and Stewart [137] perfromed flow experiments in beds packed with quartz cylindrical particles and used water displacement method to obtain voidages of magnitude $0.354 - 0.361$. Dixon [26] used water displacement techniques to measure voidage exhibited by equilateral cylinders and observed an asymptotic bed voidage of 0.36 with increase in bed diameter. Benyahia [27] employed a image

Table 2.3: Experimental studies on cylinder packed structures

Author,Year	Experiment	Measurement technique	Remarks
Dixon,1988 [26]	Packed tubular vessels with equilateral cylinders	Water displacement	Developed correlations to predict bulk voidage as function of D_B/D_p
Benyahia and O'Neil,2005 [28]	Packed tubular reactors with holed cylinders	Water displacement	Developed correlations to predict bulk voidage as function of diameter
Zhang *et al.* 2006, [37]	Packed tubes with extrudate particles	X Ray microtomography	Measured the orientation effects within the bed
Mathias and Muldowney 2000, [107]	Packed reactors with a orifice device from different heights	Measured porosity defects through temperature response methods	Observed that loading methods determine the homogeneity in packing structures
Montillet and Le Coq, 2001, [138]	Consolidated packed beds of non-isotropic particles with resin	Image analysis	Elucidated the effects of wall and floor on packing configuration
Nguyen *et al.*, 2005, [21]	Beds prepared with trilobes and cylinders	Image analysis, MRI and water displacement	Enhanced radial porosity correlations compared to water substitution method

analysis technique to obtain the bed characteristics of both equilateral and non-equilateral cylinders and concluded that non-equilateral cylinders display a dampened oscillatory profile in radila voidage when compared to their equilateral counterparts. Foumeny and Roshani [116] developed correlations for different sizes of equilateral cylinders with water displacement technique and observed a minimum voidage of 0.30. Montillet and Le Coq, [138] used image analysis to observe bed characteristics of long cylinders and flat plates. In addition to the characteristic dampened oscillations in radial voidage, they also observed that oscillations were random in nature at different axial positions along the bed.

Enhanced measurement techniques have provided better insights into the structures of cylindrical packing. Zhang *et al.* [37] used X-ray micro-tomography to study the packing patterns

exhibited by equilateral cylinders. They observed that equilateral particles exhibit a wide range of bed voidages and orientation patterns when subjected to different packing methods. Nguyen *et al.* [21] employed magnetic resonance imaging to study local voidage patterns in beds packed with different particle shapes and observed dampening oscillatory profile from wall. Caulkin *et al.* [33] performed X-ray computerized tomography to study packed structures of different particle shapes. They reported the orientation distribution exhibited by cylindrical particles as well. Sharma *et al.* [41] utilized water substitution and Magnetic Resonance Imaging(MRI) to measure bed voidage for different particle shapes. Cylinder packing demonstrated voidages in the range of 0.4 and voidage dropped to $0.28 - 0.31$ on being subjected to tapping. It can be concluded that cylindrical particles exhibit global voidages lower compared to their spherical counterparts. Structures also exhibit oscillatory patterns in the radial voidage profiles which extend few particle diameters into bed.

Synthetic packed beds generated through several modeling techniques provide a strong alternative to gain significant insights into fixed-bed structures. Simulated beds packed with spherical particles have been studied significantly [124,134,136]. These methods rely on evaluating the contact dynamics and subsequent motion of the particles. Wide range of schemes have been employed to perform force and moment balances to track motion of particles [120, 122, 123]. Among these, Discrete Element Method (DEM) has emerged to be a reliable method to study granular flows and bed packing [130, 134]. However, the aspect of non-trivial contact detection for cylindrical particles made the studies limited to spherical particles with few exceptions as mentioned in Table 2.4. Different shape representation techniques have been employed to address the problem of contact detection amongst cylindrical particles [131]. Discrete shape representation has been employed by Marek [126] to study packing configurations in equilateral cylinders. The algorithm was further extended to study orientation distribution in beds packed with cylindrical particles [139]. Eppinger *et al.* [103] used glued sphere approach where cylinder shape is replicated by a number of lumped spheres to perform DEM simulations. Kodam *et al.* enlisted different contact scenarios and obtained geometrical criteria for contact detection to be used in DEM simulations [131]. Guo *et al.*

modified these geometrical schemes and developed a contact detection scheme relevant for high aspect ratio particles [140]. Caulkin *et al.* [33] employed a digitization scheme wherein the entire bed volume is digitized into pixels and contact detection is performed by checking if more than one particles are occupying the same pixel representative of particle-particle overlap. Boccardo *et al.* [141] employed a computer graphics code Blender employing Bullet physics library(BPL) to simulate packing of different particle shapes and obtained a good match with that of experimental works. Behnam and Dixon [142] further used this framework for fluid flow simulations in beds packed with complex shapes.

Table 2.4: Modeling studies on cylinder packed structures

Author,Year	Particles packed	Modeling technique	Remarks
Caulkin *et al.*,2009 [33]	Used complex cylinder shapes with holes	Used digitization and pixel tracking for packing particles	Predicted radial and bulk voidage values
Kodam *et al.*,2010 [131]	Packed right cylinders	Used geometric calculations for contact detection and used DEM to pack cylinders	Packed column with cylinder particles and obtained values close to experimental results
Marek,2013 [126]	Packed right cylinders	Used discrete shape representation to pack cylinder particles	Matched the experimental work of Zhang *et al.*, 2006 [37]
Niegodajew and Marek, 2016 [139]	Packed cylinders with different aspect ratios	Used method of Marek,2013, [126]	Analysed the orientation of particles near wall and bulk region

2.3.3 Loading Methods

Packing methods employed for assembling fixed-beds ultimately dictate unit efficiency [143]. The development of improved filling devices has enabled reduction in bed voidage or greater compaction of the bed in order to achieve high volume catalyst loading [25, 115]. Spatial arrangement of particles near the wall has also been explored to dampen the radial voidage oscillations and thus enhancing radial flow uniformity [117, 144]. Šmid *et al.* [145] observed that addition of particles uniformly across the bed generated uniform voidage compared to loading the particles in the center of the bed. They attribute this effect to the difference in particle interactions with the column wall for each method. Mathias *et al.* [107] varied the height of the loading device from the free catalyst surface, such that as drop height increased the radial spread of catalyst particles increased resulting in greater bed voidage uniformity. Using poly-disperse particle sets for loading beds has also been shown to dampen the wall induced oscillations in radial bed porosity compared to the mono-disperse set [112, 113]. Afandizadeh *et al.* [25] noted in the case of cylindrical particles, beds prepared by slow rates of particle addition showed lower voidage compared to faster rates of particle addition. Pottbäcker *et al.* [115] showed that addition of particles with different physical

properties and filling techniques altered the global voidage as well and demonstrated the need for global voidage correlations to be inclusive of loading method employed. Given their significant impact upon resulting bed structure there is a great value in developing computational tools capable of accurately and efficiently predicting local bed structure in fixed-beds inclusive of the above discussed variants.

Non-isotropic particle structures exhibit a wide range of packing structures depending on the methodology used to pack the beds. Wooten [146] studied the packing developed by sock and dense loading and commented on the differences observed in these structures. Smid *et al.* [145] used radiogauging method to study three different loading methods to pack beds with cylindrical particles and observed that uniform filling method("rainy filling") using a grid distributor generated a homogeneous distribution of catalyst. Bazmi et al [38, 39] performed sock and dense loading of trilobe particles and observed that dense loading provided a more compact and tortuous bed which resulted in increased pressure drop resulted in maldistribution of fluids. Dense loading comprised of sharp corners and resulted into higher pressure drop. Potbacker [115] also demonstrated loading methods to significantly effect the overall voidage in fixed-beds for spherical particles.

From the above discussion, it can be concluded that DEM is capable of studying fixed bed structures. In this study, DEM methods are employed to study the effect of loading methods, particle shape and particle sample polydispersity on the resulting fixed bed structures. The generated structures are evaluated for their geometric features. This analysis is performed on two commonly found particle shapes: spheres and cylinders.

The DEM structures generated are converted to CAD geometries. The interstitial flow domain is extracted and the impact of loading strategies, particle poly-dispersity is studied using CFD analysis.

3. MATHEMATICAL MODELS

This chapter describes the mathematical models employed in this study for the fixed-bed analysis: Discrete Element Method(DEM) and Computational Fluid Dynamics(CFD). In this chapter the mathematical formulation of both these techniques are described in detail. Discrete Element Method is employed to study the packed structures comprised of spherical and cylindrical particles. Later, spherical packed structures are used to study the interstitial fluid flow using computational fluid dynamics analysis. The chapter also describes the methods employed to transfer the geometric data obtained from DEM simulations to suitably modified CAD geometries capable of generating robust meshes for solving the conservation equations of fluid flow models.

3.1 Discrete Element Method

The Discrete Element Method has been successfully employed to study granular media. DEM method has been consistently used to generate stationary solid structures to study global and local properties of the medium [134]. DEM models have been employed to study granular flows in hopper and chute devices [147]. This methodology provides significant insights into modeling of physical and chemical processes [88, 148, 149]. DEM is a Lagrangian based framework to study granular media by modeling the particle level interactions. A rigorous review of different types of DEM has been provided by Dziugys and Peters [130]. In this study, DEM based on classical Newtonian dynamics was used for generating packed bed structures and is described in detail.

3.1.1 Mathematical Model

DEM solves the Newton's second law of motion over a discretized time step to evaluate the motion of particles. [88, 90, 134, 135, 136] . Both translational and rotational motion equations are solved to calculate the displacement the particle undergoes over a given time step by evaluating surface forces $\vec{F_s}$, body forces $\vec{F_b}$ and torque $\vec{\tau}$.

$$m_p \frac{d^2 \vec{y}_p}{dt^2} = \vec{F}_s + \vec{F}_b \tag{3.1}$$

$$I \frac{d^2 \vec{\theta}_p}{dt^2} = \vec{\Gamma} \tag{3.2}$$

Particle's linear velocity, momentum, angular velocity and angular momentum are updated at each time step δt by integrating the Newton's second law over the given time step. During this time step, the velocities and acceleration are considered to be constant.

$$\vec{v}_p = \frac{d\vec{y}_p}{dt} \tag{3.3}$$

$$\vec{\omega}_p = \frac{d\vec{\theta}_p}{dt} \tag{3.4}$$

Also, the collisions between particles are considered to be elastic in nature and are modeled using coefficient of restitution and Poisson's hypothesis [130]. All the collisions are considered to be instantaneous in nature and influence the motion of the particles. The particles are allowed to undergo partial overlap during the collision, and the overlap geometry dictates the contact forces that arise from the collisions. In addition, depending on the surface roughness, frictional forces modeled after coulomb's law are also included in the simulation. A wide range of contact force models have been studied and developed for DEM simulations [150].

3.1.2 Contact Detection

Contact detection is the most rigorous part of the DEM simulations. To determine the contact forces, overlap amongst the particles has to be determined. At the end of each time step, the geometric position and orientations of particles are calculated. Based on these, contact detection algorithms are applied to calculate the overlap distances. The overlap distances are used in the force modeling and moment modeling calculations. Contact detection being the most repetitive step of the DEM simulation has received lot of attention to minimize the computation time [140].

Broadly, the contact detection can be divided into coarse and fine levels. During coarse contact detection level, the neighborhood of the particles among which possible contact could occur is established. This is followed by a fine contact detection where pairwise examination of overlap is performed. Many strategies have been proposed to optimize this procedure [131].

Contact detection among spheres is trivial owing to their isotropic geometric shape. As shown in Figure 3.1, after the neighborhood of particles with possible contact is established, the fine contact detection is performed by calculating the distance between the geometric centers. In case, the distance between the centers is less than the sum of radii of the spheres, overlap exist. Similarly, if the distance between the wall and the center of the sphere is less than the radii, overlap with the wall exist. Lastly, if the distance between center of spheres and the floor of the reactor is less than the radii, the sphere has an overlap with the floor.

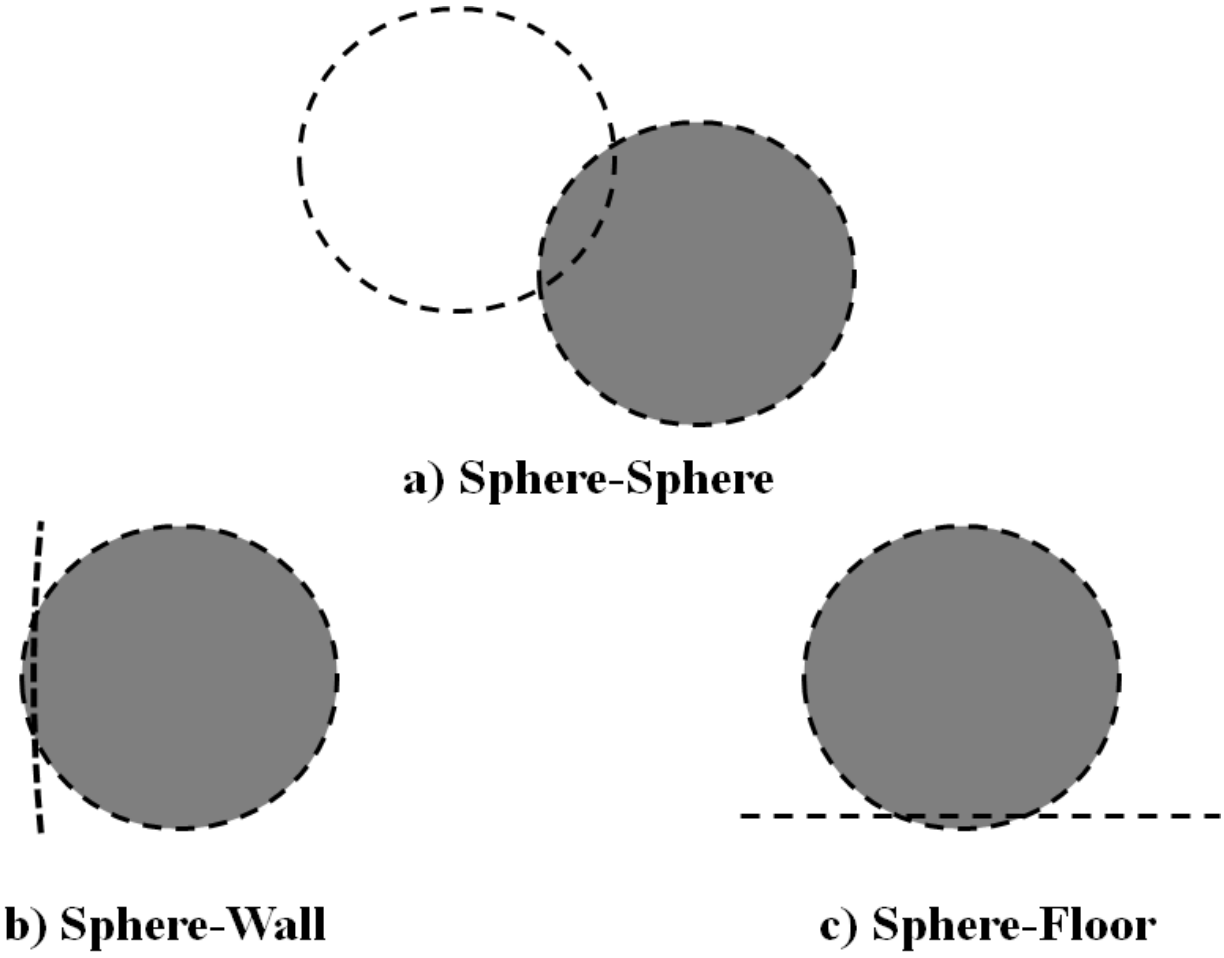

Figure 3.1: Schematic of overlap among spherical particles

However, the contact detection for the case of cylinders is a complex task and is not straightforward. The non-isotropic shape and multiple overlap configurations make contact detection amongst cylinders a non-trivial task. Several strategies have been proposed to perform contact detection among cylinders [105, 131]. The objective of these strategies is to reduce the geometrical complexity of contact detection for cylinders. Different shape representation techniques have been employed to this end to perform contact detection. Marek *et al.* [126] used discrete shape representation to represent a cylinder, wherein the surface of the cylinder was densely distributed with points. By calculating the relative position of these points with other cylinder, contact detec-

tion checks could be performed. The cylinder surface has to be densely distributed with points to ensure a good representation of the cylinder shape is obtained. Though discrete shape representation eliminates the geometrical complexity of the issue, it results in heavy computational cost and high memory allocation to achieve a desired resolution. Sphero-cylinder representation where the ends of the cylinders would be capped by hemi-spheres was also used to model contact detection among cylinders where the contact checks could be reduced to sphere-sphere,sphere-cylinder and cylinder-cylinder scenarios [123]. However, the methodology of glued spheres has been the most successful strategy applied so far to study cylindrical particles [103]. In this method, the cylinder is represented by a set of spheres lumped together to provide a cylinder shape representation. The number of spheres and their locations can be altered suitably to provide an accurate representation of the cylinder shape. The entire contact detection scheme is executed by checking intersection among spheres from different cylinders. These schemes generate the final cylinder position and can be subsequently used to represent cylinder shapes for CFD simulations. These schemes have also been employed to study granular media comprising other particle shapes as well [149]. However, the ability of these approaches to capture the sharp end effects of cylindrical particles is still debated and may result in overlaps that might not be otherwise present when studying cylindrical particles [105].

Kodam *et al.* [131] studied various overlap configurations among cylindrical particles and provided geometric rules to quantify the overlap among cylinders without any shape representation modifications. Figure 3.2 demonstrates the different contact scenarios that occur during cylinder particle simulations. A total of 9 distinct cases were identified and through a set of geometric rules, the overlap is quantified. After the overlap is obtained evaluating the contact force is performed using relevant models.

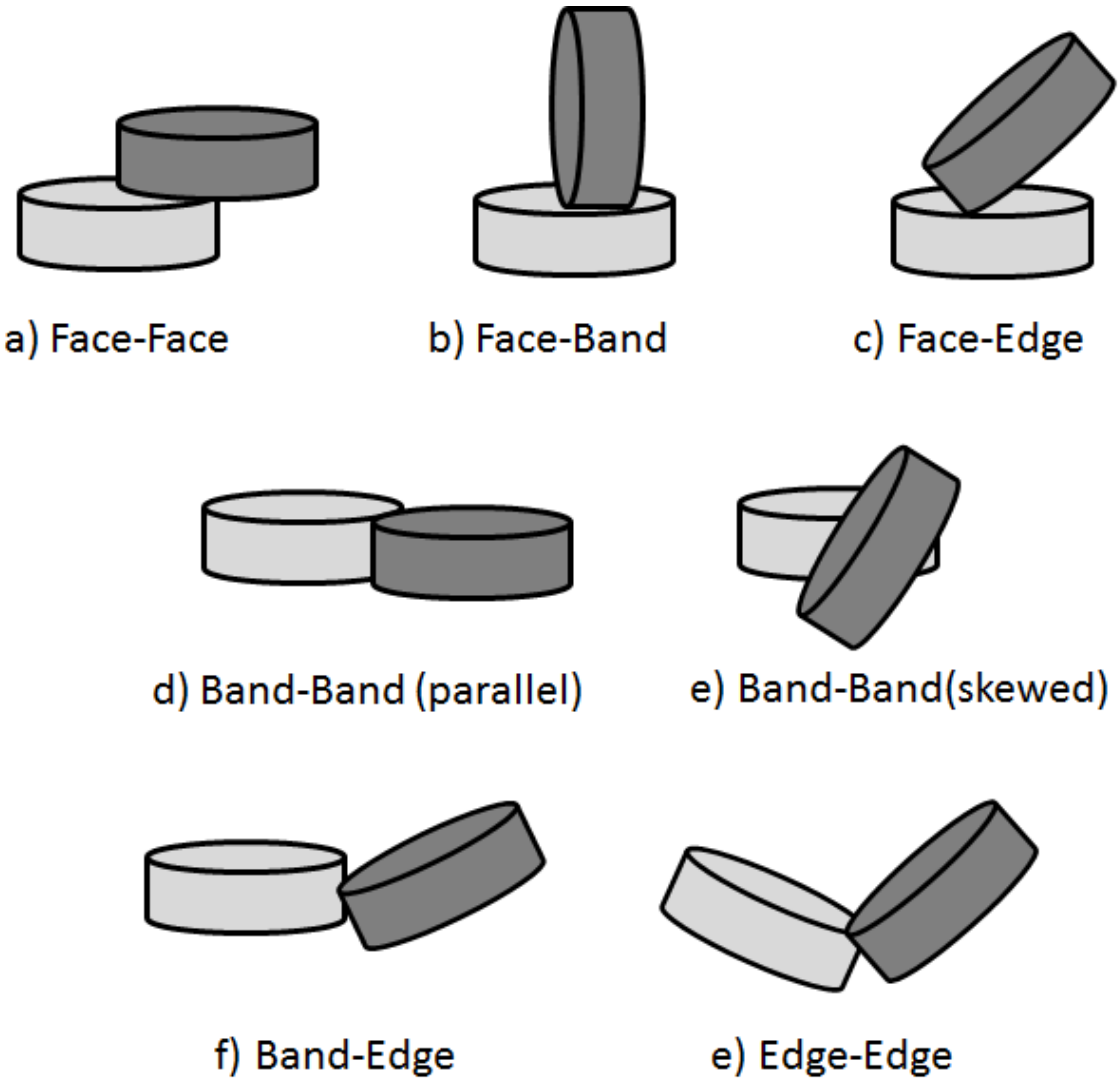

Figure 3.2: Schematic of overlap among cylindrical particles, modified from Kodam *et al.* [131]

Guo *et al.* [140] modified these rules and applied them to high aspect ratio cylinders. Recently, polyhedral meshing of cylinder particles to calculate overlap among the cylinder particles has been employed for packing studies [105, 141]. This modification provides accurate representation of cylinders resulting in better predictions for cylinder like structures.

In the current study, contact detection scheme for spherical particles was by geometric computation whereas for cylinder particles the methodology proposed by Kodam *et al.* [131] was used.

3.1.3 Force Modeling

Evaluation of contact forces during a collision is an important aspect of DEM simulations. The forces comprise of body forces like gravity and surface forces arising from contact between the particles. Among these, the calculation of contact forces has received significant attention as evidenced by the number of models that have been developed. The models either rely on empirical constants to extract the contact forces or employ constants derived from the physical properties of the solids involved. In this study, two different force models have been considered: Hertz-Mindilin Contact force model for spherical particles and Linear Spring contact model for the case of cylindrical particles. It has to be noted that the models applied in the study do not address the non-elastic deformations that might occur during the particle collisions and is major limitation of the above mentioned models [150]. Similarly, particle breakage during the practice of loading is not considered in this study.

3.1.3.1 Hertz-Mindilin Contact Model

Hertz-Mindilin Contact model is a hybrid combination of the Hertz theory for normal contact and Mindlin theory for spherical shapes [151]. The model has been commonly applied for granular media where elastic collisions are considered. The net contact force that arise when solids collide is a combination of normal and tangential forces at the contact as shown in Figure 3.3.

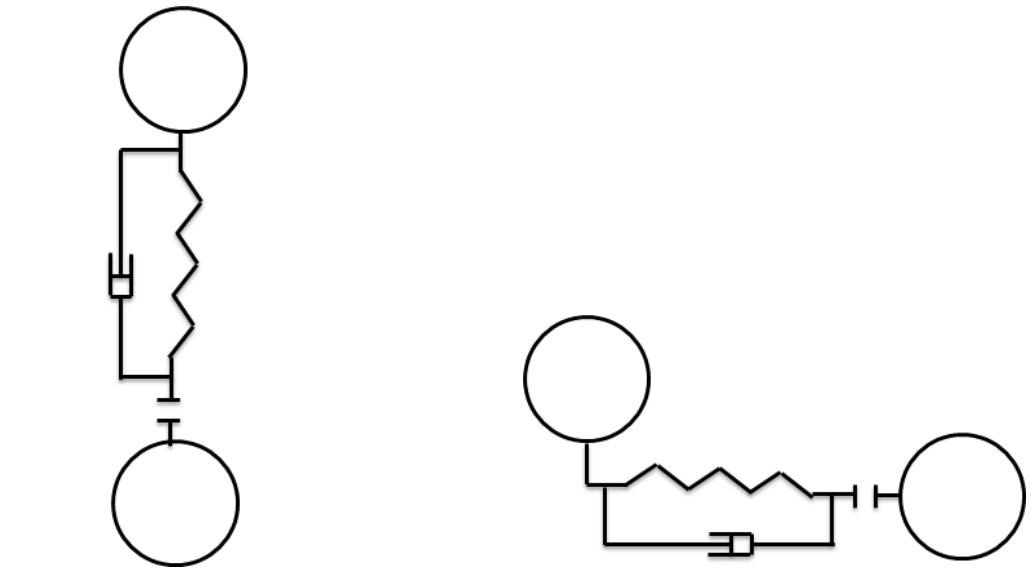

Figure 3.3: Schematic representation of a) Normal contact b) Tangential contact forces among particles

$$\vec{F}_{contact} = \vec{F}_n + \vec{F}_t \tag{3.5}$$

The normal contact force $\vec{F}_n$ is given by:

$$\vec{F}_n = -K_n d_n - N_n v_n \tag{3.6}$$

where K_n is the normal stiffness coefficient, N_n is the dampening coefficient, d_n is the normal overlap between the solids and v_n is the normal component of the velocity.

The tangential contact force $\vec{F}_t$ is given by:

$$\vec{F_t} = -K_t d_t - N_t v_t \tag{3.7}$$

where K_t is the normal stiffness coefficient, N_t is the dampening coefficient, d_t is the tangential overlap between the solids and v_t is the tangential component of the velocity. The tangential force is modified in case the magnitude of tangential force is less than frictional force.

$$\vec{F_t} = \frac{|K_n d_n| C_{fs} d_t}{|d_t|}, \qquad \textit{if} \quad |K_t d_t| < |K_n d_n| C_{fs} \tag{3.8}$$

The above mentioned stiffness coefficients are obtained from the physical properties of the materials involved through following equations:

$$K_n = \frac{4}{3} E_{eq} \sqrt{d_n R_{eq}} \tag{3.9}$$

$$N_n = \sqrt{5 K_n M_{eq}} N_{ndamp} \tag{3.10}$$

$$K_t = 8 G_{eq} \sqrt{d_t R_{eq}} \tag{3.11}$$

$$N_t = \sqrt{5 K_t M_{eq}} N_{ndamp} \tag{3.12}$$

The equivalent radius R_{eq} and equivalent mass are given by:

$$R_{eq} = \frac{1}{\frac{1}{R_A} + \frac{1}{R_B}} \tag{3.13}$$

$$M_{eq} = \frac{1}{\frac{1}{M_A} + \frac{1}{M_B}} \tag{3.14}$$

The damping coefficients are evaluated from the normal and tangential coefficients of restitution as follows:

$$N_{ndamp} = \frac{-ln(C_{nrest})}{\sqrt{\pi^2 + ln(C_{nrest})^2}} \tag{3.15}$$

$$N_{tdamp} = \frac{-ln(C_{trest})}{\sqrt{\pi^2 + ln(C_{trest})^2}} \tag{3.16}$$

The equivalent Young's modulus E_{eq} and equivalent shear modulus G_{eq} are given by:

$$E_{eq} = \frac{1}{\frac{1-\nu_A^2}{E_A} + \frac{1-\nu_B^2}{E_B}} \tag{3.17}$$

$$G_{eq} = \frac{1}{\frac{2(2-\nu_A)(1+\nu_A)}{E_A} + \frac{2(2-\nu_B)(1+\nu_B)}{E_B}} \tag{3.18}$$

In the case of wall and floor contact $R_{wall} = \infty$ and $M_{wall} = \infty$. This model is well suited for study of spherical particle packing studies.

3.1.3.2 Linear Spring Model

Linear spring model was first proposed by Cundall and Strack [128]. The model follows similar mathematical formulation as described in Hertz-Mindlin model. However, the stiffness coefficients K_n and K_t are pre-defined and normal damping coefficients are given by:

$$N_n = 2N_{ndamp}\sqrt{K_n M_{eq}} \tag{3.19}$$

$$N_t = 2N_{tdamp}\sqrt{K_t M_{eq}} \tag{3.20}$$

The linear spring model facilitates force calculation with the contact detection scheme employed for cylinder particles [131]. The stiffness coefficients are user-defined and are selected to replicate the experimental and correlations from literature. while ensuring the overlap among cylinders is as minimum as possible.

3.1.4 Time Integration

DEM method tracks the motion of particles by evaluating and updating the linear and angular velocities and thereby the position of particles. Several time integration schemes have been proposed to ensure stability of the simulation. A key aspect of stability is the critical time step called Rayleigh time step:

$$t_{critical} = 2\sqrt{\frac{m}{K_{eff}}} \tag{3.21}$$

A time step less than the critical time step ensures convergence. However, for systems with high stiffness coefficients small time steps need to be chosen which increase the computation time. To circumvent this aspect, modification of Young's Modulus which increases the stiffness coefficients is employed as a preferred strategy [152]. For the simulations performed, a time step not more than 20% of $t_{critical}$ is employed.

3.2 Computational Fluid Dynamics

Computational Fluid Dynamics provides a framework to solve the constitutive equations of continuity, conservation of momentum and conservation of energy to obtain detailed flow, pressure and temperature fields in fixed bed reactors [5, 55]. The equations are solved iteratively using finite volume methods [153] to obtain the local interstitial flow fields. In addition, temperature and species distribution can also be obtained using this technique. Although some simplified flow models have provided good insights into flow behavior [eg: Ergun equation, Darcy's Law], they do not capture the local fields and hence do not provide in depth insights into the flow configuration. However, computational fluid dynamics provides a rigorous framework to obtain numerical solution to these flow fields. The study aims at understanding the influence of the catalyst geometry on the flow phenomena. To achieve this goal, the geometrical data (particle location and orientation) and the bed tube are obtained from the DEM simulations. A sequence of boolean operations are performed to obtain the interstitial flow domain through which fluid flow occurs. This domain is

meshed using a set of constraints to obtain robust meshes. Lastly, the constitutive equations are solved over this discretized domain to obtain the local flow and pressure fields.

3.2.1 Governing Equations

The model solves for equation of continuity given as follows:

$$\frac{\partial \rho}{\partial t} + \frac{\partial \rho u_i}{\partial \chi_i} = 0 \tag{3.22}$$

The conservation of momentum is as follows:

$$\frac{\partial u_i}{\partial t} + \frac{\partial u_i u_i}{\partial \chi_j} = -\frac{\partial p}{\partial \chi_i} + \frac{\partial \tau_{ij}}{\partial \chi_j} + \rho g_i + F_i \tag{3.23}$$

In the above equation p represents static pressure, τ_{ij} is the stress tensor, ρg_i is the gravitational body force and F_i is any external force the fluid experiences. In the current study, all fluids are treated as Newtonian fluids where τ_{ij} is given by:

$$\tau_{ij} = \left[\mu(\frac{\partial u_i}{\partial \chi_j} + \frac{\partial u_j}{\partial \chi_i})\right] - \frac{2}{3}\mu \frac{\partial u_i}{\partial \chi_i}\delta_{ij} \tag{3.24}$$

Similarly, the equation for conservation of energy can be given as:

$$\frac{\partial \rho H}{\partial t} + \frac{\partial \rho u_i H}{\partial \chi_i} = \frac{\partial}{\partial \chi_i}\lambda \frac{\partial T}{\partial \chi_i} - \frac{\partial \Sigma_j H_i J_i}{\partial \chi_i} + \frac{DP}{Dt} + (\tau_{ik})\frac{\partial u_i}{\partial \chi_k} + S_H \tag{3.25}$$

Many researchers have observed that the traditional superficial velocities employed in fixed bed reactors exhibit highly unsteady and chaotic flows. Particle Reynolds Number (Re) greater than 300 are described by turbulent models.

$$Re = \frac{\rho v_{in} d_p}{\mu} \tag{3.26}$$

Several strategies have been applied to model turbulence in fluid flow. While solving the time dependent Navier-Stokes equation called as Direct Numerical Simulation (DNS) [97] is the most straightforward choice, it is highly restrictive in terms of the geometrical complexities and the computational demand for simulating fluid flow [11]. Alternatively, Large Eddy Simulations (LES) [154] and Reynolds Averaged Navier Stokes [55] models provide viable options for solving the fluid flow. The transient formulation of LES makes it less suitable for fixed-bed simulations [90]. Considering the above aspects, RANS has been successfully applied to study fluid flow in fixed-beds [99].

RANS model decomposes the vector component into a mean component and a fluctuating component.

$$v_i = \overline{v_i} + v_i' \tag{3.27}$$

The modified velocity components are substituted into the conservation of momentum equation. The resulting equations are averaged which eliminates the terms with single fluctuating components:

$$\frac{\partial(\rho\overline{v}_i)}{\partial t} + \frac{\partial}{\partial\chi_j}(\rho\overline{v_i v_j} + \rho\overline{v_i' v_j'}) + \frac{\partial\overline{p}}{\partial\chi_i} + \frac{\partial\overline{\tau}_{ij}}{\partial\chi_j} = \rho g_i \tag{3.28}$$

Several models have been developed to predict the product of the fluctuating components in the above equation and have been rigorously investigated regarding their applicability for fixed-bed analysis [23, 96]. The modified $k-\epsilon$ model has been found to be the most suitable for fixed bed analysis. Following equation shows the prediction of fluctuating components from the model .

$$(-\rho\overline{v}_i\overline{v}_j) = \mu_t\left(\frac{\partial v_i}{\partial\chi_j} + \frac{\partial v_j}{\partial\chi_i}\right) - \frac{2}{3}\left(\rho k + \mu_t\frac{\partial v_i}{\partial\chi_j}\right)\delta_{ij} \tag{3.29}$$

The above equations are solved to obtain the steady state flow, velocity and pressure fields in the fixed bed reactors. The entire model has been simulated using the academic license of STAR-CCM + package.

3.2.2 Meshing Strategies

Meshing the interstitial domain of packed beds is a challenging task. Several aspects related to the size and nature of the geometry make meshing a tedious task. CAD representation of DEM generated particle packing structures are not suitable for generating meshes that can efficiently solve and converge the governing equations for fluid flow analysis. In order to minimize memory requirements, CAD geometries only provide an approximate representation of the intended solid particle. The soft sphere approach followed during DEM simulations also results in minimal overlap among the solid particles. The above constraints often result in "dirty geometries", which need post-processing before proceeding to fluid flow simulations. The complex geometries of sphere and cylinder packing requires fine meshing to avoid highly skewed and low quality cells. However, extremely fine meshing often results large number of cells resulting in heavy computational cost. Several researchers have addressed this issue by suitable modifying the bed geometry without altering the overall bed behavior [96]. The mesh generation comprises of surface meshing and volume meshing. Following sections describe generation of meshes for reliable computations.

3.2.2.1 Surface Meshing

After obtaining the flow domain, the bed and particle surfaces are remeshed to obtain smooth surfaces. This surface mesh provides a base over which the volume mesh is generated. The surface meshing is done by either using the surface wrapper or surface remesher [57]. The motivation for surface meshing is to generate a water tight mesh which provides a smoother and continuous representation of the solid surfaces over which the volume mesh can be generated. The objective of the surface mesh is to provide the best possible representation of the solid catalyst particles that can reflect the impact of packing geometry on the fluid flow simulation.

As mentioned earlier, spherical and cylindrical particles exhibit contact points which require extremely fine meshing to avoid skewed cells [96]. In order to mitigate this issue, several modifications of the geometry have been proposed as shown in Figure 3.4. They can be broadly classified as global [55, 149] where the particle size is either increased or decreased to eliminate the fine contact points and local [103, 135] using bridges at contact points or using caps where local flattening of particle shape is performed at the contact points. Compared to the global methods where the bed geometry is modified and corrections have to be applied while post-processing [11], local methods are promising with minimal change to the actual geometry. In this study, local flattening (caps method) is applied where the contact surfaces is flattened to create a finite volume which can be meshed to provide reliable volume mesh.

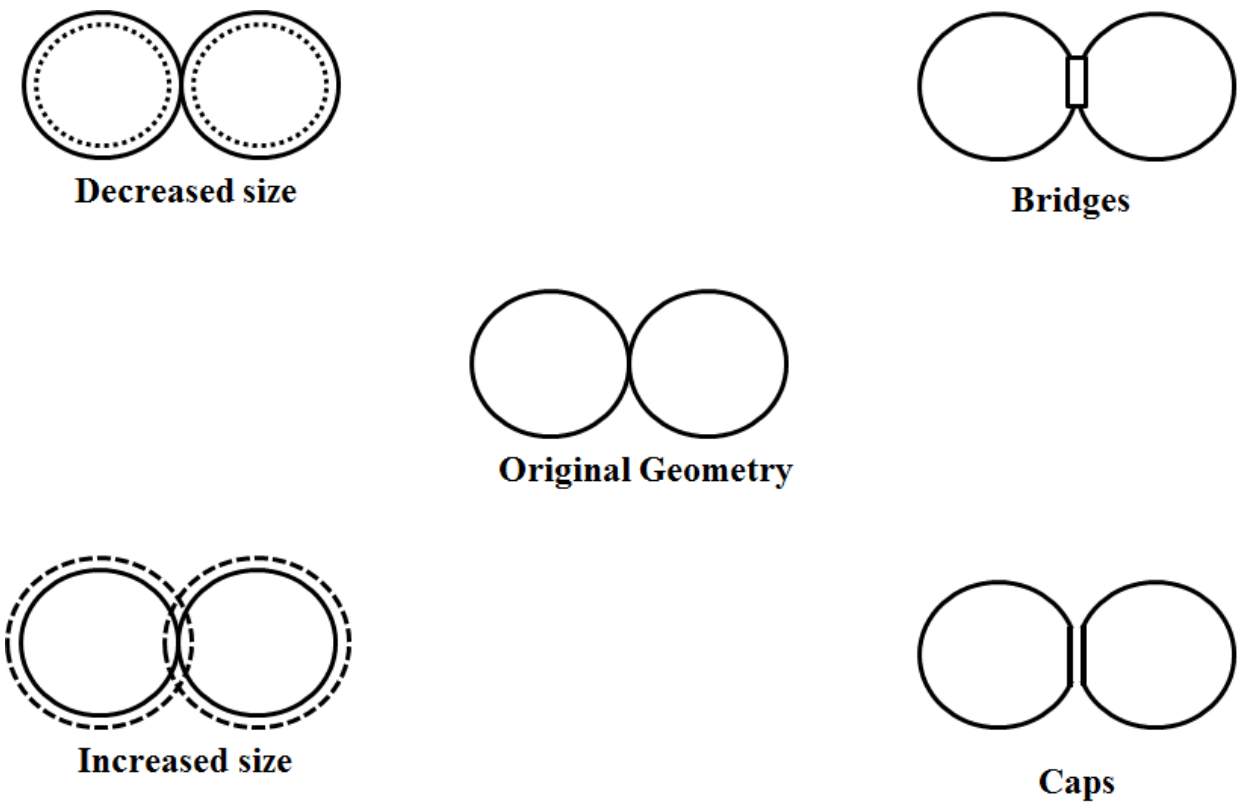

Figure 3.4: Geometry modifications to generate reliable surface and volume meshes

3.2.2.2 Volume Meshing

Volume meshing comprising of polyhedral and prism layers is used to generate the volume mesh from the bed wall and particle surfaces. The prism layers are grown along the surface of the particles to capture the boundary layer effects for velocity and temperature as shown in Figure 3.5.

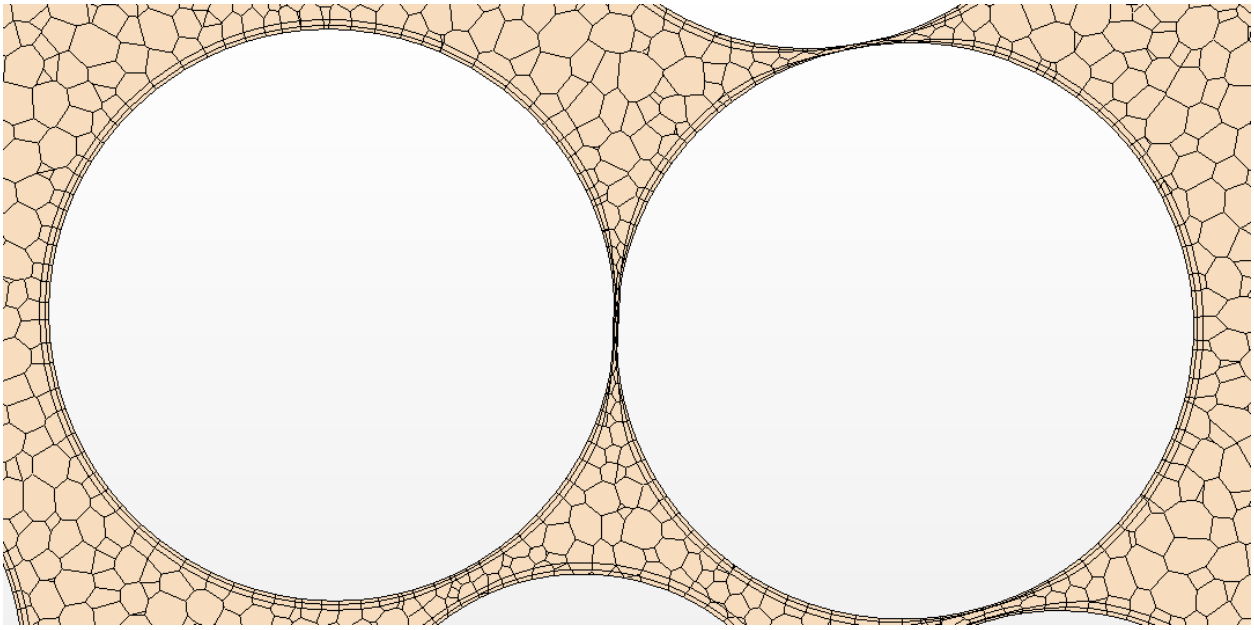

Figure 3.5: Generated prism layers along the surface to capture velocity and temperature gradients

The remainder of the volume is suitable meshed with polyhedral mesh as shown in Figure 3.6. The mesh generation process is constrained to quality parameters in order to generate reliable meshes [57, 95, 99, 103].

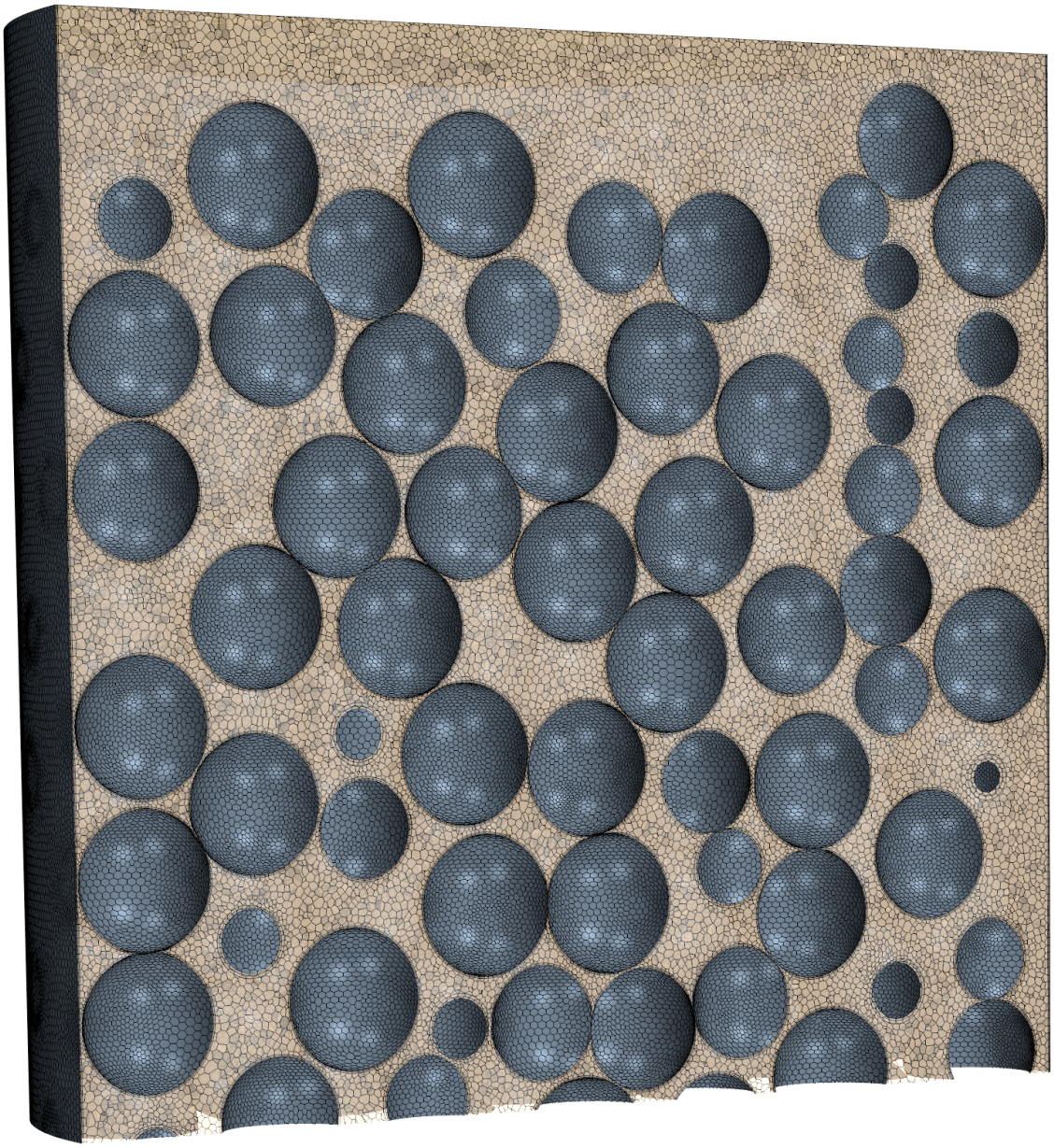

Figure 3.6: Generated volume mesh in the interstitial flow domain

4. SPHERE PARTICLE PACKING

4.1 Overview

Cylindrical vessels representing the beds to be packed are generated and spherical particles are added to bed sequentially until a minimum bed height $h = 35D_p$ is generated. Preferential loading of particles is obtained by suitably modifying the particle injector zone. After a desired loading strategy is selected, the particle positions and radii are randomized and introduced into the bed. The particles are allowed to settle under the influence of gravity and simulation is stopped when the maximum velocity of the particles in the bed falls below a magnitude of $0.0001\ m/s$.

4.1.1 Loading Methods

Figure 4.1 depicts three loading methods simulated by modifying injector zone to introduce particles at desired radial positions. *Uniform loading* refers to particles added uniformly across the bed cross-section, and *sock loading* introduced the particles in the center of the bed whereas *wall loading* introduced the particles along the bed wall.

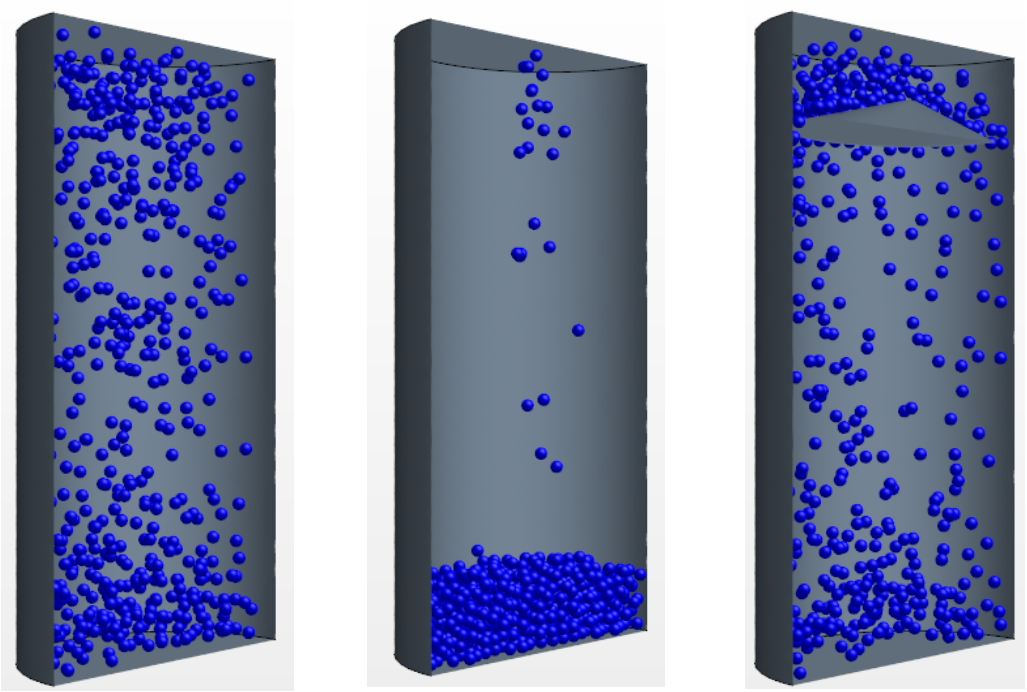

(a) Uniform (b) Sock (c) Wall

Figure 4.1: Initial loading positions and corresponding initial packing structure of monodisperse spherical particles for (a) Uniform (b) Sock and (c) Wall loading in $D_B/D_p = 20$

4.1.2 Discrete Element Method

Discrete Element method[DEM] solves Newton's second law over a discretized time step to evaluate the motion of particles and has been effectively employed to study fixed-beds as well. [88, 90, 95, 117, 134, 135, 136]. Both translational and rotational motion equations are solved to calculate the displacement the particle undergoes over a given time step by evaluating surface forces $\vec{F_s}$, body forces $\vec{F_b}$ and torque $\vec{\Gamma}$.

Interactive forces between particles are calculated using the Hertz-Mindlin contact model where the normal and dampening forces are calculated from the overlap and velocities of particles involved [128, 130]. The rolling resistance model was used for friction calculations. Glass was used as material for both particles and the wall. However, a reduced Young's modulus was used for the calculation which results in faster computation by increasing the time step over which calcu-

lations can be performed [152, 155, 156]. DEM simulations were performed using STAR-CCM + (academic license) software package [90, 95, 117, 157].

4.1.3 Implementation

The entire set of simulations were performed on a LINUX based IBM/Lenovo x86 HPC Cluster super computer facility capable of parallelization provided by Texas A&M University. In all cases, output was collected comprising of tabular data representing the particle number, radial, vertical and angular positions and radii of the sphere.

4.1.4 Analysis Of Results

Sufficiently long beds were generated to mitigate any end effects produced by the reactor floor [32]. Also, the topmost layer of the bed can be loosely packed and hence the top five particle diameters are not included for voidage analysis [103] The bulk and radial voidages of the simulated fixed-beds are calculated as follows:

A plane perpendicular to the axis of the cylindrical bed is drawn at an arbitrary height h from the base. The number of particles N_p with geometrical centers enclosed within the resulting cylindrical volume can be obtained from the output file. Through a set of geometric computations, the net solid volume(v_{solid}) enclosed is evaluated. The resulting bulk voidage ϵ_B is given as:

$$\epsilon_B = 1 - \frac{v_{solid}}{\pi D_B^2 h/4} \tag{4.1}$$

The edge-based technique proposed by Mueller [36] is used to predict the radial voidage at a specific axial and radial position as follows. Firstly, the bed is dissected into planes perpendicular to the axis of the cylindrical bed, secondly this plane is divided into annular rings from center of the bed towards the wall with an increment in the radius by $R/100$ as suggested by [34] where R is the mean radius of the particle sample. For each annular ring, the length of the arc intersecting a spherical particle $s(r)$ is evaluated using the following equation:

$$s(r) = 2\theta r \tag{4.2}$$

where r is the radius of the annular ring and θ is angle subtended at the center of the bed by the intersecting arc passing through the sphere [36]. Such evaluation is performed for the entire annular ring to obtain the radial porosity at that specific radial position and height,

$$\epsilon(r, h) = 1 - \frac{\Sigma s(r)}{2\pi r} \tag{4.3}$$

which can be further averaged across multiple vertical planes to obtain the axially averaged radial voidage.

Tortuosity represents the ratio of length of the path traversed by the fluid to actual length of bed (vertical direction in current case). PathFinder algorithm [158, 159, 160] has been used to estimate the geometrical tortuosity demonstrated by simulated beds. The algorithm evaluates the shortest possible path the fluid can travel through by connecting adjacent void throats throughout the bed. The bed base is discretized into a set of points from which these possible paths can be traced. Through this process, localized tortuosity values can be obtained across the bed and have been presented in this study for different loading methods. In addition to the tortuosity analysis, particle segregation induced by the loading methods has been studied for poly-disperse mixtures for the case of $D_B/D_P = 20$.

4.2 Results And Discussion

4.2.1 Parameter Selection And Validation

Table 4.1 provides the particle and bed dimensions used for simulations aimed at investigating the relative impact of loading method and poly-dispersity of particle sample.

Table 4.1: Particle and Bed dimensions used for investigating the effect of loading method on bed structure

$D_p(m)$	D_B/D_p
0.00635	8
0.00635	14
0.00635	20

In order to study the reproducibility of the model, a total of 15 beds across the three bed-particle diameter ratios were generated using Uniform loading. The bulk voidage calculated showed a maximum standard deviation of 0.3 % establishing the reproducibility of the models. Table 4.2 shows the relevant parameters used for the model employed in this study.

Table 4.2: Simulation parameters used for generation of sphere packed structures

Parameters	Values	Units
Young's modulus Y	$1e7$	N/m^2
Density ρ	2500	kg/m^3
Poisson's Ratio ν	0.235	-
Restitution e	0.94	-
Static friction α	0.4	-
Time step Δ t	0.0001	s

Bulk voidage characteristics of the fixed-beds were compared with correlation provided by Benayahia and O' Niell [28]. Figure 4.2 shows the bulk voidage values for monodisperse beds with D_B/D_P $8, 14$ and 20 compared with correlation [28] with a multiple correlation coefficient of 93% and a standard deviation of 1.5% with DEM simulations for the cases of $D_B/D_P = 8, 14$ and

20. The plot also shows decrease in bulk voidage with increase in bed diameter due to elimination of constraining effects of the wall. The bulk voidage profiles stabilize to an asymptotic value of 0.39 as observed in other similar studies [136, 157].

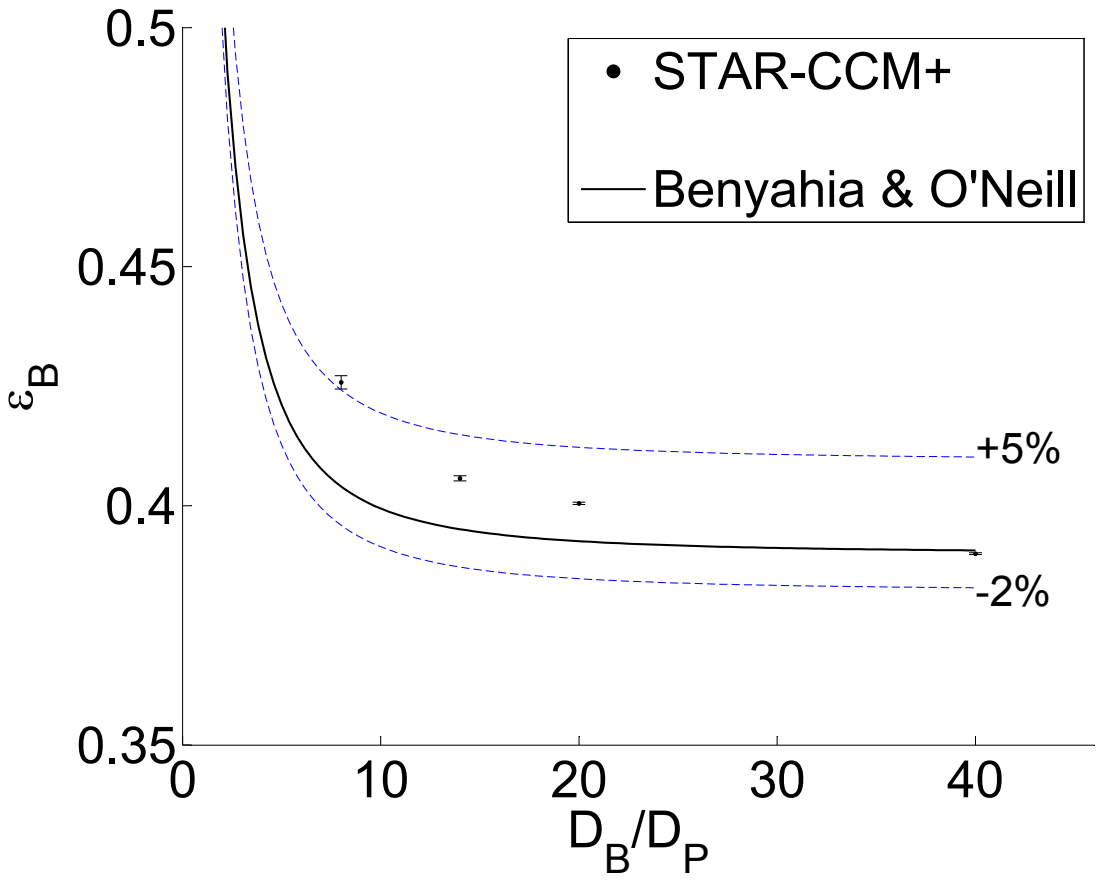

Figure 4.2: Bulk voidage measurements of the simulations compared with Benyahia and O'Neill correlation [28]

Radial voidage profiles for the monodisperse beds were compared with correlation of deKlerk [43] in Figure 4.3 and show good agreement.

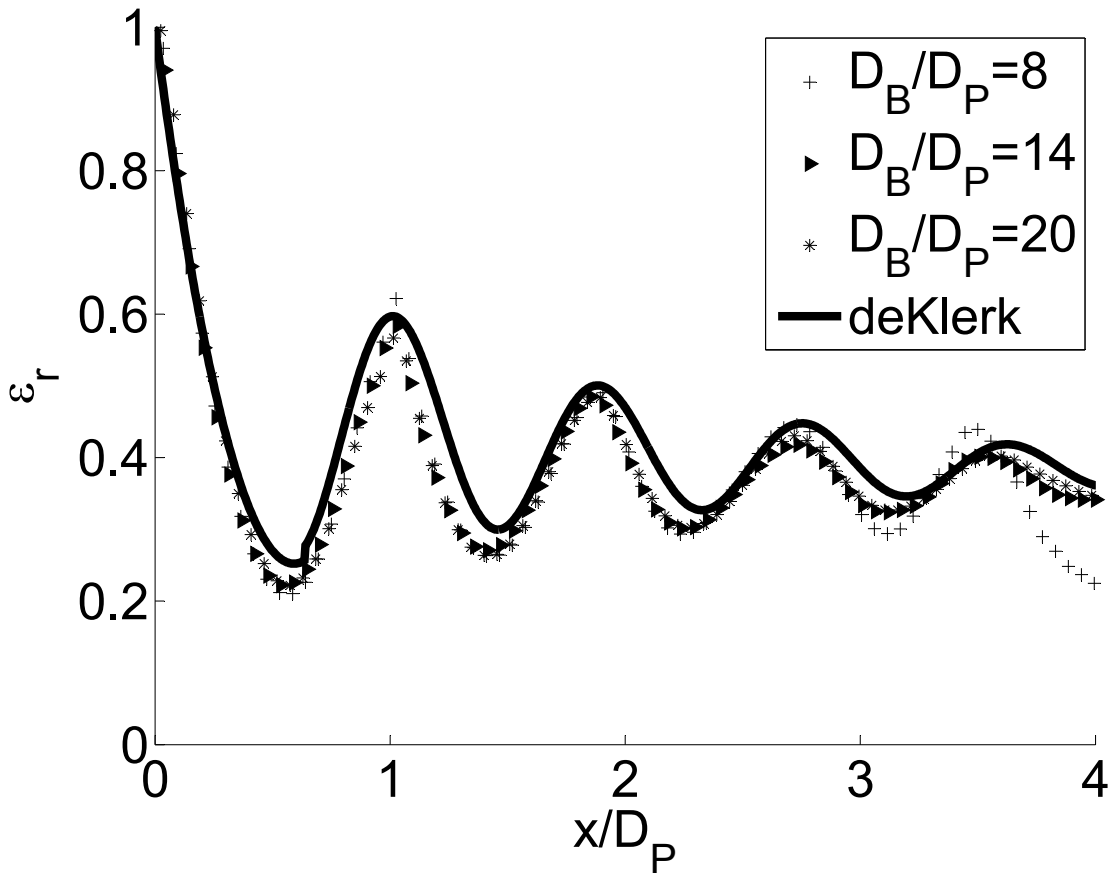

Figure 4.3: Radial voidage profiles of simulated beds compared with deKlerk correlation [43]

4.2.2 Relative Influence Of Loading Methods

Figure 4.4 and 4.5 depict the bulk and radial voidage profiles obtained for monodisperse particle beds with D_B/D_P $8, 14$ and 20 respectively. The bulk voidage profiles for the monodisperse beds show similar trends irrespective of the loading methodology employed. In line with experimental measurements of [44], the radial voidage patterns demonstrate an oscillatory profile in the proximity of wall caused by the ordering of particles. The tortuosity plots for the monodisperse packing are presented in Figure 4.6. The tortuosity plots provide show that the beds exhibit a tortuosity distribution with a mean value of 1.18. It can be seen that loading methods do not influence the packing configurations generated by monodisperse spherical particles.

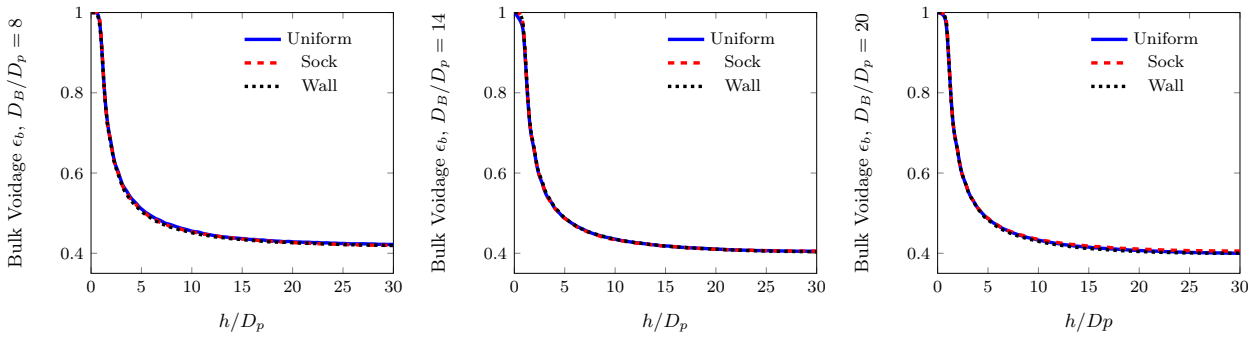

Figure 4.4: Bulk voidage of simulated monodisperse particle beds obtained from Uniform, Sock and Wall loading for $D_B/D_P = 8, 14, 20$

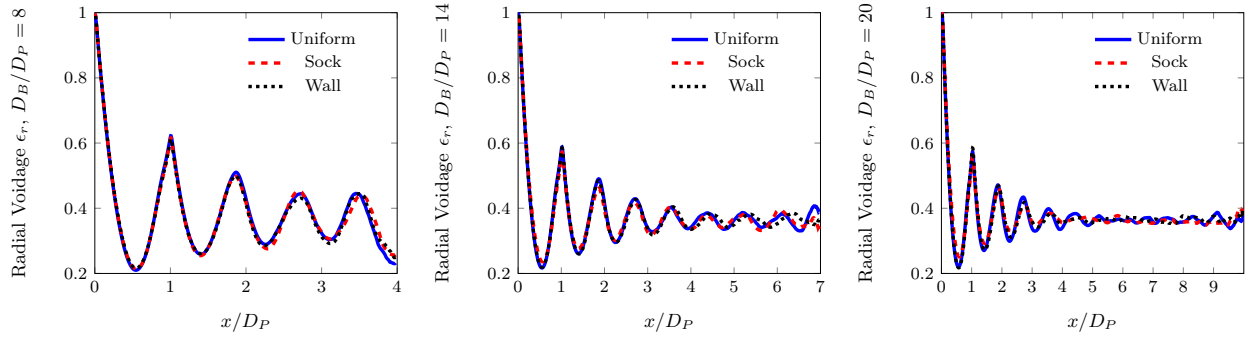

Figure 4.5: Radial voidage of simulated monodisperse beds obtained from Uniform, Sock and Wall loading for $D_B/D_P = 8, 14, 20$

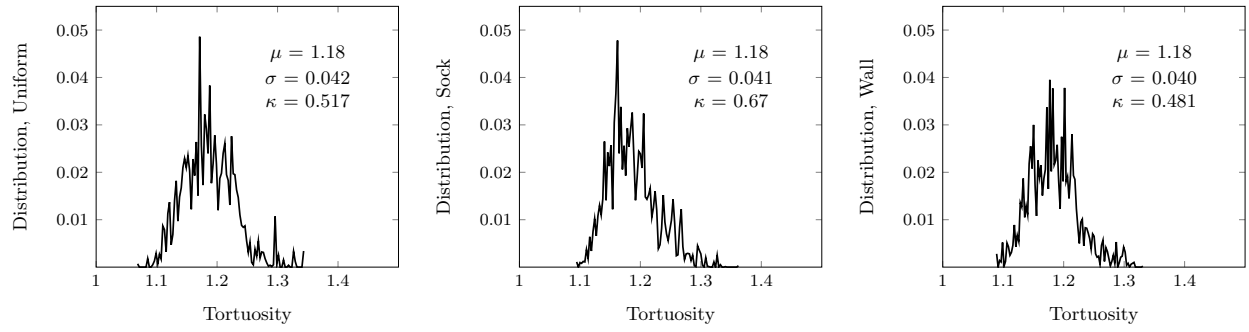

Figure 4.6: Tortuosity distribution of monodisperse beds obtained from Uniform, Sock and Wall loading for $D_B/D_P = 20$

4.2.3 Relative Influence Of Particle Size Distribution

In addition to studying the impact of loading methods on the mentioned particle-bed dimensions, each run was performed with three particle size distributions. Monodisperse particle sample comprised of spheres with uniform diameter of 6.35 mm and polydisperse samples with a mean diameter of 6.35 mm and spread of 10% and 20% were used. Figure 4.7 shows the distribution of polydispersity obtained from the packing simulation and depicts a normal distribution with a mean diameter of 6.35 mm and desired standard deviations.

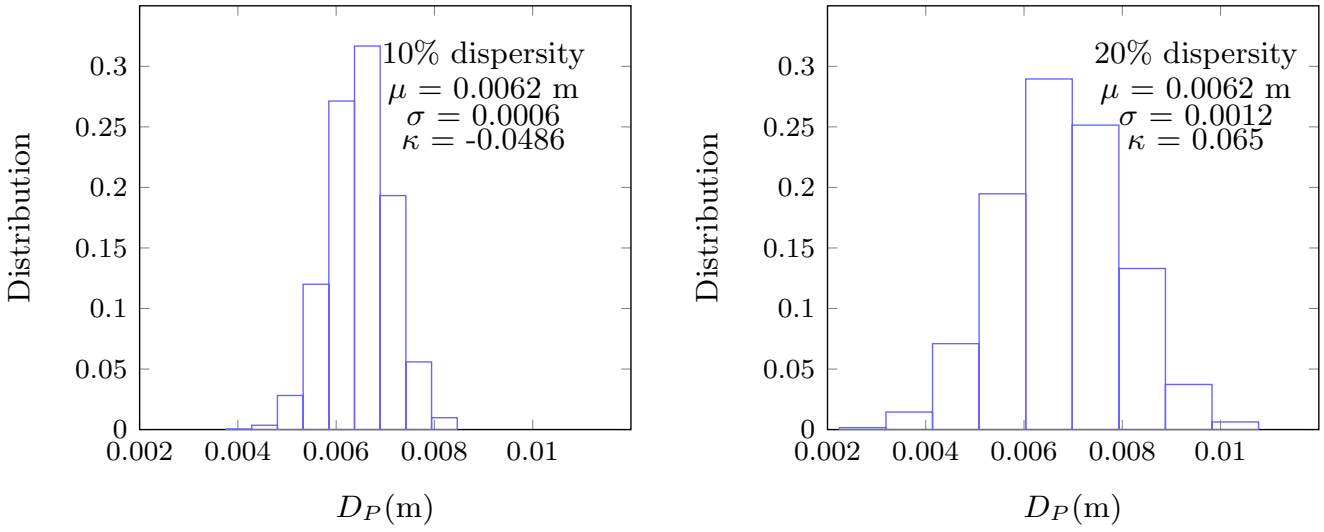

Figure 4.7: Polydispersity distribution generated from Uniform Loading for $D_B/D_P = 20$

The bulk and radial voidage profiles for beds generated with polydisperse samples are shown in Figure 4.8 and 4.9 respectively. It can be seen that bulk voidage profiles are similar to the case of mono-disperse loading and lead to an asymptotic value with increase in bed diameter. The impact of polydispersity is noticed in the dampening of oscillatory profiles of radial voidage. The oscillations exhibit higher amplitude in case of monodisperse packing and decreases with increase in polydispersity. The void spaces present in between larger particles are occupied by smaller particles and results in dampening of voidage profiles.

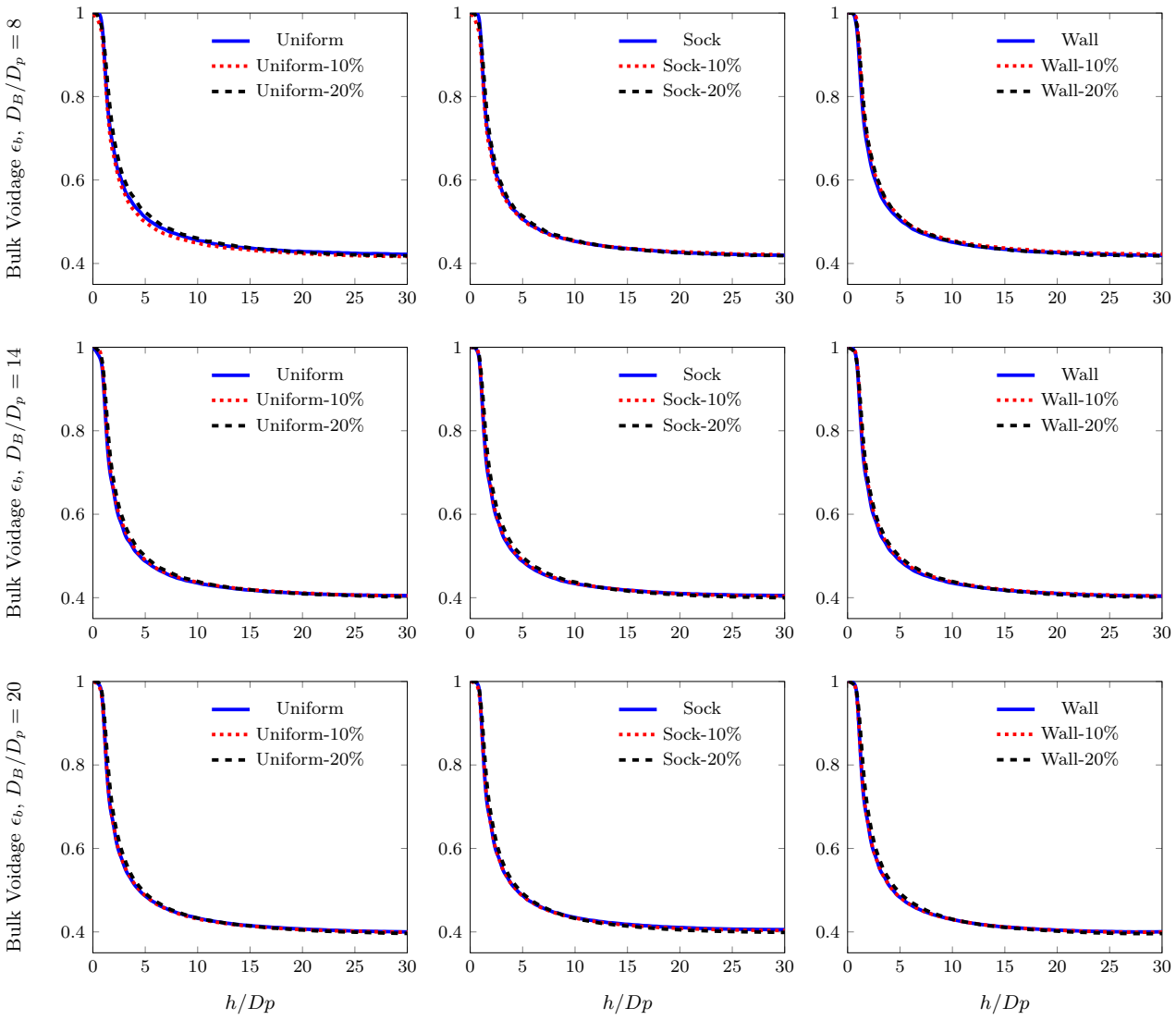

Figure 4.8: Bulk voidage profiles of monodisperse and polydisperse beds obtained from Uniform, Sock and Wall loading for $D_B/D_P = 8, 14, 20$

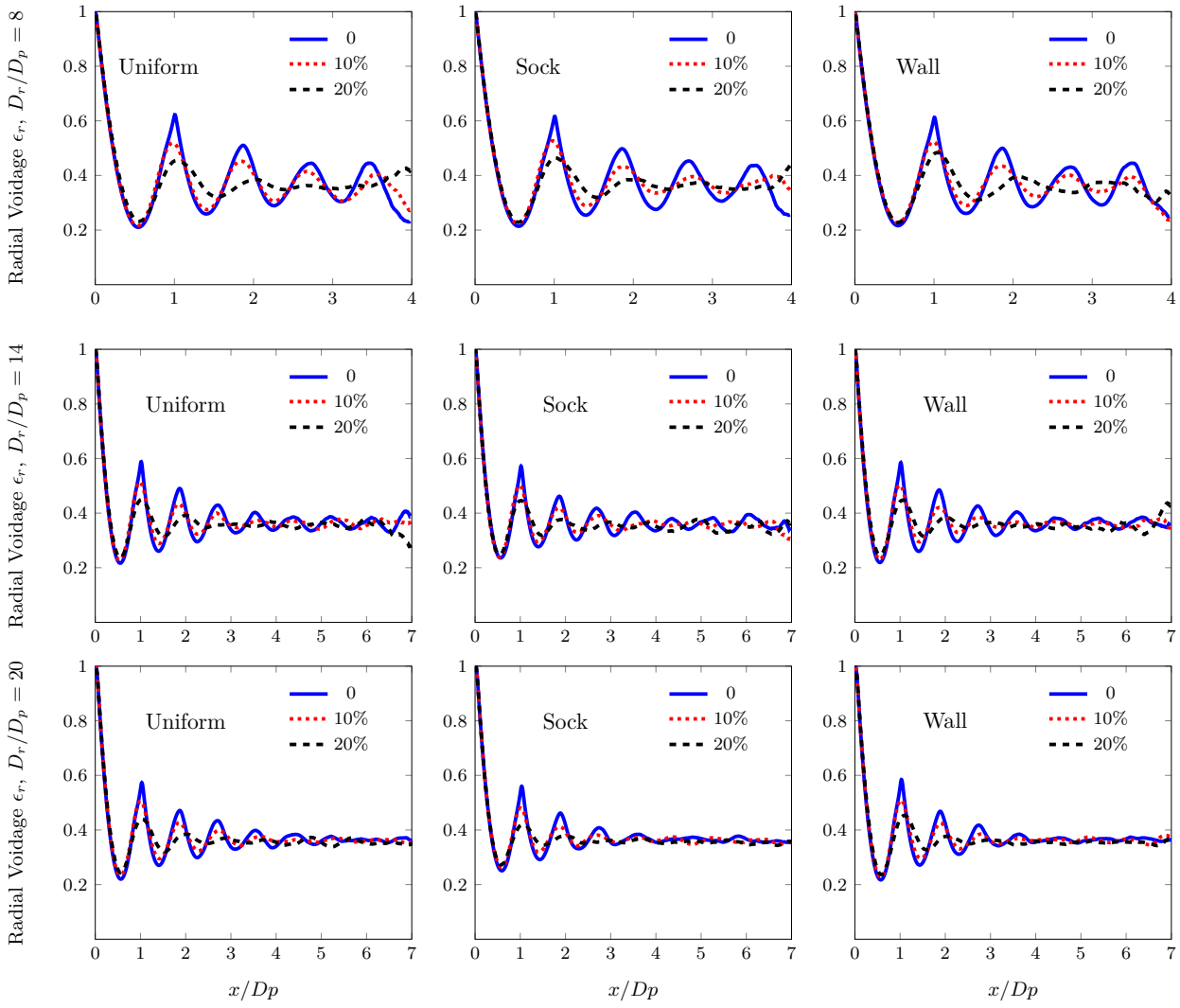

Figure 4.9: Radial voidage profiles of monodisperse and polydisperse beds obtained from Uniform, Sock and Wall loading for $D_B/D_P = 8, 14, 20$

Preferential loading of polydisperse particles by varying the radial entry positions into the bed tends to create particle segregation [161, 162]. D_B/D_p of 20 was used for this study and three different beds corresponding to each loading and polydispersity were generated for this study. The entire bed was divided into annular rings of thickness D_p. For each of the annular rings, the mean particle diameter of the particles with centers in the given annular rings is evaluated. Figure 4.10 represents the variation of the mean particle diameter along the radial position of the bed from center to the wall. It can be seen that for the case of uniform loading the mean particle diameter

does not show significant variation across the bed radius, however for the case of sock loading, the mean particle diameter tends to decrease from center towards the wall and for wall loading mean particle diameter tends to increase from the center towards the wall of the bed. This behavior is further validated by the skewness values presented in Figure 4.11 where sock loading demonstrated positive skewness towards the wall and wall loading shows positive skewness towards the center of the bed. As larger particles tend to experience higher resistance to be displaced when compared to smaller particles, larger particles are found in the vicinity of introduction zone whereas smaller particles are displaced further. Thus for the case of poly-disperse mixtures, the loading techniques tend to create a gradient of particle sizes from the zone of the introduction. This will bound to create non-isotropic void behavior and needs to be taken account of while packing the fixed-beds.

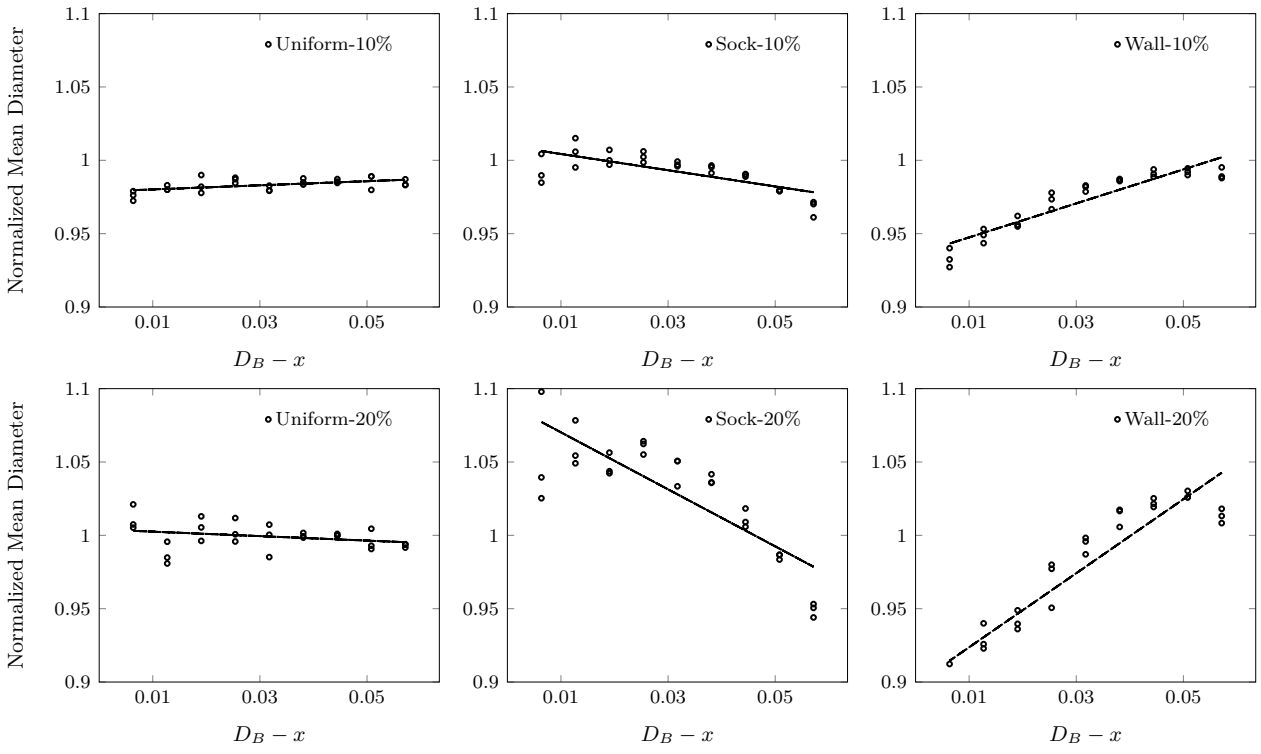

Figure 4.10: Normalized mean diameter along the radial distance from center to wall for 10 % and 20 % polydisperse beds for $D_B/D_p = 20$

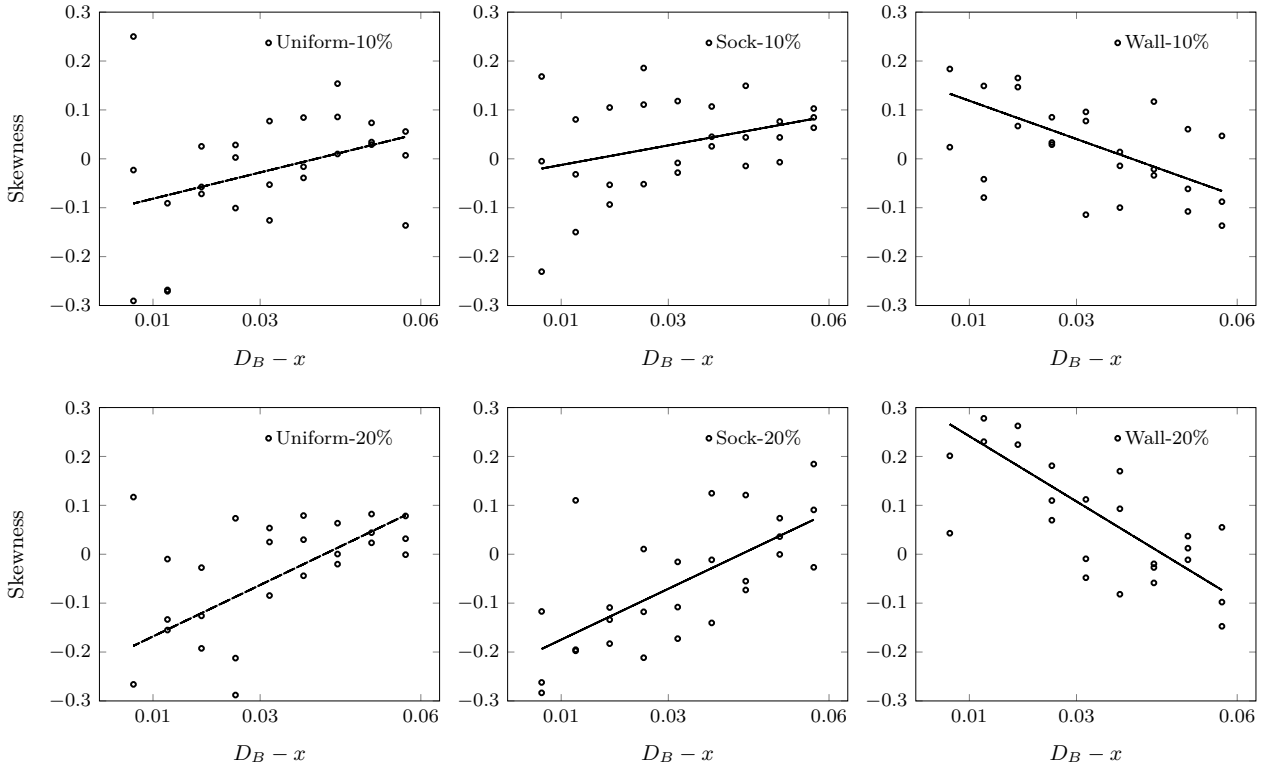

Figure 4.11: Skewness of particle size distribution along the radial distance from center to wall for 10 % and 20 % polydisperse beds for $D_B/D_p = 20$

Lastly, the tortuosity plots for polydisperse beds were generated using the PathFinder algorithm and are presented in Figure 4.12. The tortuosity values depicted by the bed are similar to the values . However, more rigorous interstitial fluid flow studies have to be performed to gain better understanding of the influence of polydispersity and loading methods.

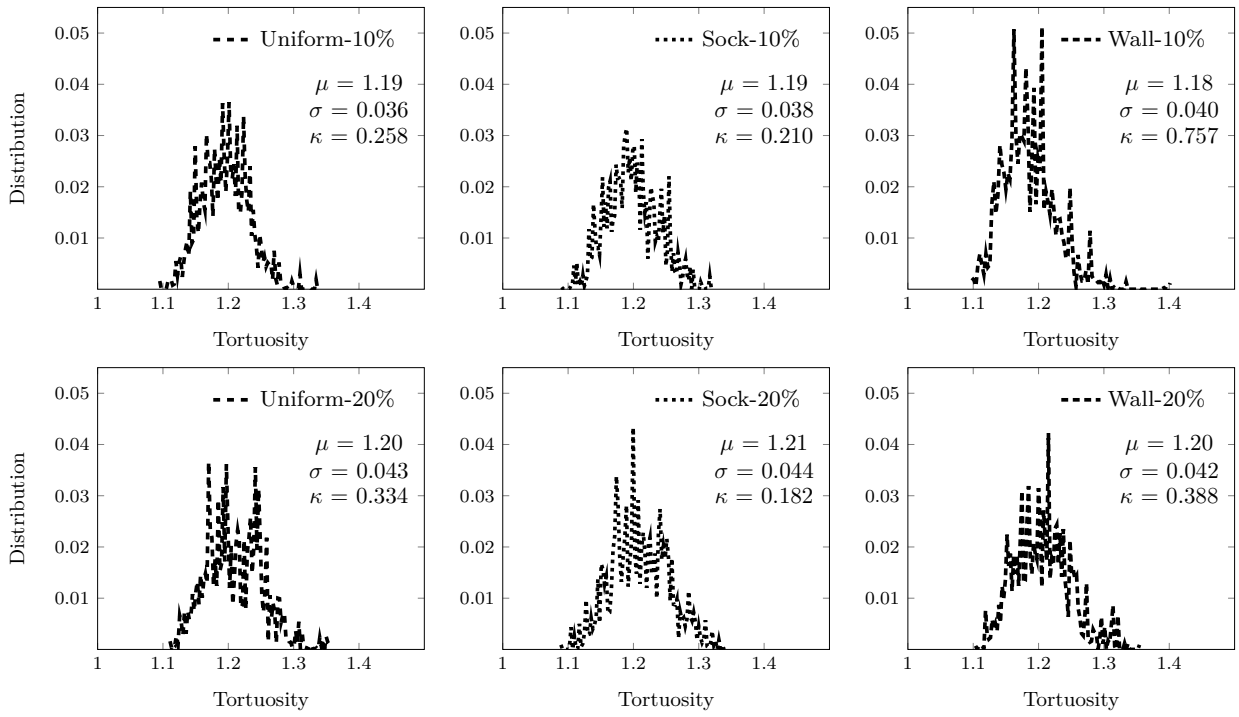

Figure 4.12: Tortuosity distribution for 10 % and 20 % polydisperse beds for $D_B/D_p = 20$

4.3 Conclusions

DEM simulations were performed to study the influence of different loading methodologies on spherical packing structures. STAR-CCM+ was used for performing the packing simulations and generated beds showed good match with the correlations from literature. The loading methods did not show any significant difference in the voidage and tortuosity behavior of the generated bed structures and could be attributed to the isotropic nature of spherical particles. However, for the case of polydisperse mixtures along with dampening of oscillations in the radial voidage profiles, segregation of particles depending on the loading methodology employed was noticed. This may lead to significantly altering the subsequent fluid flow behavior observed in the beds.

5. CYLINDER PARTICLE PACKING

5.1 Overview

DEM has been employed in this study to generate fixed-beds comprised of cylindrical particles. Rigid cylinder particle model provided by STAR-CCM+ was used for the packing simulations [104]. Particles are introduced into the bed via different loading methods wherein the radial entry position of the cylinders is varied specific to the method chosen. This is achieved by suitably modifying the injector and bed geometry. After selecting the loading method, particle positions and orientation are randomized at the top of bed and are allowed to settle under the influence of gravity. Particles are introduced simultaneously into the bed until a minimum packing height h $\sim 30D_P$ is generated. The simulation is stopped after the bed reaches the desired height and particles reach a state of rest. As the simulation is completed, the position and orientation vector of the cylinder are exported for further analysis.

5.1.1 Loading Methods

The loading methods employed in this study test the effect of preferential loading of particles across the cross-section of bed. Three different loading methods are employed in this study. Particles are added uniformly across the bed cross-section which is a commonly practiced loading method in earlier packing studies. In addition, simultaneous addition of particles in the central zone of bed and addition of particles along the wall of bed are taken up to study effect of wall on structures developed in fixed beds. Figure 5.1demonstrates the three loading methods used in this study. *Uniform* loading is performed where particles are added uniformly across the bed, *Sock* loading is performed to add particles in the center of the bed and *Wall* loading is performed to add particles along the wall of the bed.

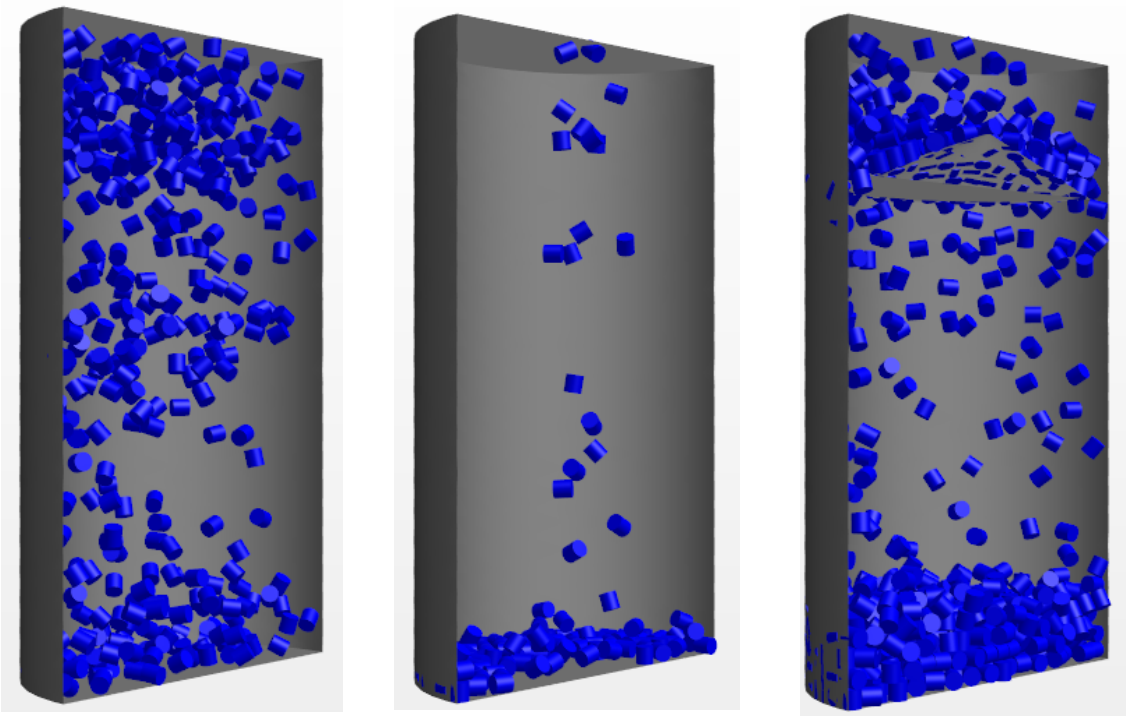

(a) Uniform (b) Sock (c) Wall

Figure 5.1: Loading methods and corresponding initial packing structure of cylindrical particles (a) Uniform (b) Sock and (c) Wall loading in $D_B/L_p = 20$

5.1.2 Discrete Element Method

Discrete Element methods (DEM) have been accepted as a reliable method to perform random packing generation and have been used for subsequent fluid flow analysis [88, 95, 103, 104, 163]. The method solves Newton's second law of motion to track the translational and rotational motion of particles. This is performed by evaluating the contact forces arising from particle-particle and particle-wall interactions. Linear spring model is used to determine the contact forces along with rolling resistance model for friction calculations. Glass was used as a material for both particle and wall. However, a reduced Young's modulus was used for the calculation which results in faster computation by increasing the time step over which calculations can be performed [152, 155, 156].

5.1.3 Implementation

The entire set of simulations were performed using STAR-CCM + 12.06.011 on a LINUX based IBM/Lenovo x86 HPC Cluster super computer facility capable of parallelization provided by Texas A&M University. The output comprises of tabular data representing the particle number, geometric position and orientation of the cylinder.

5.1.4 Analysis Of Results

Bulk voidage and radial voidage for the simulated fixed-bed structures were calculated as follows. For any given cylindrical volume of height h, the number of cylindrical particles enclosed can be obtained from the output file. From this, the geometric volume enclosed by the solid particles is evaluated and resultant bulk voidage is given as:

$$\epsilon_B = 1 - \frac{v_{solid}}{\pi D_B^2 h/4}$$

The non-isotropic shape of cylindrical particles makes geometric evaluation of radial voidage non-trivial. In order to overcome this issue, the entire bed volume is densely distributed with points. Entire bed is divided into annular volumes of thickness $d_p/5$. In each of the annular rings, the number of points interior to cylindrical particles N_p are evaluated. The ratio of these points to the total points in the annular region M_p provides a measure of the voidage at the corresponding radial positions.

Orientation distribution is an important aspect of cylinder packing structures [40, 139]. Apart from the bulk and radial voidage, they provide additional insights into spatial arrangements of cylindrical particles. The orientation distribution of cylindrical particles with the vertical and the radial of the bed are reported in this study.

5.2 Results And Discussion

5.2.1 Parameter Selection And Validation

Table 5.1 provides the details of the particle and bed dimensions used in this study. All the particle samples were mono-disperse with aspect ratios of 1 and 5. To establish reproducibility of the model, five different beds for each bed diameter to particle length ratio were generated using equilateral cylinders employing uniform loading. Figure 5.2 shows the bulk voidage of the beds generated compared with correlation of Benyahia and O'Neill [28]. It can be seen that the beds generated exhibit a mean value close to the correlation with a maximum standard deviation of 0.79%.

Table 5.1: Particle and Bed dimensions used for investigating the effect of loading method on bed structure

D_P(mm)	L_P/D_P	D_B/L_p
6.35	1	10
6.35	1	20
6.35	5	10
6.35	5	20

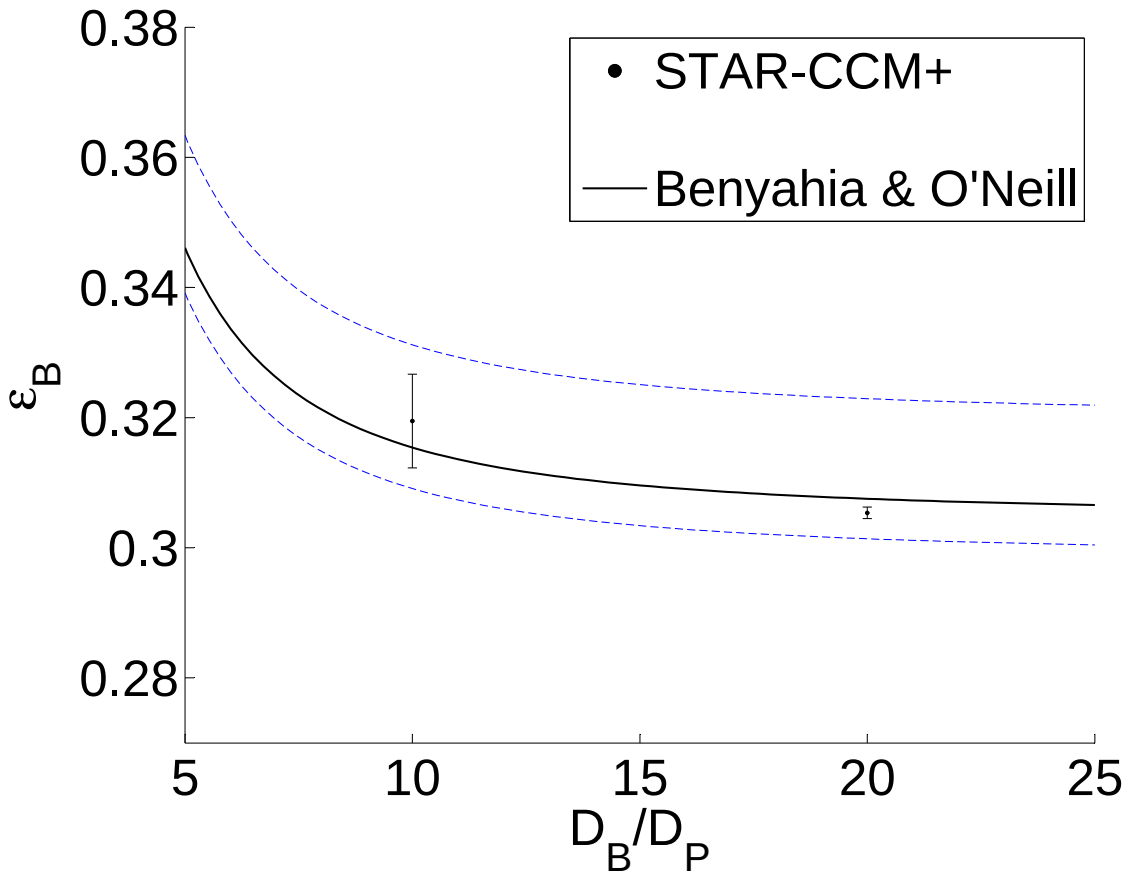

Figure 5.2: Bulk voidage of simulated beds compared with Benyahia and O'Neill correlation [28]

Caulkin *et al.* [33] generated fixed-beds comprising of cylinder particles with diameter 3.42 mm and length of 3.46 mm. X-ray tomography analysis was performed on these beds to obtain

X-ray tomography study [33] performed on fixed-beds packed with cylinder particles provided significant insights into the radial voidage and particle orientation distribution. Beds were generated comprising of cylindrical particles with a diameter of 3.42 mm and length of 3.46 mm similar to the study [33]. The radial voidage and particle orientation profiles for generated beds were compared with reported results of tapped bed packing. Figure 5.3 shows that the generated radial voidage profiles exhibit oscillatory patterns which propagate from wall into the bed similar to the tomographic data.

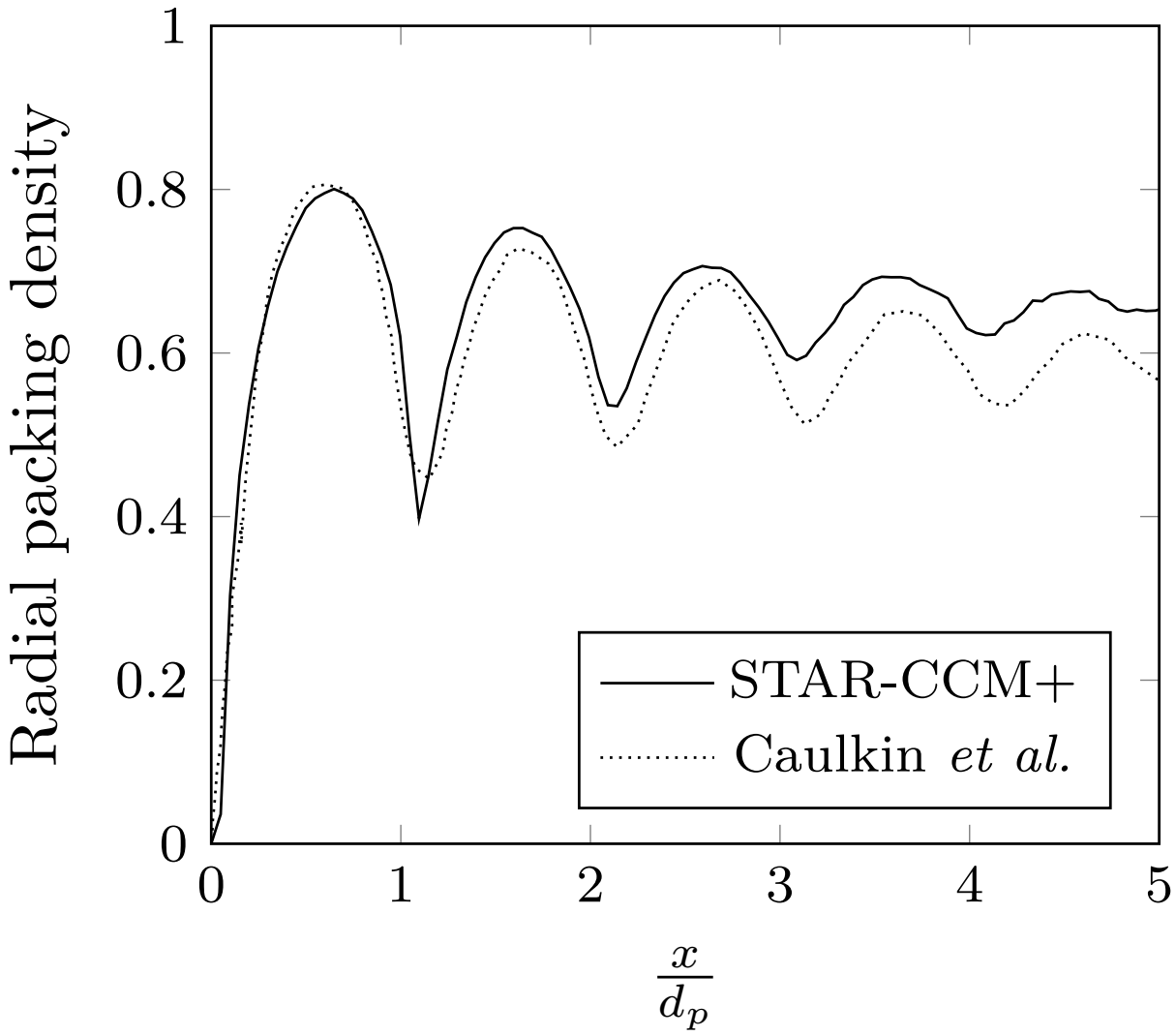

Figure 5.3: Radial voidage profile generated and compared with experimental data of Caulkin *et al.* [33]

Figure 5.4 shows a good agreement between the orientation distributions of the generated beds and tomographic data. However, the DEM simulations under predict the orientation distribution in the range of 0-10 degrees as observed in other studies as well [33, 139] and is usually attributed to differences in the material properties and constants used for simulation.

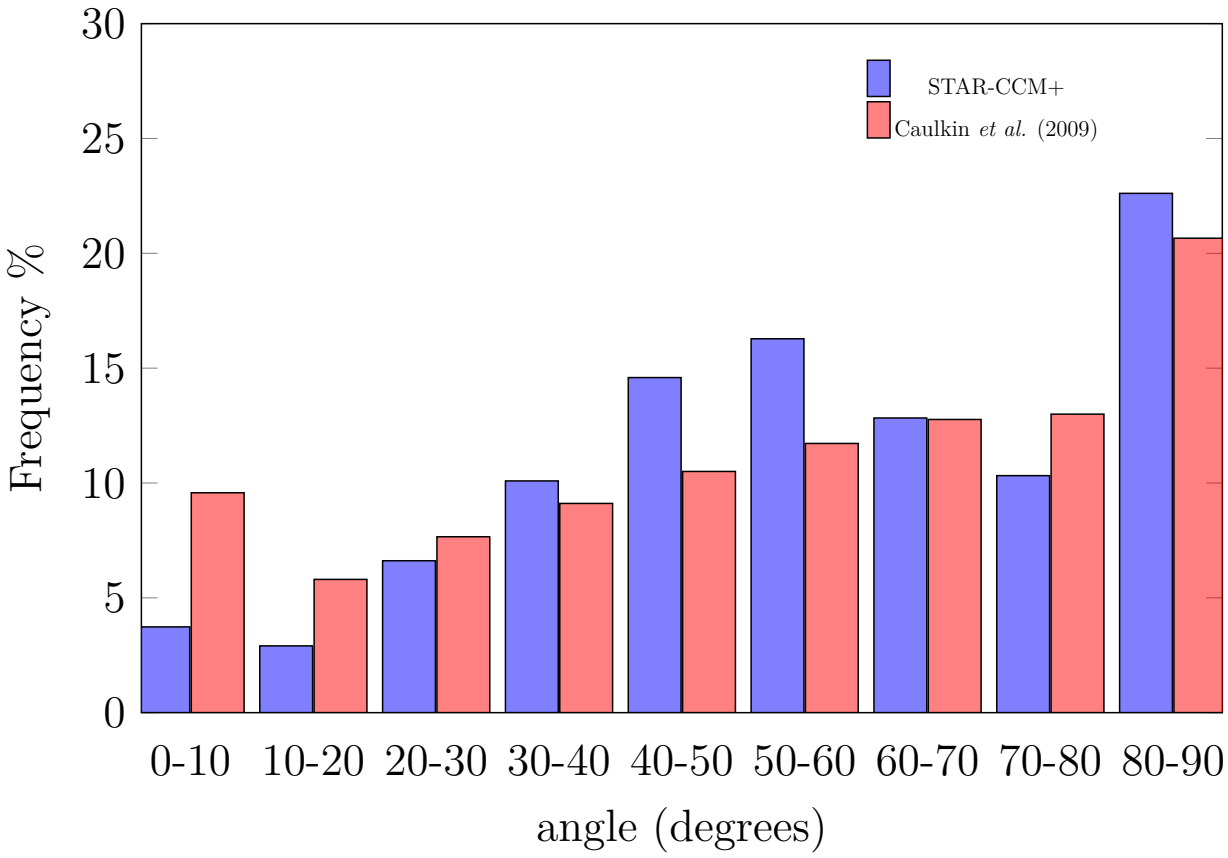

Figure 5.4: Orientation distribution of simulated beds compared with experimental data of Caulkin *et al.* [33]

Table 5.2 shows the final set of parameters used in this study. The resulting beds were analyzed for bulk voidage, radial voidage and orientation distribution.

Table 5.2: Simulation parameters used for generating cylinder packed structures

Parameters	Values	Units
Young's modulus Y	$1e7$	N/m^2
Density ρ	2500	kg/m^3
Poisson's Ratio ν	0.235	-
Restitution e	0.5	-
Static friction α	0.1	-
Time step Δ t	0.0001	s

5.2.2 Bulk Voidage

The bulk voidage of the beds for a packing height of $h \sim 25D_P$ were calculated and presented in Table 5.3. The values are in agreement with the correlation provided by Benyahia and O'Neill [28] and show a maximum deviation of 4.5%. It can be seen that the bulk voidage values are not effected by the loading method employed for both equilateral and non-equilateral cylinders.

Table 5.3: Bulk voidage values obtained from simulated cylinder packed beds

L_P/D_P	D_B/L_P	Loading	Mean	Standard Dev	Correlation	Error(%)
		Uniform	0.329	0.016		4.47
1	10	Sock	0.314	0.002	0.315	0.22
		Wall	0.324	0.001		3.015
		Uniform	0.305	0.003		0.65
1	20	Sock	0.303	0.002	0.307	1.30
		Wall	0.309	0.003		0.84
		Uniform	0.415	0.001		2.35
5	10	Sock	0.401	0.009	0.425	5.43
		Wall	0.419	0.005		1.29
		Uniform	0.410	7E-4		1.55
5	20	Sock	0.410	4E-4	0.417	1.65
		Wall	0.400	0.011		4.07

5.2.3 Radial Voidage

Figure 5.5 provides the radial voidage plots for the case of equilateral cylinders for D_B/L_p of 10 and 20. It can be seen that the radial voidage shows an oscillatory pattern in the vicinity of the wall which gradually dampens out as the distance from wall increases. This behavior which is also demonstrated by spherical structure packing arises from the ordering of particles near the wall.

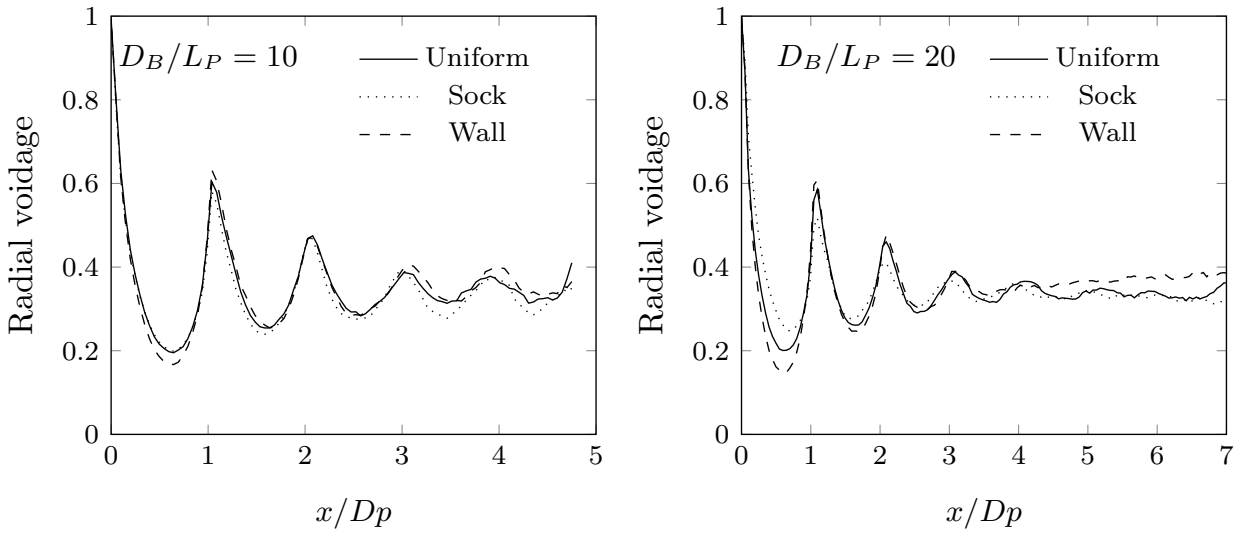

Figure 5.5: Radial voidage profiles of simulated beds generated with equilateral cylinders

However for the case of non-equilateral cylinders in Figure 5.6 the oscillations dampen out rapidly when compared to case of equilateral cylinders. High aspect ratio cylinders tend to minimize the wall ordering effect as a consequence of the non-isotropic particle shape. Among the different loading methods, wall loading induces strong order compared to others. Addition of particles along the wall creates an ordering effect resulting in increased amplitude of voidage oscillation.

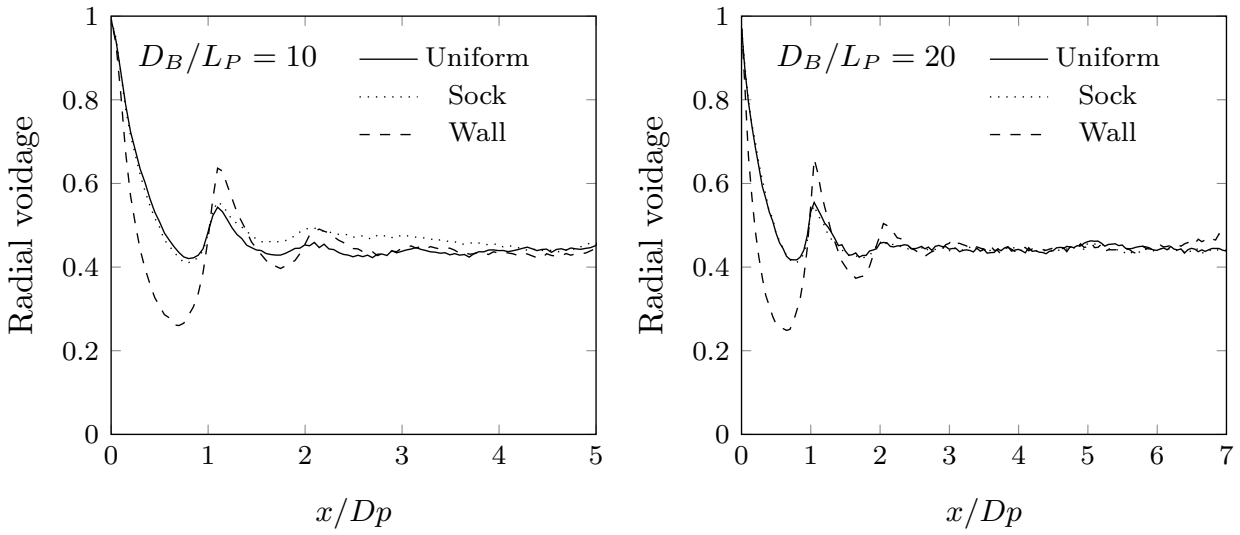

Figure 5.6: Radial voidage profiles of simulated beds generated with non equilateral cylinders

5.2.4 Orientation Analysis

Particle orientation distribution is an important characteristic of cylindrical particles. Figure 5.7 shows the alignment of equilateral particles with the vertical axis of bed. The loading methods tend to create similar orientation distribution for the case of equilateral cylinders and is similar in nature to tomographic studies of Caulkin *et al.* [33]. High aspect ratio cylinders exhibits different behavior compared to equilateral cylinders in Figure 5.8. In this case particles exhibit a strong tendency to align perpendicular to the vertical which is the most stable position for the case of long cylinders. The tendency to align horizontally becomes stronger with increase in bed diameter. Wall loading provides unhindered settling of particles which results in particles aligning in the most stable position. This results in creation of isotropic voidage profiles which ensures better fluid distribution [164, 165].

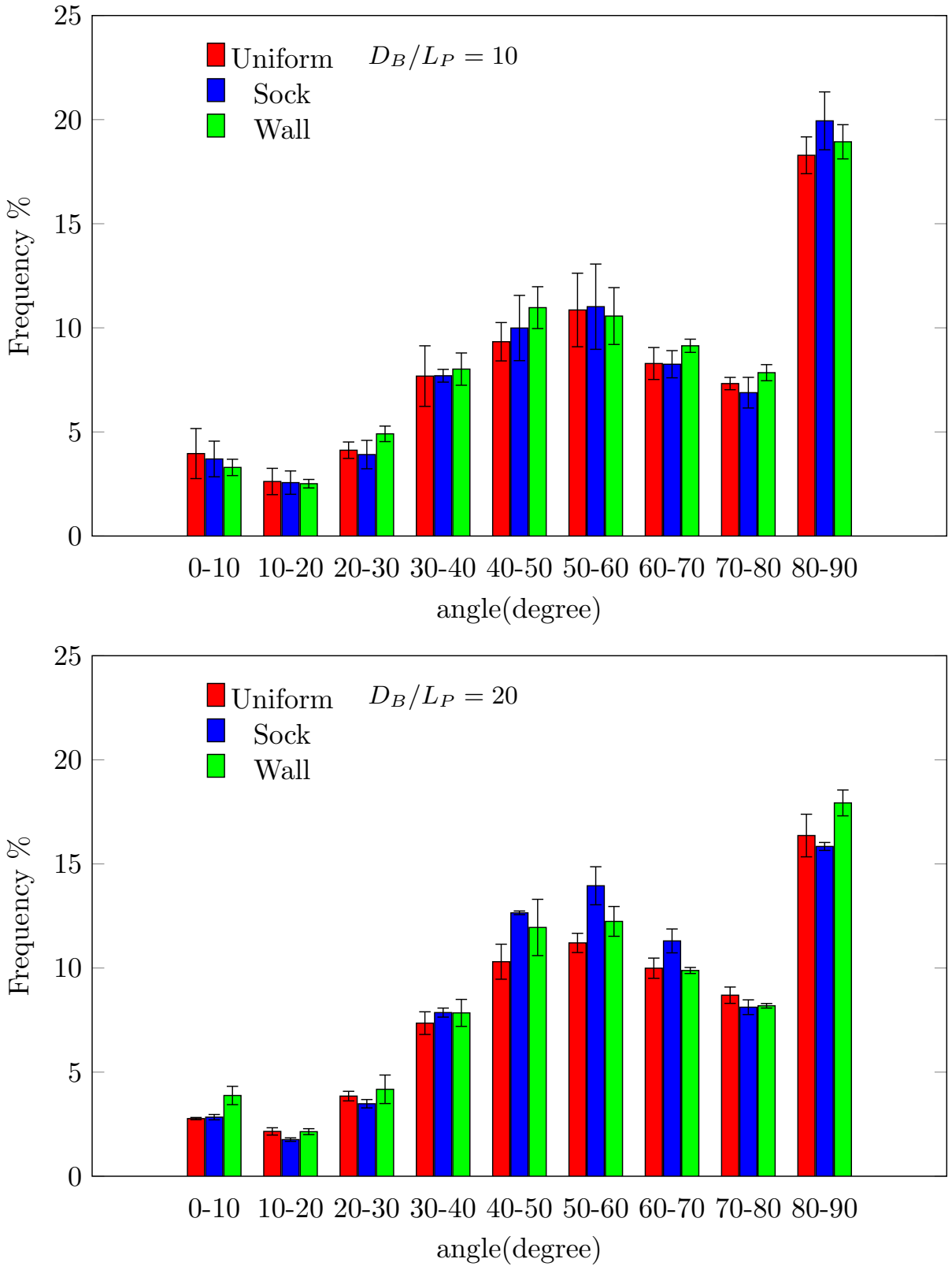

Figure 5.7: Orientation distribution with vertical axis for equilateral cylinders

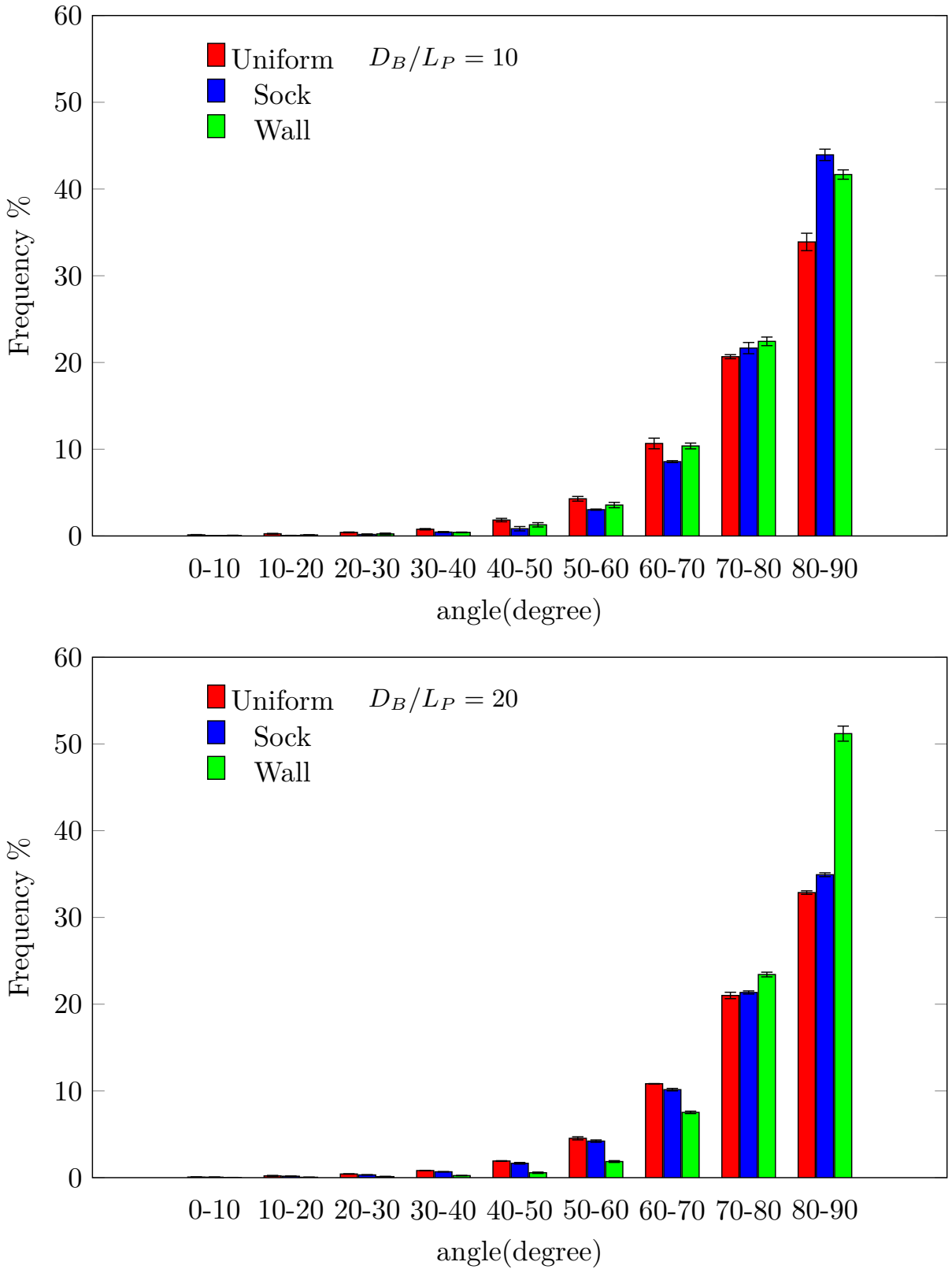

Figure 5.8: Orientation distribution with vertical axis for non equilateral cylinders

Figure 5.9 shows the alignment of particles in radial direction for case of equilateral cylinders. As can be seen particles show a preference to align either along the radial direction or perpendicular to it with other alignments present as well. This behavior is consistently seen with all loading methods. Figure 5.10 shows the study for non equilateral cylinders. Wall loading shows an increased alignment of particles in the radial direction. A possible reason for this preferential alignment is due to the unhindered settlement of particles along the wall.

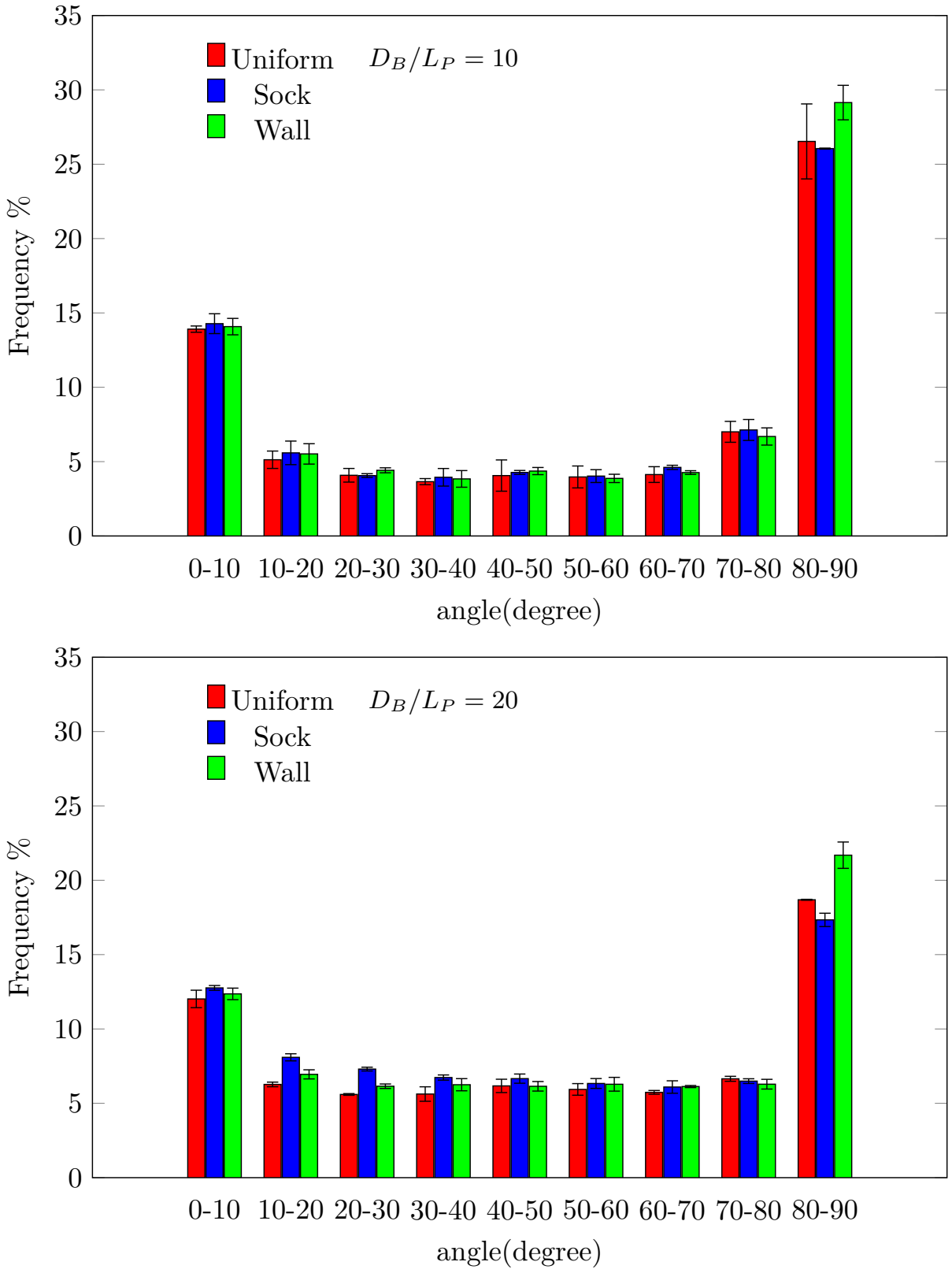

Figure 5.9: Orientation distribution with radial direction for equilateral cylinders

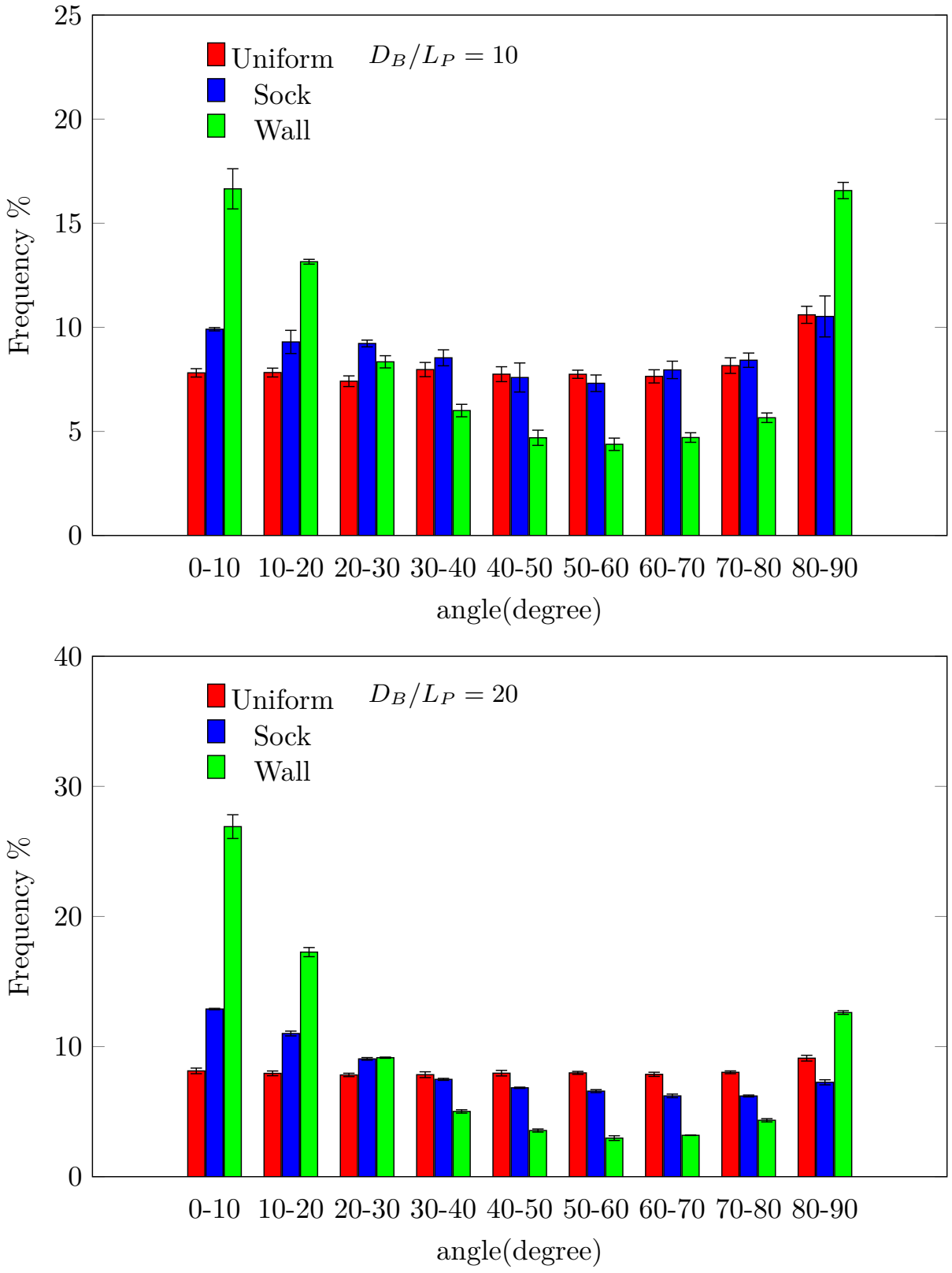

Figure 5.10: Orientation distribution with radial direction for non-equilateral cylinders

From the above results, it can be inferred that loading methods do not influence the voidage parameters. While voidage parameters are important, they do not truly capture the intricate details of packing structures. As can be seen, structures with similar voidage parameters can exhibit varied local orientation resulting in different flow patterns altering the transport properties.

5.3 Conclusions

Discrete Element Method was employed to study the impact of loading methods on the packing configurations generated using cylindrical particles in a circular tube. Three different loading methods employing preferential addition of particles uniformly, in the center of the bed and towards the wall of the bed were studied. Also, the studies were carried out using equilateral cylinders with aspect ratio of 1 and non equilateral cylinders with aspect ratio of 5. While equilateral cylinders exhibited dampening oscillatory profiles in radial voidage towards the center of the bed, non-equilateral cylinders did not show strong oscillations except for the case of wall loading where particles were added along the wall. Also, there was strong difference in the orientation distribution profiles for equilateral and non-equilateral cylinders. While equilateral cylinders showed a range of alignment orientations with the vertical, high aspect ratio cylinders were predominantly horizontal. The equilateral cylinder packing was not influenced by the loading methods employed similar to the behavior of mono disperse spherical particles. Whereas wall loading employed in the study aligned the high aspect ratio particles in the radial direction when compared to other loading methods. It can be concluded that loading methods tend to impact the packing configurations generated in the beds and should be taken into consideration for future studies especially in low bed-particle diameter cases.

6. FLUID FLOW MODELING

6.1 Overview

The bed geometries generated from the DEM simulations using different loading methods were studied using Computational Fluid Dynamics. Initial set of validation studies were performed on monodisperse sphere beds packed with uniform loading for $D_B/D_p \sim 8$ and a bed height $h \sim 15D_P$. The model validation was performed by comparing the interstitial velocities profiles and overall pressure drop with experimental data and correlations. Mesh independence was established by varying the mesh size until no further change in the accuracy of solution was noticed. After finalizing the model and mesh parameters, the influence of loading methods and polydispersity was studied using beds with $D_B/D_p \sim 20$. Among bed generation, meshing and solving for the constitutive equations, meshing is the most computationally intensive parts and limits the size of geometries that can be investigated [103] . This addressed by suitably modifying the size of geometries investigated for fluid flow analysis. In the initial mesh parametric studies of spherical particle packing, beds with D_B/D_p of 8 and height of $15D_p$ was chosen for the simulation. After finalizing the mesh parameters, the influence of polydispersity and loading methods was studied using D_B/D_p of 20. As meshing of the entire bed is not viable, the volume of the bed investigated is modified. The symmetry of the bed is exploited to prepare a suitable flow domain. Tabib *et al.* [148] has demonstrated that CFD analysis of sections of large scale industrial reactors can provide insights into velocity profiles and pressure drop within the bed. They identified a bed length $\sim 5D_P$ to simulate flow fields devoid of entrance effects. Also, as the loading methods employed exhibit radial symmetry, the fluid flow simulation was performed in a quarter of the bed volume. Thus for beds with larger diameters, flow analysis was performed over a bed height of $5D_P$ and a quarter section of the bed.

6.2 Geometry Description and Meshing

The stationary bed obtained by employing different loading methods serves as the geometry for fluid flow analysis. The solid particles (spheres and cylinders) and the bed tube obtained from the DEM simulations are converted to CAD geometries. CAD geometries are topographical representations of the solid particles and bed tube using faces, edges and vertices and provide an approximate representation of the particle and bed shape. The interstitial flow domain is obtained through a series of boolean and meshing operations over which the conservation equations are solved.

The CAD geometries imported from DEM simulations are initially remeshed using a surface remesher. This remeshing performs two important operations of generating a smooth mesh and eliminating the contact points by using the method of caps [11, 103]. After generating the surface mesh, the volume of the interstitial domain is meshed with a combination of prism layer and polyhedral meshing. Velocity inlet was set as the boundary condition at the inlet of the bed and the outlet of the bed was set to atmospheric pressure. The catalyst and bed wall were set to no-slip boundary condition. For the case of large beds, the planes restricting the bed to a quarter segment were set to symmetric plane conditions. The bed was extruded outward for a length of $2D_P$ at inlet and $15D_P$ at outlet to minimize re-circulations and facilitate smooth convergence.

6.3 Implementation

The entire set of simulations were performed using STAR-CCM + 12.06.011 version on a LINUX based IBM/Lenovo x86 HPC Cluster super computer facility capable of parallelization provided by Texas A&M University.

6.4 Results And Discussions

6.4.1 Parameter Selection and Validation

Initial hydrodynamic investigations were performed to obtain the overall pressure drop and the results were compared with the correlation of Einsfeld and Schnitzlen [30]. This correlation was chosen as it accounts for the influence of bed-particle diameter ratio give by

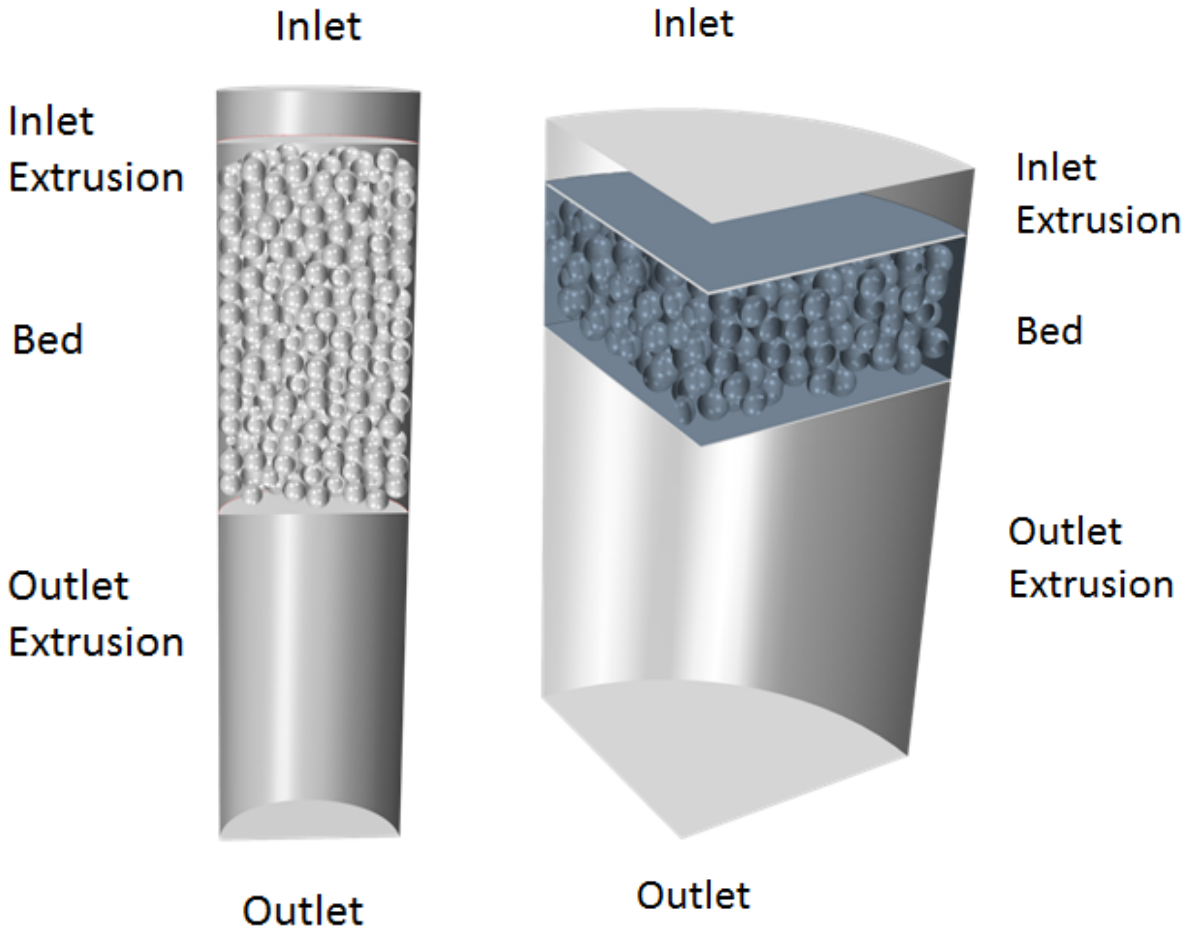

(a) Validation studies

(b) Loading studies

Figure 6.1: Bed geometries used for fluid dynamics analysis

$$\frac{\Delta p}{H} = A\frac{\mu_g(1-\epsilon)^2}{d_p^2\epsilon^3}U_{in} + B\frac{(1-\epsilon)\rho_g U_{in}^2}{d_p\epsilon^3} \tag{6.1}$$

$$A = 154\left(1 + \frac{1}{3}\frac{d_p}{R(1-\epsilon}\right)^2 \qquad B = \left[1 + \frac{1}{3}\frac{d_p}{R}\frac{1}{1-\epsilon}\right]\left[1.50\left(\frac{d_p}{2R}\right)^2 + 0.87\right]^{-2}$$

Simulations were carried out with air as the fluid and the properties listed in Table 6.1.

Table 6.1: Thermophysical properties of air used for simulation

Property	**Value**	**Units**
Density	1.18415	kg/m^3
Dynamic Viscosity	1.855e-5	Pa-s

Hydrodynamic studies were performed by varying the particle Reynolds Number between $100, 200, 300, 500$ and 1000. A base size representative of the geometry is chosen and the remaining parameters related to surface proximity, surface size, prism layer thickness and polyhedral mesh fixed relative to the base size. The parameters were obtained from similar studies used to study fluid flow among spherical particles and are listed in Table 6.2 [104, 157].

Table 6.2: Mesh Parameters used for the simulation

Property	**Value**
Base size	3 - 6.35 mm
Surface Size	4-10 %
Surface Growth Rate	1.5
Prism Thickness	3 %
Number of Prism layers	2
Minimum distance between Surfaces	10 %

Figure 6.2 shows the predicted pressure drop compared with Eisfeld and Schnitzlien correlation [30]. It can be seen that the overall pressure drop increases with inlet velocity. A maximum deviation of 17% was observed for all the meshes which is within the engineering approximations for design. With mesh refinement, it can be seen that the results do not change significantly establishing grid independence. As can be seen from Table 6.3 selection of fine mesh increases the mesh cells without any significant increase in the accuracy of the predictions. Therefore, a mesh with base size of 3.5 mm was used for the rest of the simulations.

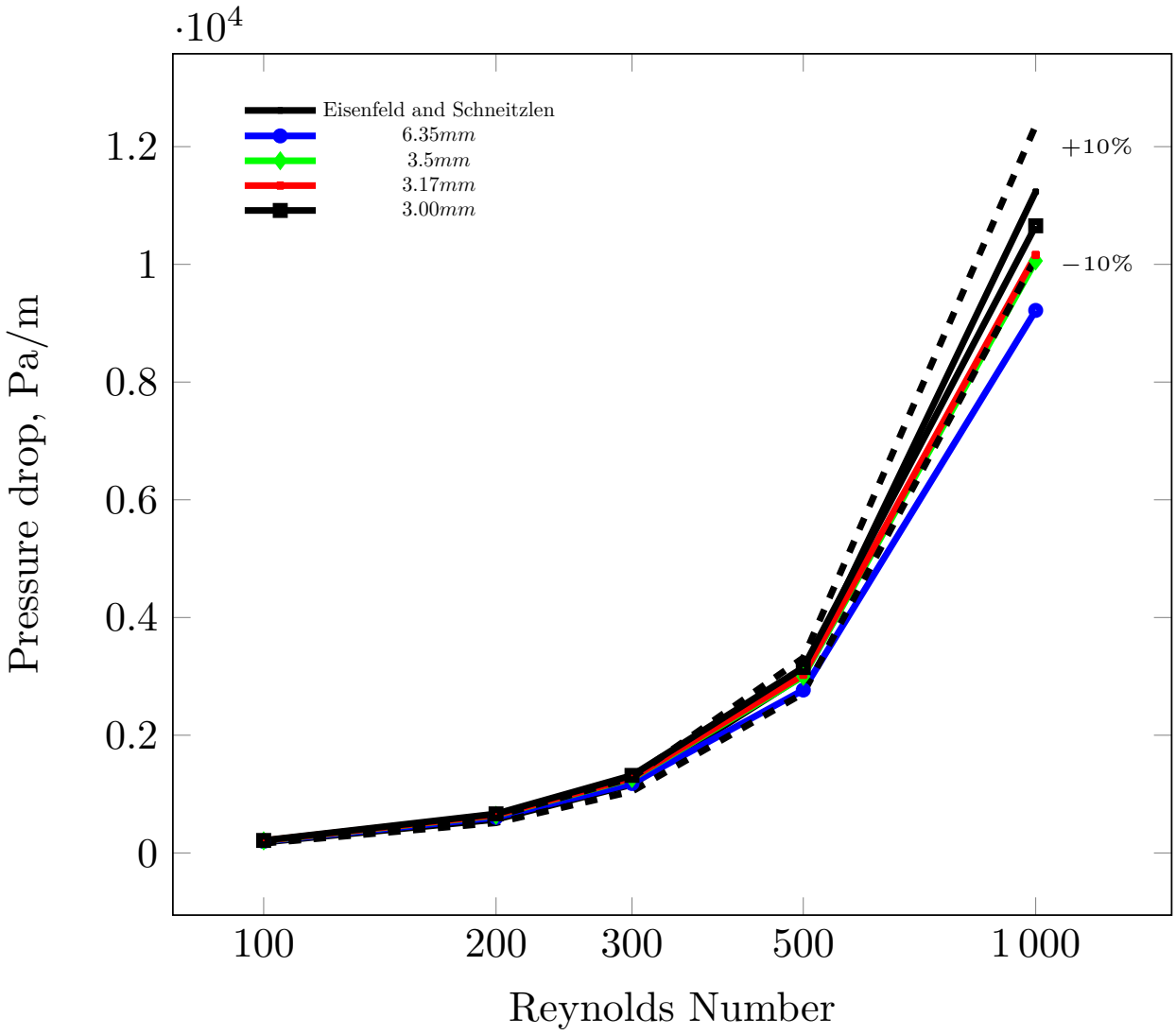

Figure 6.2: Predicted pressure drop compared with Eisenfeld and Schneitzlen correlation [30]

Table 6.3: Mesh cells and error% with base size parameter

Base Size	**Number of cells** $[10^6]$	**Maximum Error**
6.35 mm	2.20	17.95
3.50 mm	6.89	10.46
3.17 mm	8.89	9.56
3.00 mm	11.36	5.16

Further model validation was performed by comparing the normalized axial velocities in a bed with $D_B/D_P = 8$ for $Re = 532$ with the work of Giese *et al.* [166] where light dopplometry was used to measure axial velocities in beds with $D_B/D_P = 9.3$. It can be seen from Figure 6.3 that the model predictions are in good agreement with the experimental work near the wall with deviations increasing towards the center of the bed. A possible difference could be arising from the different packing material and bed diameters in both the studies.

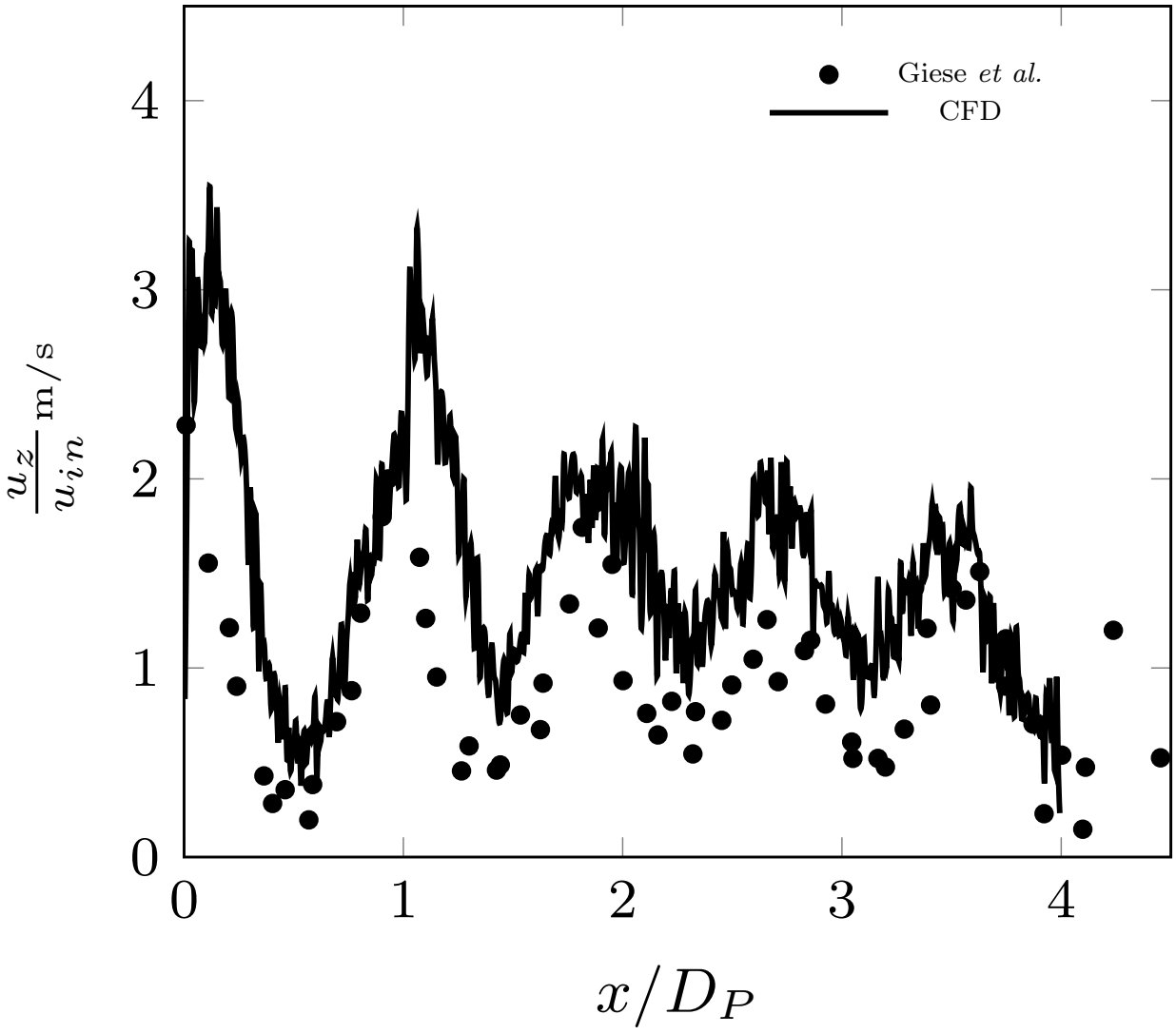

Figure 6.3: Comparison of axial velocities with experimental data [166]

Figure 6.4 represents the velocity magnitudes in the interstitial flow domain along the plane $z = 0$. The interstitial flow velocities reach magnitudes ~ 10 the inlet velocity and show significant deviations from the assumed plug flow behavior. This is a significant deviation from the ideal behavior predicted by the homogeneous or porous models discussed in Chapter 2. As can be seen from the Figure 6.4, the distribution of these velocities is dependent on the presence of narrow throats in the fixed bed and has to accounted for while analyzing the reactors. This mandates study of the local solid structure in fixed beds to develop mechanistic models.

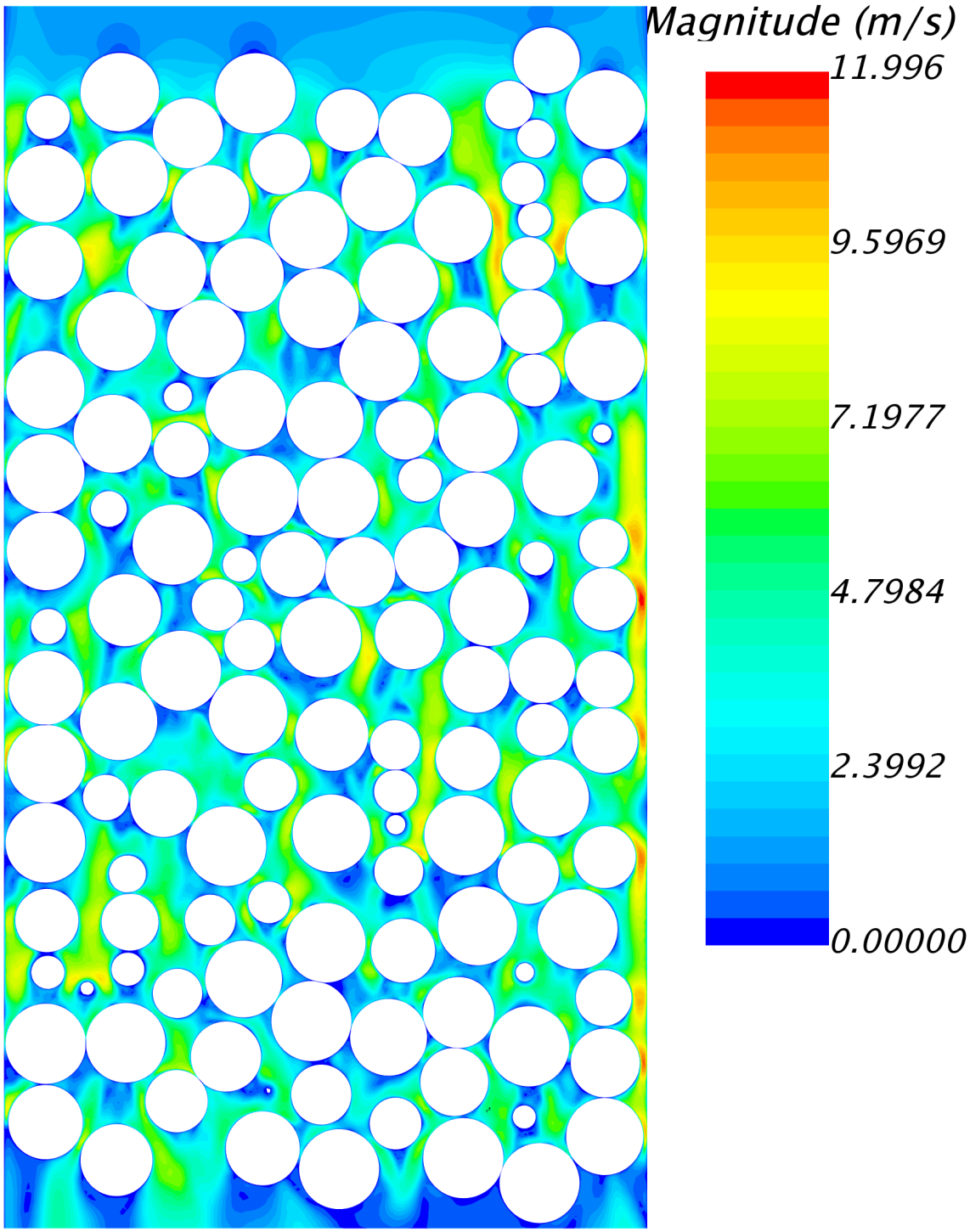

Figure 6.4: Velocity profiles of interstitial flow for $Re = 532$ along the plane $y = 0$

After the initial validation studies, impact of the loading methods and the polydispersity on fluid flow were studied. Prior to this analysis, the minimum bed length required to capture developed flow profile was investigated . Pressure drop measurements were made against the bed height as shown in Figure 6.5. It can be seen that after an entry length of $2.5D_P$, the variation of pressure drop with length becomes linear indicative of developed flow. This length will further decrease in case of poly-disperse mixtures and cylinders as the re-distribution of fluid is more significant in them owing to their random nature of packing.

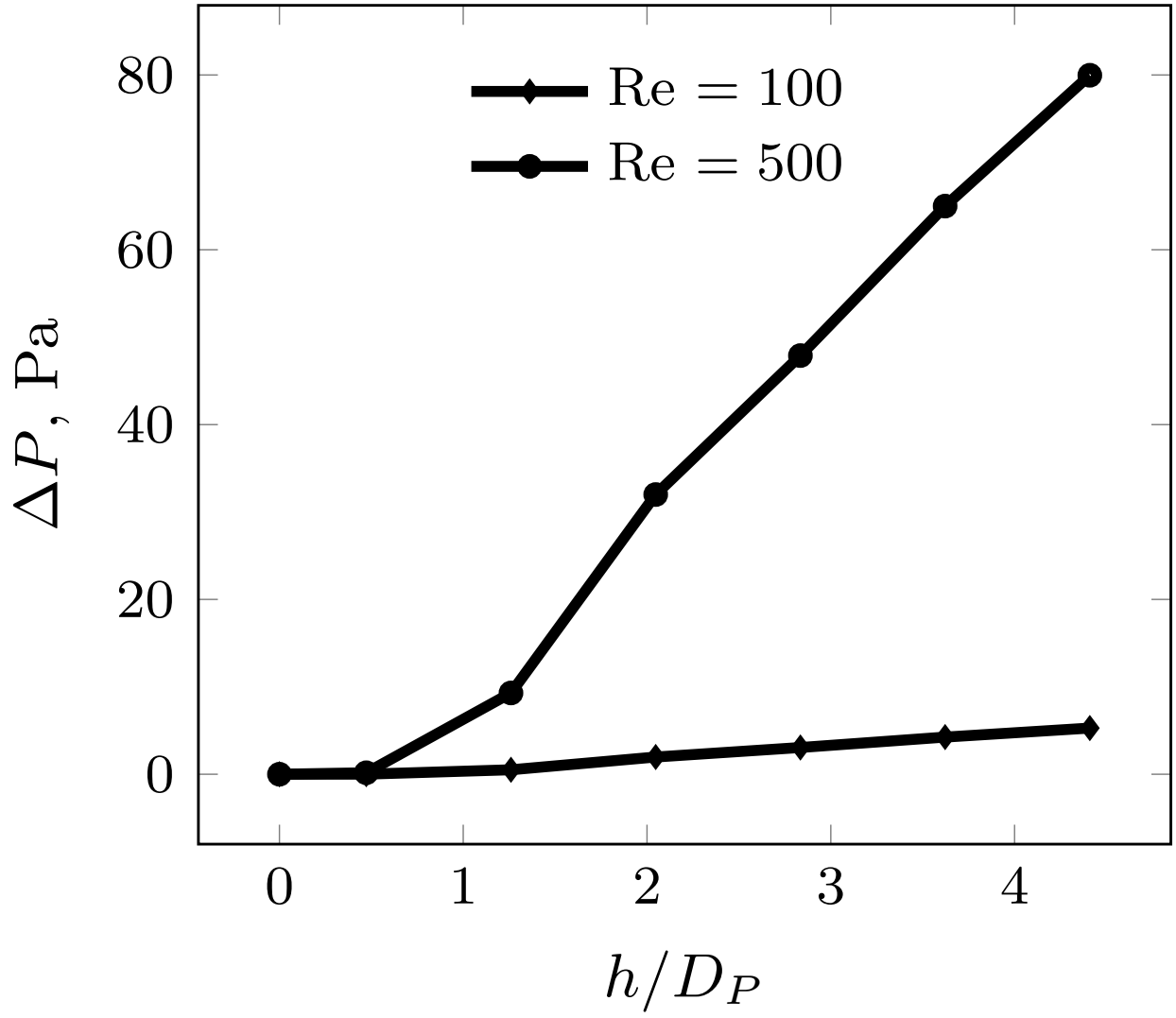

Figure 6.5: Variation of pressure drop with bed height

A total of six beds (three monodisperse and three polydisperse) corresponding to each loading method were studied. Each of the bed was simulated for two different inlet velocities of $v = 0.246m/s$ with $Re = 100$ corresponding to laminar flow and $v = 1.23m/s$ with $Re = 500$ corresponding to turbulent flow.

6.4.2 Velocity Profiles

Figure 6.6 shows the circumferential averaged velocity profiles across the bed height. The averaged velocity profiles do not show any dependency on the loading methods or the polydispersity.

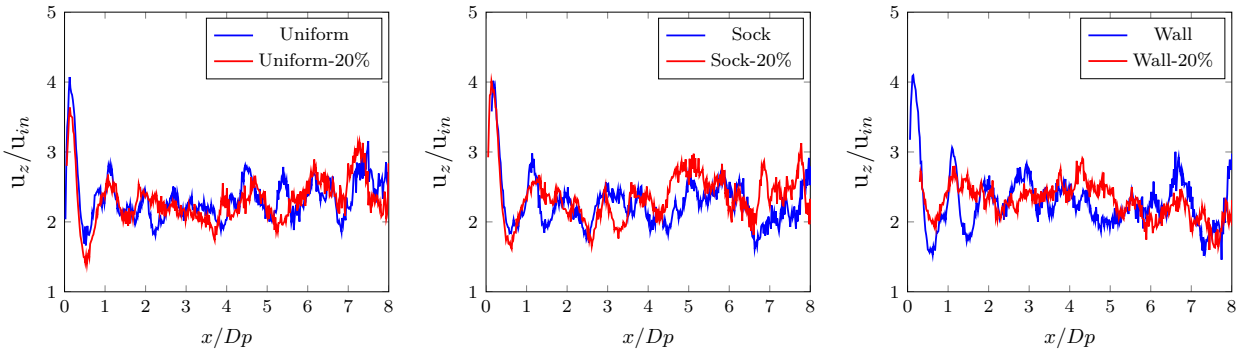

Figure 6.6: Circumferential averaged velocities across the bed height on a radial plane $\theta = 45$ for $Re = 100$

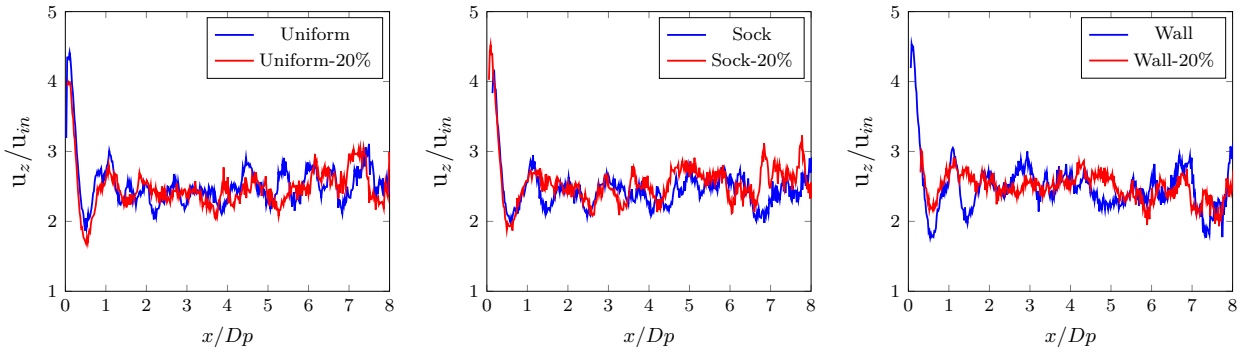

Figure 6.7: Circumferential averaged velocities across the bed height on a radial plane $\theta = 45$ for $Re = 500$

Figure 6.8 shows the interstitial velocity profiles on a radial plane. The plane shows distribution of the spheres and the interstitial velocities. It can be seen that zones with interstitial velocity ~ 10 times inlet velocity are observed. The position of these zones is dependent on the presence of narrow throats and is more prominent in the case of poly-disperse mixtures. Also wall loading shows higher distribution of the narrow throats when compared to sock and wall loading. The behavior is similar for the case of $Re = 500$ with increase in magnitudes of interstitial velocity.

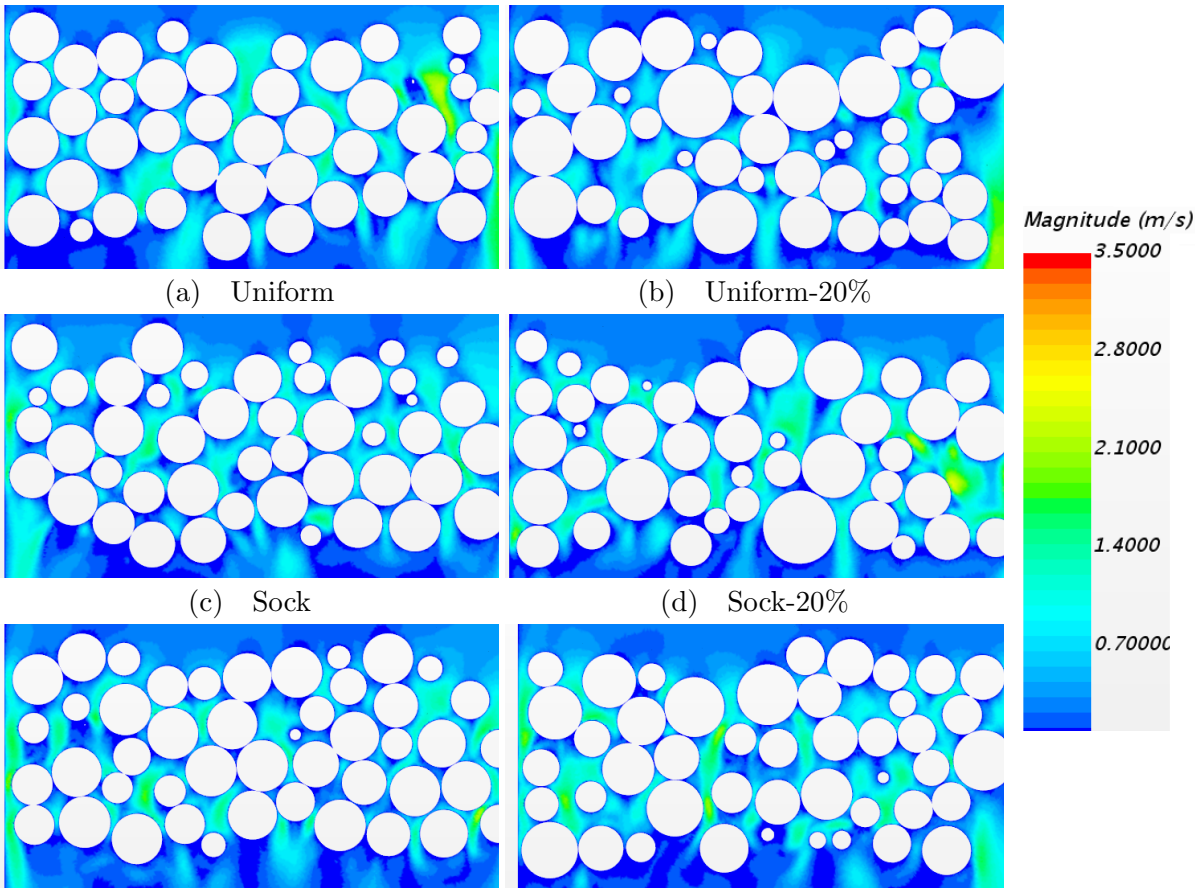

(a) Uniform (b) Uniform-20%

(c) Sock (d) Sock-20%

(e) Wall (f) Wall -20%

Figure 6.8: Velocity profiles on a radial plane $\theta = 45$ for $Re = 100$

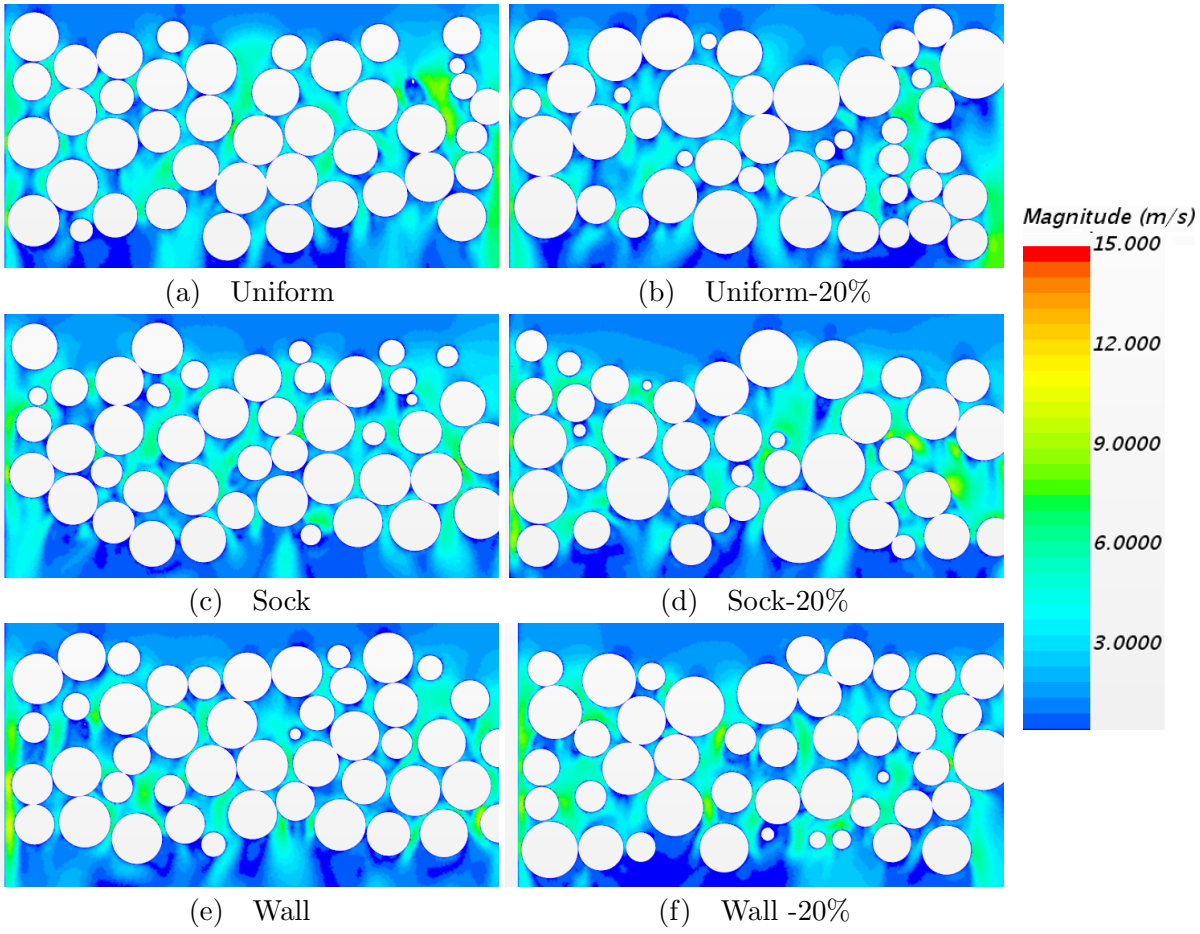

(a) Uniform (b) Uniform-20%

(c) Sock (d) Sock-20%

(e) Wall (f) Wall -20%

Figure 6.9: Velocity profiles on a radial plane $\theta = 45$ for $Re = 500$

6.5 Conclusions

The loading and poly-dispersity samples of spherical particles developed using DEM simulations were subjected to fluid dynamics analysis. Suitable mesh processing was performed on these geometries to develop robust meshes. The model validity was established by comparing the velocity profiles and pressure drop with experimental data and correlations. The analysis was further extended to larger beds to study the influence of loading methods and poly-dispersity. In order to minimize the meshing and computational issues, bed length required for developed flow was identified as $\sim 5D_p$. This bed height was used to compare interstitial flow profiles in DEM gen-

erated beds. Although, averaged axial velocity profiles did not show any variation with loading methods and poly-dispersity, the interstitial flow profiles were different for loading methods and poly-dispersity. Local velocities as high as ~ 10 inlet velocities were noticed and distribution of these velocities is dependent on the presence of narrow throats within the bed. From this study, it can be concluded that local velocity distributions can be significantly different to the inlet velocity. The velocity profiles are strongly dependent on the solid structure, which needs to be accounted for analyzing fixed beds and this study provided a reliable workflow to draw insights into fixed bed operation, which were otherwise not possible with homogeneous and lumped models.

7. CONCLUSIONS AND RECOMMENDATIONS

The current work intended to develop a workflow which could investigate the effect of the loading methods, particle shape and poly-dispersity on fixed-bed behavior through following three aims:

- Develop a methodology to assemble a packing of spherical particles inclusive of the poldispersity of packing sample and loading methodology.
- Develop a methodology to assemble a packing of cylinders of different aspect ratios inclusive of loading methodology.
- Develop a computational fluid dynamics framework to study the impact of the particle scale geometry on the fluid flow behavior in a gas-solid downflow reactor.

The objectives were attained by employing a combination of Discrete Element Methods and Computational Fluid Dynamic tools using the academic license of STAR-CCM + v $12.06.011$ package.

In Chapter 4, three different loading methods *Uniform, Sock* and *Wall* were employed to study packing of spherical particles. Sphere particle packing was generated using glass particles in a cylindrical tube. The simulations were carried out in D_B/D_P of $8, 14$ and 20 representative of commonly used multi-tube reactors and for D_P of $0.00635m$. In addition, the particle sample poly-dispersity was varied with 0%,10% and 20% dispersity. The packing structures were evaluated by measuring the bulk voidage, radial voidage and bed tortuosity. It was observed that polydisperisty alters the radial voidage by dampening the wall induced oscillations. Loading methods did not alter the packing structure in the case of mono-disperse spheres, however segregation of particles based on the particle size was observed in the case of poly-disperse mixtures. Sock loading lead to a decrease in particle size from center to wall, whereas the wall loading created an opposite trend where larger particles settled at the wall and smaller particles were found in the center of the bed.

In Chapter 5, similar packing exercises were carried out for cylinder particles with D_P of $0.00635m$ and aspect ratio of 1 and 5. The simulations were performed for D_B/D_P of 10 and 20. The beds were analyzed for radial voidage and particle orientation distributions. The behavior of uniform cylinders was similar to the trends exhibited with mono-disperse particle packing. However, the oscillations in radial voidage were dampened when compared to the spherical counterparts. For the case of high aspect ratio cylinders, the behavior was significantly different with minimized oscillations. Among the three loading methods for high aspect ratio cylinders, wall loading showed stronger oscillations compared to uniform and sock loading. The loading methods impacted the particle orientation distributions for the cylinder particles. While all the three loading methods created particles being aligned with the floor, wall loading created a strong alignment in the radial direction when compared to uniform and sock loading. This results in creation of isotropic voidages.

In Chapter 6, Computational Fluid Dynamics analysis was carried on the packed beds of spherical particles prepared with different loading methods and polydisperse mixtures of dispersity $\sim 20\%$. The model was validated by comparing overall pressure drop and axial velocity profiles and a good match with experimental data was observed. As scale of geometry that can be analyzed is a limiting factor, suitable representative geometries were identified that could provide good insights into operation of fixed-bed reactors. Model predicts varying velocity profiles across the bed cross-section dependent on the local solid structure. This causes different transport and reactive activity in the bed and needs to be accounted for while modeling fixed beds.

The research work developed a workflow to analyze loading methods and their impact on the behavior of fixed-beds. The Discrete Element Method has been proven to be an effective strategy to study the fixed bed structures and has been applied to study loading. The methodology could be extended to following studies:

- In the current study, loading of particles was studied in presence of air as surrounding fluid. Settling of particles is impacted by the viscous drag of surrounding fluid and can be investigated using the DEM methods.

- The DEM methods were applied to spherical and cylindrical particle packing structures and can be extended to trilobes and other cylinder like particles.
- The aging behavior of these beds could be studied by subjecting beds to vibration and tapping.
- The flow behavior among spherical particles was analyzed in this study and could be extended to other shapes of relevance.
- In addition to flow studies, energy distribution can also be studied using CFD to obtain the axial and radial conductivity parameters in fixed beds.
- Species balance can be performed to study the behavior of relevant industrial reactions.
- The models can be suitably extended to two phase flow analysis which are quite pivotal in Trickle Bed Reactors.

REFERENCES

[1] P. N. Dwivedi and S. Upadhyay, "Particle-fluid mass transfer in fixed and fluidized beds," *Industrial and Engineering Chemistry Process Design and Development*, vol. 16, no. 2, pp. 157–165, 1977.

[2] J. Ellenberger and R. Krishna, "Counter-current operation of structured catalytically packed distillation columns: pressure drop, holdup and mixing," *Chemical Engineering Science*, vol. 54, no. 10, pp. 1339–1345, 1999.

[3] M. P. Dudukovic, F. Larachi, and P. L. Mills, "Multiphase reactors–revisited," *Chemical Engineering Science*, vol. 54, no. 13-14, pp. 1975–1995, 1999.

[4] M. P. Duduković, F. Larachi, and P. L. Mills, "Multiphase catalytic reactors: a perspective on current knowledge and future trends," *Catalysis Reviews*, vol. 44, no. 1, pp. 123–246, 2002.

[5] V. V. Ranade, R. Chaudhari, and P. R. Gunjal, *Trickle bed reactors: Reactor engineering and applications*. Elsevier, 2011.

[6] G. Eigenberger and W. Ruppel, "Catalytic fixed-bed reactors," *Ullmann's Encyclopedia of Industrial Chemistry*, 2000.

[7] G. Q. Wang, X. G. Yuan, and K. T. Yu, "Review of mass-transfer correlations for packed columns," *Industrial and Engineering Chemistry Research*, vol. 44, no. 23, pp. 8715–8729, 2005.

[8] J. B. Powell, "Application of multiphase reaction engineering and process intensification to the challenges of sustainable future energy and chemicals," *Chemical Engineering Science*, vol. 157, pp. 15–25, 2017.

[9] M. P. Dudukovic, "Challenges and innovations in reaction engineering," *Chemical Engineering Communications*, vol. 196, no. 1-2, pp. 252–266, 2008.

[10] M. P. Dudukovic, "Reaction engineering: Status and future challenges," *Chemical Engineering Science*, vol. 65, no. 1, pp. 3–11, 2010.

[11] A. G. Dixon, "Local transport and reaction rates in a fixed bed reactor tube: Endothermic steam methane reforming," *Chemical Engineering Science*, vol. 168, pp. 156–177, 2017.

[12] R. K. Lyon and J. A. Cole, "Unmixed combustion: an alternative to fire," *Combustion and Flame*, vol. 121, no. 1-2, pp. 249–261, 2000.

[13] Z. A. Aboosadi, M. Rahimpour, and A. Jahanmiri, "A novel integrated thermally coupled configuration for methane-steam reforming and hydrogenation of nitrobenzene to aniline," *International Journal of Hydrogen Energy*, vol. 36, no. 4, pp. 2960–2968, 2011.

[14] R. Anderson, L. Bates, E. Johnson, and J. F. Morris, "Packed bed thermal energy storage: A simplified experimentally validated model," *Journal of Energy Storage*, vol. 4, pp. 14–23, 2015.

[15] J.-C. Charpentier and M. Favier, "Some liquid holdup experimental data in trickle-bed reactors for foaming and nonfoaming hydrocarbons," *AIChE Journal*, vol. 21, no. 6, pp. 1213–1218, 1975.

[16] C. N. Satterfield, "Trickle-bed reactors," *AIChE Journal*, vol. 21, no. 2, pp. 209–228, 1975.

[17] Y. Wu, M. R. Khadilkar, M. H. Al-Dahhan, and M. P. Duduković, "Comparison of upflow and downflow two-phase flow packed-bed reactors with and without fines: experimental observations," *Industrial and Engineering Chemistry Research*, vol. 35, no. 2, pp. 397–405, 1996.

[18] F. Larachi, A. Laurent, N. Midoux, and G. Wild, "Experimental study of a trickle-bed reactor operating at high pressure: two-phase pressure drop and liquid saturation," *Chemical Engineering Science*, vol. 46, no. 5-6, pp. 1233–1246, 1991.

[19] W. Wammes, J. Middelkamp, W. Huisman, C. DeBass, and K. Westerterp, "Hydrodynamics in a cocurrent gas-liquid trickle bed at elevated pressures," *AIChE journal*, vol. 37, no. 12, pp. 1849–1862, 1991.

[20] M. Ellman, N. Midoux, A. Laurent, and J. Charpentier, "A new, improved pressure drop correlation for trickle-bed reactors," in *Tenth International Symposium on Chemical Reaction Engineering*, pp. 2201–2206, Elsevier, 1988.

[21] N. L. Nguyen, V. van Buren, R. Reimert, and A. von Garnier, "Determination of porosity and flow distribution in packed beds by magnetic resonance imaging," *Magnetic Resonance Imaging*, vol. 23, no. 2, pp. 395–396, 2005.

[22] L. Gladden, L. Anadon, C. Dunckley, M. Mantle, and A. Sederman, "Insights into gas–liquid–solid reactors obtained by magnetic resonance imaging," *Chemical Engineering Science*, vol. 62, no. 24, pp. 6969–6977, 2007.

[23] R. J. Lopes and R. M. Quinta-Ferreira, "Cfd modelling of multiphase flow distribution in trickle beds," *Chemical Engineering Journal*, vol. 147, no. 2-3, pp. 342–355, 2009.

[24] K. M. Brunner, H. D. Perez, R. P. Peguin, J. C. Duncan, L. D. Harrison, C. H. Bartholomew, and W. C. Hecker, "Effects of particle size and shape on the performance of a trickle fixed-bed recycle reactor for fischer–tropsch synthesis," *Industrial and Engineering Chemistry Research*, vol. 54, no. 11, pp. 2902–2909, 2015.

[25] S. Afandizadeh and E. Foumeny, "Design of packed bed reactors: guides to catalyst shape, size, and loading selection," *Applied Thermal Engineering*, vol. 21, no. 6, pp. 669 – 682, 2001.

[26] A. G. Dixon, "Wall and particle-shape effects on heat transfer in packed beds," *Chemical Engineering Communications*, vol. 71, no. 1, pp. 217–237, 1988.

[27] F. Benyahia, "On the global and local structural properties of packed beds of nonequilateral cylindrical particles," *Particulate Science and Technology*, vol. 14, no. 3, pp. 221–237, 1996.

[28] F. Benyahia and K. E. O'Neill, "Enhanced Voidage Correlations for Packed Beds of Various Particle Shapes and Sizes," *Particulate Science and Technology*, vol. 23, no. 2, pp. 169–177, 2005.

[29] S. Ergun and A. A. Orning, "Fluid flow through randomly packed columns and fluidized beds," *Industrial and Engineering Chemistry*, vol. 41, no. 6, pp. 1179–1184, 1949.

[30] B. Eisfeld and K. Schnitzlein, "The influence of confining walls on the pressure drop in packed beds," *Chemical Engineering Science*, vol. 56, no. 14, pp. 4321–4329, 2001.

[31] D. Nemec and J. Levec, "Flow through packed bed reactors: 1. single-phase flow," *Chemical Engineering Science*, vol. 60, no. 24, pp. 6947–6957, 2005.

[32] J. Reimann, J. Vicente, E. Brun, C. Ferrero, Y. Gan, and A. Rack, "X-ray tomography investigations of mono-sized sphere packing structures in cylindrical containers," *Powder Technology*, vol. 318, pp. 471–483, 2017.

[33] R. Caulkin, X. Jia, C. Xu, M. Fairweather, R. A. Williams, H. Stitt, M. Nijemeisland, S. Aferka, M. Crine, A. Léonard, D. Toye, and P. Marchot, "Simulations of structures in packed columns and validation by x-ray tomography," *Industrial and Engineering Chemistry Research*, vol. 48, no. 1, pp. 202–213, 2009.

[34] G. E. Mueller, "Radial void fraction distributions in randomly packed fixed beds of uniformly sized spheres in cylindrical containers," *Powder Technology*, vol. 72, pp. 269–275, nov 1992.

[35] G. E. Mueller, "Radial porosity in packed beds of spheres," *Powder Technology*, vol. 203, no. 3, pp. 626–633, 2010.

[36] G. E. Mueller, "A simple method for determining sphere packed bed radial porosity," *Powder Technology*, vol. 229, pp. 90–96, 2012.

[37] W. Zhang, K. E. Thompson, A. H. Reed, and L. Beenken, "Relationship between packing structure and porosity in fixed beds of equilateral cylindrical particles," *Chemical Engineering Science*, vol. 61, pp. 8060–8074, dec 2006.

[38] M. Bazmi, S. H. Hashemabadi, and M. Bayat, "Extrudate trilobe catalysts and loading effects on pressure drop and dynamic liquid holdup in porous media of trickle bed reactors," *Transport in Porous Media*, vol. 99, no. 3, pp. 535–553, 2013.

[39] M. Bazmi, S. H. Hashemabadi, and M. Bayat, "Flow maldistribution in dense and sock loaded trilobe catalyst trickle bed reactors: Experimental data and modeling using neural network," *Transport in Porous Media*, vol. 97, no. 1, pp. 119–132, 2013.

[40] A. G. Dixon, "CFD study of effect of inclination angle on transport and reaction in hollow cylinder catalysts," *Chemical Engineering Research and Design*, vol. 92, no. 7, pp. 1279 – 1295, 2014.

[41] S. Sharma, M. D. Mantle, L. F. Gladden, and J. M. Winterbottom, "Determination of bed voidage using water substitution and 3D magnetic resonance imaging, bed density and pressure drop in packed-bed reactors," *Chemical Engineering Science*, vol. 56, no. 2, pp. 587–595, 2001.

[42] C. Du Toit, "Radial variation in porosity in annular packed beds," *Nuclear Engineering and Design*, vol. 238, no. 11, pp. 3073–3079, 2008.

[43] A. de Klerk, "Voidage variation in packed beds at small column to particle diameter ratio," *AIChE Journal*, vol. 49, no. 8, pp. 2022–2029, 2003.

[44] M. Suzuki, T. Shinmura, K. Iimura, and M. Hirota, "Study of the wall effect on particle packing structure using x-ray micro computed tomography," *Advanced Powder Technology*, vol. 19, pp. 183–195, mar 2008.

[45] D. Gunn, "Transfer of heat or mass to particles in fixed and fluidised beds," *International Journal of Heat and Mass Transfer*, vol. 21, no. 4, pp. 467–476, 1978.

[46] O. Bey and G. Eigenberger, "Fluid flow through catalyst filled tubes," *Chemical Engineering Science*, vol. 52, no. 8, pp. 1365–1376, 1997.

[47] C. Boyer, A. Koudil, P. Chen, and M. Dudukovic, "Study of liquid spreading from a point source in a trickle bed via gamma-ray tomography and cfd simulation," *Chemical Engineering Science*, vol. 60, no. 22, pp. 6279–6288, 2005.

[48] R. Holub, M. Duduković, and P. Ramachandran, "A phenomenological model for pressure drop, liquid holdup, and flow regime transition in gas-liquid trickle flow," *Chemical Engineering Science*, vol. 47, no. 9-11, pp. 2343–2348, 1992.

[49] K. Grosser, R. Carbonell, and S. Sundaresan, "Onset of pulsing in two-phase cocurrent downflow through a packed bed," *AIChE Journal*, vol. 34, no. 11, pp. 1850–1860, 1988.

[50] P. Kawatra, S. Panyaram, and B. A. Wilhite, "Hydrodynamics in a pilot-scale cocurrent trickle-bed reactor at low gas velocities," *AIChE Journal*, vol. 64, no. 7, pp. 2560–2569, 2018.

[51] W. Yang and S. Liu, "Role of tomography in gas/solids flow measurement," *Flow measurement and Instrumentation*, vol. 11, no. 3, pp. 237–244, 2000.

[52] Y. T. Makkawi and P. C. Wright, "Electrical capacitance tomography for conventional fluidized bed measurements—remarks on the measuring technique," *Powder Technology*, vol. 148, no. 2-3, pp. 142–157, 2004.

[53] J. Lerou and G. Froment, "Velocity, temperature and conversion profiles in fixed bed catalytic reactors," *Chemical Engineering Science*, vol. 32, no. 8, pp. 853–861, 1977.

[54] V. Balakotaiah and S. M. Dommeti, "Effective models for packed-bed catalytic reactors," *Chemical Engineering Science*, vol. 54, no. 11, pp. 1621–1638, 1999.

[55] A. G. Dixon, M. Nijemeisland, and E. H. Stitt, "Packed tubular reactor modeling and catalyst design using computational fluid dynamics," *Advances in Chemical Engineering*, vol. 31, pp. 307–389, 2006.

[56] R. Carbonell, "Multiphase flow models in packed beds," *Oil and Gas Science and Technology*, vol. 55, no. 4, pp. 417–425, 2000.

[57] CD-Adapco 2014, "STAR- CCM +," 2014.

[58] J. Tallmadge, "Packed bed pressure drop—an extension to higher reynolds numbers," *AIChE Journal*, vol. 16, no. 6, pp. 1092–1093, 1970.

[59] A. Bos, L. V. DE BELD, J. Overkamp, and K. Westerterp, "Behaviour of an adiabatic packed bed reactor part 1: Experimental study," *Chemical Engineering Communications*, vol. 121, no. 1, pp. 27–53, 1993.

[60] R. Westerterp, R. Bos, R. Wijngaarden, W. Kusters, and A. Martens, "Selective hydrogenation of acetylene in an ethylene stream in an adiabatic reactor," *Chemical Engineering and Technology*, vol. 25, no. 5, pp. 529–539, 2002.

[61] N. Wakao, S. Kaguei, and T. Funazkri, "Effect of fluid dispersion coefficients on particle-to-fluid heat transfer coefficients in packed beds: correlation of nusselt numbers," *Chemical Engineering Science*, vol. 34, no. 3, pp. 325–336, 1979.

[62] N. Wakao and S. Kagei, *Heat and mass transfer in packed beds*, vol. 1. Taylor and Francis, 1982.

[63] V. W. Weekman Jr and D. M. Nace, "Kinetics of catalytic cracking selectivity in fixed, moving, and fluid bed reactors," *AIChE Journal*, vol. 16, no. 3, pp. 397–404, 1970.

[64] S. M. Jacob, B. Gross, S. E. Voltz, and V. W. Weekman Jr, "A lumping and reaction scheme for catalytic cracking," *AIChE Journal*, vol. 22, no. 4, pp. 701–713, 1976.

[65] A. Atta, S. Roy, F. Larachi, and K. D. P. Nigam, "Cyclic operation of trickle bed reactors: a review," *Chemical Engineering Science*, vol. 115, pp. 205–214, 2014.

[66] B. Wilhite, B. Blackwell, J. Kacmar, A. Varma, and M. McCready, "Origins of pulsing regime in cocurrent packed-bed flows," *Industrial and Engineering Chemistry Research*, vol. 44, no. 16, pp. 6056–6066, 2005.

[67] J. Guilleminot, A. Choisier, J. Chalfen, S. Nicolas, and J. Reymoney, "Heat transfer intensification in fixed bed adsorbers," *Heat Recovery Systems and CHP*, vol. 13, no. 4, pp. 297–300, 1993.

[68] H. Deans and L. Lapidus, "A computational model for predicting and correlating the behavior of fixed-bed reactors: I. derivation of model for nonreactive systems," *AIChE Journal*, vol. 6, no. 4, pp. 656–663, 1960.

[69] M. Sheintuch and O. Nekhamkina, "Pattern formation in homogeneous reactor models," *AIChE Journal*, vol. 45, no. 2, pp. 398–409, 1999.

[70] G. Viswanathan, D. Luss, A. Bindal, and J. Khinast, "Stationary transversal hot zones in adiabatic packed-bed reactors," *AIChE Journal*, vol. 51, no. 11, pp. 3028–3038, 2005.

[71] P. Ramachandran and J. Smith, "Mixing-cell method for design of trickle-bed reactors," *The Chemical Engineering Journal*, vol. 17, no. 2, pp. 91–99, 1979.

[72] V. Balakotaiah and D. Luss, "Global analysis of the multiplicity features of multi-reaction lumped-parameter systems," *Chemical Engineering Science*, vol. 39, no. 5, pp. 865–881, 1984.

[73] S. Sundaresan, "Modeling the hydrodynamics of multiphase flow reactors: current status and challenges," *AIChE Journal*, vol. 46, no. 6, pp. 1102–1105, 2000.

[74] P. Ravindra, D. Rao, and M. Rao, "Liquid flow texture in trickle-bed reactors: an experimental study," *Industrial and Engineering Chemistry Research*, vol. 36, no. 12, pp. 5133–5145, 1997.

[75] W. van der Merwe and W. Nicol, "Characterization of multiple flow morphologies within the trickle flow regime," *Industrial and Engineering Chemistry Research*, vol. 44, no. 25, pp. 9446–9450, 2005.

[76] T. Dumas, F. Lesage, and M. Latifi, "Modelling and measurements of the velocity gradient and local flow direction at the pore scale of a packed bed," *Chemical Engineering Research and Design*, vol. 88, no. 3, pp. 379–384, 2010.

[77] E. Tsotsas and H. Martin, "Thermal conductivity of packed beds: a review," *Chemical Engineering and Processing: Process Intensification*, vol. 22, no. 1, pp. 19–37, 1987.

[78] P. C. Watson and M. P. Harold, "Dynamic effects of vaporization with exothermic reaction in a porous catalytic pellet," *AIChE Journal*, vol. 39, no. 6, pp. 989–1006, 1993.

[79] J. Hanika, K. Sporka, V. Ružička, and J. Hrstka, "Measurement of axial temperature profiles in an adiabatic trickle bed reactor," *Chemical Engineering Journal*, vol. 12, no. 3, pp. 193–197, 1976.

[80] W. L. Luyben, "Catalyst dilution to improve dynamic controllability of cooled tubular reactors," *Computers and Chemical Engineering*, vol. 37, pp. 184–190, 2012.

[81] A. Attou, C. Boyer, and G. Ferschneider, "Modelling of the hydrodynamics of the cocurrent gas–liquid trickle flow through a trickle-bed reactor," *Chemical Engineering Science*, vol. 54, no. 6, pp. 785 – 802, 1999.

[82] K. Schnitzlein and H. Hofmann, "An alternative model for catalytic fixed bed reactors," *Chemical Engineering Science*, vol. 42, no. 11, pp. 2569–2577, 1987.

[83] S. Schwidder and K. Schnitzlein, "A new model for the design and analysis of trickle bed reactors," *Chemical Engineering Journal*, vol. 207, pp. 758–765, 2012.

[84] G. A. Funk, M. P. Harold, and K. M. Ng, "A novel model for reaction in trickle beds with flow maldistribution," *Industrial and Engineering Chemistry Research*, vol. 29, no. 5, pp. 738–748, 1990.

[85] M. Khadilkar, M. Al-Dahhan, and M. Duduković, "Multicomponent flow-transport-reaction modeling of trickle bed reactors: application to unsteady state liquid flow modulation," *Industrial and Engineering Chemistry Research*, vol. 44, no. 16, pp. 6354–6370, 2005.

[86] Y. Jiang, J. Guo, and M. H. Al-Dahhan, "Multiphase flow packed-bed reactor modeling: combining cfd and cell network model," *Industrial and Engineering Chemistry Research*, vol. 44, no. 14, pp. 4940–4948, 2005.

[87] W. Du, L. Zhang, S. Lv, P. Lu, J. Xu, and W. Wei, "Numerical study of liquid coverage in a gas–liquid–solid packed bed," *Particuology*, vol. 23, pp. 90–99, 2015.

[88] S. Das, N. G. Deen, and J. Kuipers, "A dns study of flow and heat transfer through slender fixed-bed reactors randomly packed with spherical particles," *Chemical Engineering Science*, vol. 160, pp. 1–19, 2017.

[89] C. Wang and P. Cheng, "A multiphase mixture model for multiphase, multicomponent transport in capillary porous media—i. model development," *International Journal of Heat and Mass Transfer*, vol. 39, no. 17, pp. 3607–3618, 1996.

[90] G. D. Wehinger, T. Eppinger, and M. Kraume, "Evaluating catalytic fixed-bed reactors for dry reforming of methane with detailed cfd," *Chemie Ingenieur Technik*, vol. 87, no. 6, pp. 734–745, 2015.

[91] Z. Solomenko, Y. Haroun, M. Fourati, F. Larachi, C. Boyer, and F. Augier, "Liquid spreading in trickle-bed reactors: Experiments and numerical simulations using eulerian–eulerian two-fluid approach," *Chemical Engineering Science*, vol. 126, pp. 698–710, 2015.

[92] W. J. S. Van der Merwe, *Analysis of flow through cylindrical packed beds with small cylinder diameter to particle diameter ratios*. PhD thesis, 2014.

[93] A. G. Dixon and M. Nijemeisland, "Cfd as a design tool for fixed-bed reactors," *Industrial and Engineering Chemistry Research*, vol. 40, no. 23, pp. 5246–5254, 2001.

[94] Y. Haroun, D. Legendre, and L. Raynal, "Volume of fluid method for interfacial reactive mass transfer: application to stable liquid film," *Chemical Engineering Science*, vol. 65, no. 10, pp. 2896–2909, 2010.

[95] G. D. Wehinger, C. Fütterer, and M. Kraume, "Contact modifications for cfd simulations of fixed-bed reactors: cylindrical particles," *Industrial and Engineering Chemistry Research*, vol. 56, no. 1, pp. 87–99, 2016.

[96] A. G. Dixon, M. Nijemeisland, and E. H. Stitt, "Systematic mesh development for 3d cfd simulation of fixed beds: Contact points study," *Computers and Chemical Engineering*, vol. 48, pp. 135–153, 2013.

[97] F. Mousazadeh, H. van Den Akker, and R. F. Mudde, "Direct numerical simulation of an exothermic gas-phase reaction in a packed bed with random particle distribution," *Chemical Engineering Science*, vol. 100, pp. 259–265, 2013.

[98] M. Behnam, A. G. Dixon, M. Nijemeisland, and E. H. Stitt, "A New Approach to Fixed Bed Radial Heat Transfer Modeling Using Velocity Fields from Computational Fluid Dynamics Simulations BT - Industrial and Engineering Chemistry Research," *Industrial and Engineering Chemistry Research*, vol. 52, pp. 15244–15261, 2013.

[99] G. D. Wehinger, M. Kraume, V. Berg, O. Korup, K. Mette, R. Schlögl, M. Behrens, and R. Horn, "Investigating dry reforming of methane with spatial reactor profiles and particle-resolved cfd simulations," *AIChE Journal*, vol. 62, no. 12, pp. 4436–4452, 2016.

[100] B. Partopour and A. G. Dixon, "Reduced microkinetics model for computational fluid dynamics (cfd) simulation of the fixed-bed partial oxidation of ethylene," *Industrial and Engineering Chemistry Research*, vol. 55, no. 27, pp. 7296–7306, 2016.

[101] B. Partopour and A. G. Dixon, "Computationally efficient incorporation of microkinetics into resolved-particle cfd simulations of fixed-bed reactors," *Computers and Chemical Engineering*, vol. 88, pp. 126–134, 2016.

[102] P. R. Gunjal, V. V. Ranade, and R. V. Chaudhari, "Computational study of a single-phase flow in packed beds of spheres," *AIChE Journal*, vol. 51, no. 2, pp. 365–378, 2005.

[103] T. Eppinger, K. Seidler, and M. Kraume, "DEM-CFD simulations of fixed bed reactors with small tube to particle diameter ratios," *Chemical Engineering Journal*, vol. 166, no. 1, pp. 324–331, 2011.

[104] M. Zhang, H. Dong, and Z. Geng, "Computational study of flow and heat transfer in fixed beds with cylindrical particles for low tube to particle diameter ratios," *Chemical Engineering Research and Design*, vol. 132, pp. 149–161, 2018.

[105] B. Partopour and A. G. Dixon, "An integrated workflow for resolved-particle packed bed models with complex particle shapes," *Powder Technology*, vol. 322, pp. 258–272, 2017.

[106] F. Bazer-Bachi, F. Augier, and B. Santos, "1d and 2d simulations of partially wetted catalyst particles: A focus on heat transfer limitations," *Chemical Engineering Science*, vol. 66, no. 9, pp. 1953–1961, 2011.

[107] M. F. Mathias and G. P. Muldowney, "Effect of solids loading method on bed porosity and gas flux distribution in a fixed-bed reactor," *Chemical Engineering Science*, vol. 55, no. 21, pp. 4981 – 4991, 2000.

[108] Y. S. Shyr and W. R. Ernst, "Preparation of nonuniformly active catalysts," *Journal of Catalysis*, vol. 63, no. 2, pp. 425 – 432, 1980.

[109] L. H. S. Roblee, R. M. Baird, and J. W. Tierney, "Radial porosity variations in packed beds," *AIChE Journal*, vol. 4, no. 4, pp. 460–464, 1958.

[110] R. F. Benenati and C. B. Brosilow, "Void fraction distribution in beds of spheres," *AIChE Journal*, vol. 8, no. 3, pp. 359–361, 1962.

[111] M. C. Thadani and F. N. Peebles, "Variation of local void fraction in randomly packed beds of equal spheres," *Industrial and Engineering Chemistry Process Design and Development*, vol. 5, no. 3, pp. 265–268, 1966.

[112] J. Ismail, M. Fairweather, and K. Javed, "Structural properties of beds packed with ternary mixtures of spherical particles: Part I- global properties," *Chemical Engineering Research and Design*, vol. 80, no. 6, pp. 637 – 644, 2002.

[113] J. Ismail, M. Fairweather, and K. Javed, "Structural Properties of Beds Packed with Ternary Mixtures of Spherical Particles: Part II- Local Properties," *Chemical Engineering Research and Design*, vol. 80, pp. 645–653, sep 2002.

[114] D. P. Haughey and G. S. G. Beveridge, "Structural properties of packed beds—a review," *The Canadian Journal of Chemical Engineering*, vol. 47, no. 2, pp. 130–140, 1969.

[115] J. Pottbäcker and O. Hinrichsen, "Experimental study on the influence of filling method and particle material on the packed-bed porosity," *Chemie Ingenieur Technik*, vol. 89, no. 4, pp. 454–458, 2017.

[116] E. Foumeny and F. Benyahia, "Predictive characterization of mean voidage in packed beds," *Heat Recovery Systems and CHP*, vol. 11, no. 2-3, pp. 127–130, 1991.

[117] N. Zobel, T. Eppinger, F. Behrendt, and M. Kraume, "Influence of the wall structure on the void fraction distribution in packed beds," *Chemical Engineering Science*, vol. 71, pp. 212–219, 2012.

[118] F. Larachi, R. Hannaoui, P. Horgue, F. Augier, Y. Haroun, S. Youssef, E. Rosenberg, M. Prat, and M. Quintard, "X-ray micro-tomography and pore network modeling of single-phase fixed-bed reactors," *Chemical Engineering Journal*, vol. 240, pp. 290–306, mar 2014.

[119] R. Hannaoui, P. Horgue, F. Larachi, Y. Haroun, F. Augier, M. Quintard, and M. Prat, "Pore-network modeling of trickle bed reactors: Pressure drop analysis," *Chemical Engineering Journal*, vol. 262, pp. 334 – 343, 2015.

[120] S. Chan and K. Ng, "Geometrical characteristics of a computer-generated three-dimensional packed column of equal and unequal sized spheres with special reference to wall effects," *Chemical Engineering Communications*, vol. 48, no. 4-6, pp. 215–236, 1986.

[121] Y. Shi and Y. Zhang, "Simulation of random packing of spherical particles with different size distributions," *Applied Physics A*, vol. 92, pp. 621–626, may 2008.

[122] K. Nandakumar, Y. Shu, and K. T. Chuang, "Predicting geometrical properties of random packed beds from computer simulation," *AIChE Journal*, vol. 45, pp. 2286–2297, nov 1999.

[123] C. R. Abreu, F. W. Tavares, and M. Castier, "Influence of particle shape on the packing and on the segregation of spherocylinders via monte carlo simulations," *Powder Technology*, vol. 134, no. 1–2, pp. 167 – 180, 2003.

[124] W. Salvat, N. Mariani, G. Barreto, and O. Martínez, "An algorithm to simulate packing structure in cylindrical containers," *Catalysis Today*, vol. 107-108, pp. 513–519, oct 2005.

[125] R. Caulkin, M. Fairweather, X. Jia, N. Gopinathan, and R. Williams, "An investigation of packed columns using a digital packing algorithm," *Computers and Chemical Engineering*, vol. 30, pp. 1178–1188, may 2006.

[126] M. Marek, "Numerical generation of a fixed bed structure," *Chemical and Process Engineering*, vol. 34, no. 3, pp. 347–359, 2013.

[127] P. Niegodajew and M. Marek, "Analysis of orientation distribution in numerically generated random packings of Raschig rings in a cylindrical container," *Powder Technology*, vol. 297, pp. 193–201, 2016.

[128] O. Strack and P. A. Cundall, *The distinct element method as a tool for research in granular media*. Department of Civil and Mineral Engineering, University of Minnesota, 1978.

[129] P. Cundall and O. Strack, "A discrete numerical model for granular assemblies.," *Geotechnique*, vol. 29, no. 1, pp. 47–65, 1979.

[130] A. Džiugys and B. Peters, "An approach to simulate the motion of spherical and non-spherical fuel particles in combustion chambers," *Granular Matter*, vol. 3, no. 4, pp. 231–266, 2001.

[131] M. Kodam, R. Bharadwaj, J. Curtis, B. Hancock, and C. Wassgren, "Cylindrical object contact detection for use in discrete element method simulations, Part II Experimental validation," *Chemical Engineering Science*, vol. 65, pp. 5863–5871, nov 2010.

[132] E. Rougier, A. Munjiza, and N. John, "Numerical comparison of some explicit time integration schemes used in dem, fem/dem and molecular dynamics," *International Journal for Numerical Methods in Engineering*, vol. 61, no. 6, pp. 856–879, 2004.

[133] H. Kruggel-Emden, M. Sturm, S. Wirtz, and V. Scherer, "Selection of an appropriate time integration scheme for the discrete element method (dem)," *Computers and Chemical Engineering*, vol. 32, no. 10, pp. 2263–2279, 2008.

[134] J. Theuerkauf, P. Witt, and D. Schwesig, "Analysis of particle porosity distribution in fixed beds using the discrete element method," *Powder Technology*, vol. 165, pp. 92–99, jul 2006.

[135] S. Ookawara, M. Kuroki, D. Street, and K. Ogawa, "High-fidelity dem-cfd modeling of packed bed reactors for process intensification," in *Proceedings of European Congress of Chemical Engineering (ECCE-6), Copenhagen*, pp. 16–20, 2007.

[136] S. Schulze, P. A. Nikrityuk, and B. Meyer, "Porosity distribution in monodisperse and polydisperse fixed beds and its impact on the fluid flow," *Particulate Science and Technology*, vol. 33, no. 1, pp. 23–33, 2015.

[137] J. L. Stephenson and W. E. Stewart, "Optical measurements of porosity and fluid motion in packed beds," *Chemical Engineering Science*, vol. 41, no. 8, pp. 2161–2170, 1986.

[138] A. Montillet and L. Le Coq, "Characteristics of fixed beds packed with anisotropic particles—Use of image analysis," *Powder Technology*, vol. 121, pp. 138–148, nov 2001.

[139] P. Niegodajew and M. Marek, "Analysis of orientation distribution in numerically generated random packings of raschig rings in a cylindrical container," *Powder Technology*, vol. 297, pp. 193–201, 2016.

[140] Y. Guo, C. Wassgren, W. Ketterhagen, B. Hancock, and J. Curtis, "Some computational considerations associated with discrete element modeling of cylindrical particles," *Powder Technology*, vol. 228, pp. 193 – 198, 2012.

[141] G. Boccardo, F. Augier, Y. Haroun, D. Ferré, and D. L. Marchisio, "Validation of a novel open-source work-flow for the simulation of packed-bed reactors," *Chemical Engineering Journal*, vol. 279, pp. 809 – 820, 2015.

[142] B. Partopour and A. G. Dixon, "Resolved-pore simulation of co oxidation on rh/al2o3 in a catalyst layer," *ChemEngineering*, vol. 2, no. 1, p. 2, 2017.

[143] M. H. Al-Dahhan, Y. Wu, and M. P. Dudukovic, "Reproducible technique for packing laboratory-scale trickle-bed reactors with a mixture of catalyst and fines," *Industrial and Engineering Chemistry Research*, vol. 34, no. 3, pp. 741–747, 1995.

[144] J. D. Mcwhirter, M. E. Crawford, and D. E. Klein, "Wall region porosity distributions for packed beds of uniform spheres with modified and unmodified walls," *Transport in Porous Media*, vol. 27, no. 1, pp. 99–118, 1997.

[145] J. Šmid, P. Van Xuan, and D. J. Thyn, "Effect of filling method on the packing distribution of a catalyst bed," *Chemical Engineering and Technology*, vol. 16, no. 2, pp. 114–118, 1993.

[146] J. Wooten, "Dense and sock catalyst loading compared," *Oil and Gas Journal*, vol. 96, no. 41, pp. 66 – 70, 1998.

[147] R. Balevičius, R. Kačianauskas, Z. Mroz, and I. Sielamowicz, "Analysis and dem simulation of granular material flow patterns in hopper models of different shapes," *Advanced Powder Technology*, vol. 22, no. 2, pp. 226–235, 2011.

[148] M. V. Tabib, S. T. Johansen, and S. Amini, "A 3d cfd-dem methodology for simulating industrial scale packed bed chemical looping combustion reactors," *Industrial and Engineering Chemistry Research*, vol. 52, no. 34, pp. 12041–12058, 2013.

[149] H. Bai, J. Theuerkauf, P. A. Gillis, and P. M. Witt, "A coupled DEM and CFD simulation of flow field and pressure drop in fixed bed reactor with randomly packed catalyst particles," *Industrial and Engineering Chemistry Research*, vol. 48, no. 8, pp. 4060–4074, 2009.

[150] A. Di Renzo and F. P. Di Maio, "Comparison of contact-force models for the simulation of collisions in dem-based granular flow codes," *Chemical Engineering Science*, vol. 59, no. 3, pp. 525–541, 2004.

[151] B. Peng, *Discrete element method (DEM) contact models applied to pavement simulation*. PhD thesis, Virginia Tech, 2014.

[152] C. O'Sullivan and J. D. Bray, "Selecting a suitable time step for discrete element simulations that use the central difference time integration scheme," *Engineering Computations*, vol. 21, no. 2/3/4, pp. 278–303, 2004.

[153] S. V. Patankar and D. B. Spalding, "A calculation procedure for heat, mass and momentum transfer in three-dimensional parabolic flows," in *Numerical Prediction of Flow, Heat Transfer, Turbulence and Combustion*, pp. 54–73, Elsevier, 1983.

[154] Y. A. Hassan, "Large eddy simulation in pebble bed gas cooled core reactors," *Nuclear Engineering and Design*, vol. 238, no. 3, pp. 530–537, 2008.

[155] T. Li, Y. Peng, Z. Zhu, S. Zou, and Z. Yin, "Discrete element method simulations of the inter-particle contact parameters for the mono-sized iron ore particles," *Materials*, vol. 10, no. 5, p. 520, 2017.

[156] S. Lommen, D. Schott, and G. Lodewijks, "Dem speedup: Stiffness effects on behavior of bulk material," *Particuology*, vol. 12, pp. 107–112, 2014.

[157] T. Eppinger, N. Jurtz, and R. Aglave, "Automated workflow for spatially resolved packed bed reactors with spherical and non-spherical particles," in *10th International Conference on CFD in Oil andGas, Metallurgical and Process Industries, SINTEF, Trondheim, Norway*, 2014.

[158] W. Sobieski, Q. Zhang, and C. Liu, "Predicting tortuosity for airflow through porous beds consisting of randomly packed spherical particles," *Transport in Porous Media*, vol. 93, pp. 431–451, Jul 2012.

[159] W. Sobieski, W. Dudda, and S. Lipiński, "A new approach for obtaining the geometric properties of a granular porous bed based on dem simulations," *Technical Sciences/University of Warmia and Mazury in Olsztyn*, pp. 165–187, 2016.

[160] W. Sobieski, "The use of path tracking method for determining the tortuosity field in a porous bed," *Granular Matter*, vol. 3, no. 18, pp. 1–9, 2016.

[161] P. TANG and V. M. PURI, "Methods for minimizing segregation: A review," *Particulate Science and Technology*, vol. 22, no. 4, pp. 321–337, 2004.

[162] Y. Guo, C.-Y. Wu, and C. Thornton, "The effects of air and particle density difference on segregation of powder mixtures during die filling," *Chemical Engineering Science*, vol. 66, no. 4, pp. 661 – 673, 2011.

[163] J. Yang, J. Wu, L. Zhou, and Q. Wang, "Computational study of fluid flow and heat transfer in composite packed beds of spheres with low tube to particle diameter ratio," *Nuclear Engineering and Design*, vol. 300, pp. 85–96, 2016.

[164] J.-D. Llamas, F. Lesage, and G. Wild, "Radial dispersion in trickle-bed reactors: Comparison between sock and dense loadings," *Chemical Engineering Science*, vol. 65, no. 1, pp. 538–541, 2010.

[165] M. Salimi, S. H. Hashemabadi, S. Noroozi, A. Heidari, and M. Bazmi, "Numerical and experimental study of catalyst loading and body effects on a gas-liquid trickle-flow bed," *Chemical Engineering and Technology*, vol. 36, no. 1, pp. 43–52, 2013.

[166] M. Giese, K. Rottschäfer, and D. Vortmeyer, "Measured and modeled superficial flow profiles in packed beds with liquid flow," *AIChE Journal*, vol. 44, no. 2, pp. 484–490, 1998.